A FAMILY OF STRUCTURALLY RELATED SECRETED PROTEINS

OF *Staphylococcus aureus*

A Dissertation

by

SHEILA ESTHER THOMAS

Submitted to the Office of Graduate and Professional Studies of
Texas A&M University
in partial fulfillment of the requirements for the degree of

DOCTOR OF PHILOSOPHY

Chair of Committee,	Magnus Höök
Co-Chair of Committee,	Ya-Ping Ko
Committee Members,	Peter J. A. Davies
	Margarita Martinez-Moczygemba
	Rick Wetsel
	Yi Xu
Head of Department,	Warren E. Zimmer, Jr.

August 2019

Major Subject: Medical Sciences

ABSTRACT

The opportunistic pathogen, *Staphylococcus aureus* (*S. aureus*) can create a number of infections. The bacterium can assemble a two-layered structure composed of fibrinogen (Fg)/fibrin around itself, called the Fg shield to protect itself from being phagocytized by the immune response cells. The *S. aureus* proteins, Coagulase (Coa), Extracellular fibrinogen-binding protein (Efb) and von Willebrand factor-binding protein (vWbp) contribute to shield formation. Efb can contribute by binding to both soluble Fg and the complement component C3b that is deposited on the bacterial surface. The two coagulases, Coa and vWbp, can bind Fg and coagulate plasma and blood by non-proteolytically activating the coagulation factor, prothrombin that cleaves Fg to fibrin, which can contribute to the formation of the Fg/fibrin layers of the shield. The Fg interactions between Coa and Efb have been characterized to some detail. Coa and vWbp often appear to be redundant in function. However, the mechanism(s) of the interaction between vWbp and Fg appears to be unclear.

In this study, I show that vWbp and Coa do not interact with Fg in the same way. Coa shows a conformation preference in binding to soluble Fg, whereas, vWbp demonstrates no preference for binding to either soluble or immobilized Fg. Both the N- and C-terminal halves of vWbp and Coa (vWbp-N, -C; Coa-N, -C, respectively) harbor Fg-binding activities. The Fg-binding activity of Coa lies in the C-terminal region, whereas, vWbp-N harbors the higher affinity Fg-binding region. vWbp and Coa do not share the same binding sites on Fg. The N-terminal regions of both coagulases interact with the Fg β-chain, but they bind to different sites. Coa-N also appears to recognize the Fg α-chain. Both the Fg-binding motifs of Coa-C and the N-terminal region of Efb do not inhibit vWbp-C from binding to Fg, indicating that vWbp-C does

not harbor a similar motif. The predicted structure of vWbp-C appears to be structurally related to the C3b-binding motif of Efb. My data shows that the Fg interactions of vWbp and Coa are different and complex, and from this, it appears that *S. aureus* expresses a family of structurally related secreted proteins.

DEDICATION

I dedicate this dissertation to God and my family, for the love and continuous support I have received throughout this arduous yet exciting journey.

ACKNOWLEDGEMENTS

I would like to thank my advisor, Dr. Magnus Höök. He has been a wonderful mentor and a great encouragement to me during this graduate training period. Joining this lab with no strong research experience, had me a little apprehensive of how I would fare in this graduate program, but Dr. Höök had confidence in me. His confidence in my work, taught me to be confident in myself. He has provided me with opportunities that are highly beneficial to my graduate studies and especially for my future career in science.

I would also like to thank my co-mentor Dr. Ya-Ping Ko. She has been a great support to me. She has always been very willing to help me and answer any questions I had. Dr. Ko would always encourage me to strive to do better, such as giving me advice in how to improve in my presentations. Dr. Ko and Dr Höök would not only give me professional advice, but also personal advice that will be highly beneficial to me as begin my life in the world of science.

I would like to thank my committee members, Dr. Davies, Dr. Moczygemba, Dr. Xu, and Dr. Wetsel, for their guidance and support throughout the course of this research, especially for their valuable feedback through committee meetings that have allowed me to grow in knowledge as a student and scientist.

I would also like to thank my friends and colleagues and the department faculty and staff for making my time at IBT Texas A&M University a worthwhile experience.

And finally most importantly, thank you to my father and mother for their encouragement and support, as well as my siblings and my grandmother.

CONTRIBUTORS AND FUNDING SOURCES

Contributors

This work was supervised by a dissertation committee consisting of Professor Höök, Professor Ko, Professor Davies, Professor Moczygemba, Professor Xu, and Professor Zimmer of the Department of Medical Physiology and Professor Rick Wetsel of the Center of Immunology and Autoimmune Diseases.

The data analyzed for Chapters IV-VI was provided by Professor Magnus Höök and Professor Ya-Ping Ko. Critical reading of the manuscript depicted in Chapter IV and the first part of Chapter V was conducted in part by Professor Moczygemba of the Center for Infectious and Inflammatory Diseases and was published in 2019.

All other work conducted for the dissertation was completed by the student independently.

Funding Sources

Graduate study was supported by from the Training grant T32 under Grant Number AI55449-11. This work was also made possible in part by NIH/NIAID under Grant number AI020624 to Dr. Höök and support from the Hamill Foundation to Dr. Ko. Its contents are solely the responsibility of the authors and do not necessarily represent the official views of the NIH/NIAID.

NOMENCLATURE

SSTI	Skin and soft tissue infections
fI-XIII	Factor I…XIII
Fg	Fibrinogen
ST	Sequence type
Coa	Coagulase
vWbp	von Willebrand factor-binding protein
Efb	Extracellular fibrinogen-binding protein
Ecb	Extracellular complement-binding protein
SdrG	Serine-aspartate repeat-containing protein G
ClfA	Clumping factor A
MRSA	Methicillin Resistant *Staphylococcus aureus*
VRSA	Vancomycin-Resistant *Staphylococcus aureus*
vWF	von Willebrand factor
C3	Complement component 3
MGE	Mobile genetic element(s)
GST	Glutathione-S-transferase
PBS	Phosphate- Buffered Saline
TBS	Tris-Buffered Saline

TABLE OF CONTENTS

LIST OF FIGURES

LIST OF TABLES

CHAPTER I

INTRODUCTION AND LITERATURE REVIEW[1]

The immune response system

The immune response system serves as a protective mechanism towards invading microorganisms, due to a tissue injury of an animal or a human, as well as protection against molecules that are recognized as non-self, such as allergens (Chaplin, 2010). The system consists of two arms of defense, the innate and adaptive immunity that function to recruit and activate immune response cells to prevent microbial invasion. The immune response cells include the leukocytes, such as neutrophils, macrophages and lymphocytes such as B-cells, T-cells and natural killer (NK) cells (Chaplin, 2010). These immune cells play a critical role in innate and adaptive immunity with the goal of eliminating invading microorganisms (Smith et al., 2015).

A breach to the physical barrier i.e. skin, can allow an invading microorganism to enter into the tissues, resulting in the activation of the innate immune response system (Merle et al., 2015; Smith et al., 2015). Upon microbial entry, the complement system is immediately triggered (Merle et al., 2015; Nesargikar et al., 2012). The function of the complement system is to directly or indirectly kill bacteria by activating a series of complement component proteins that are either deposited on the bacterial surface or released to recruit leukocytes to the site of infection (Fig 1; (Merle et al., 2015)). In addition, vascular injury also leads to activation of coagulation cascade to prevent further blood loss and to impede bacterial entry by the formation of a blood clot, composed of fibrin and platelets (Fig 2; (Smith et al., 2015)).

[1] Part of this chapter is reprinted with permission from "The Complex Fibrinogen Interactions of the Staphylococcus aureus Coagulases" by Thomas, S., Liu, W., Arora, S., Vannakambodi, G., Ko, Y-P., and Höök, M. 2019. *Front. Cell. Infect. Microbiol.* 9:106.

Each step of the complement and coagulation pathways serve to activate enzymes downstream of the pathways, which results in amplification and propagation of the signal to recruit more immune cells to the site of infection (Palta, et al., 2014; Peetermans et al., 2015). The two dynamic pathways of innate immunity also activate immune response cells for bacterial clearance (Smith et al., 2015; Nesargikar et al., 2012). The fibrinolytic pathway then follows, which results in the breakdown of the clot to allow for wound healing (Davalos and Akassoglou, 2012).

The function of the adaptive immune response system is to activate lymphocytes for recognizing pathogens via antibody production, kill bacteria by cytotoxic T-cells and NK cells and establish immune memory cells in case of recurrent exposure to the pathogen (Alberts et al., 2002; Jorgensen et al., 2017). The immune response cells responsible for activating the lymphocytes are the B cells, dendritic cells and macrophages that are known as professional antigen presenting cells (APCs) (Chen and Jensen, 2008). APCs activate naïve helper T cells and cytotoxic T cells by processing antigens such as bacterial proteins, and presenting the bacterial fragments to the receptors on the cell surfaces of T-cells (Schuijs et al., 2018). The helper T-cells can activate cytotoxic T-cells and B-cells via the secretion of cytokines (Alberts et al., 2002). Activated B cells, called plasma cells, secrete antibodies that via the complement system are deposited on the surface of pathogens and lead to complement activation (Dunkelberger and Song, 2010; Nesargikar et al., 2012).

The immune response system is able to recognize self from non-self by complement proteins and antibodies deposited on the bacterial surface that can be detected by complement and Fc receptors, respectively, on neutrophils and macrophages (Chaplin, 2010). In addition, the presence of pathogen-associated molecular patterns (PAMPs), such as endotoxins on the

bacterial membrane can also trigger immune response cells (Chaplin, 2010; Alberts et al., 2002). Neutrophils and macrophages can recognize these PAMPs via their toll-like receptors (TLRs) (Chaplin, 2010).

Recognition of the pathogens, leads to neutrophils and macrophages engulfing the microorganisms through a process called phagocytosis that results in bacterial death (Chaplin, 2010). In adaptive immunity, activated cytotoxic T-cells kill bacteria by the release of perforin and granzymes that mediate programmed cell death of cells infected with bacteria known as apoptosis (Jorgensen et al., 2017; Alberts et al., 2002; Voskoboinik et al., 2015).

Since the complement system and coagulation cascade are critical players of the innate and adaptive immune responses, bacteria often target these two pathways for immune evasion (Foster, 2005).

The complement system

The complement system opsonizes bacteria for recruitment of leukocytes for phagocytosis, generates small complement fragments termed as anaphylatoxins that trigger an inflammatory response, and assembles the membrane attack complex (MAC) for the lysis of bacterial cells (Nesargikar et al., 2012; Noris and Remuzzi, 2013). The system is composed of about 30 soluble complement proteins that circulate in blood plasma and extracellular fluid (Nesargikar et al., 2012; Alberts et al., 2002). Three pathways make up the complement system, classical, mannose-binding lectin (MBL) and alternative pathways (Fig 1; (Merle et al., 2015; Nesargikar et al., 2012; Noris and Remuzzi, 2013)).

The classical pathway is activated by the complement component C1q that recognizes and binds to the Fc region of the antibody that is bound to the bacterial surface (Noris and Remuzzi, 2013). C1q can also bind to the pathogen surface without the presence of an antibody

to initiate the event (Nesargikar et al., 2012). C1q is composed of 18 polypeptide chains, six A-chains, six B-chains and six C-chains (Thielens et al., 2017). Each chain contains a collagen-like region at the N-terminus and a C-terminal globular head. One A, B, C chain forms a subunit of triple peptide helices, which are responsible for binding to the Fc portion of a bound antibody (Thielens et al., 2017; Nesargikar et al., 2012; Duncan and Winter, 1988; Dunkelberger and Song, 2010). Two zymogen serine proteases each of C1r and C1s are attached to C1q, for the C1 complex (Nesargikar et al., 2012). The C1 complex that is bound to the bacterial surface undergoes a conformational change of the complex that triggers the autocatalytic activation of C1r. Activated C1r then cleaves C1s, activating C1s of the complex (Nesargikar et al., 2012). Activated C1s cleaves C4 and then C2 to generate fragments C4b and C2a. C4b bound to C2a on the bacterial surface form the C3 convertase (C4b2a) that is capable of cleaving C3 to generate C3b (Noris and Remuzzi, 2013).

The mannose-binding lectin (MBL) pathway is activated by recognition and binding to carbohydrates on the bacterial surface, such as mannose (Petersen et al., 2001). The events upstream of MBL pathway are considered to be homologous to the complement proteins upstream of the classical pathway (Nesargikar et al., 2012). The complement protein, MBL, is similar in structure to that of C1q that consists of six subunits of triple helices. Each polypeptide chain of C1q is different from each other; however, the polypeptide chains of MBL are identical to each other (Jensen et al., 2005). Each chain contains a collagen-like region at the N-terminus and a globular head at the C-terminus (Jensen et al., 2005). Linked to the stalk are two zymogens each MASP-1 and MASP-2 molecules that resemble Clr and C1s, respectively (Petersen et al., 2001; Nesargikar et al., 2012). Upon subsequent activation of the zymogens, MASP-2 cleaves C4 and C2, releasing C2b and C4a and generating C3 convertase (C4b2a) (Petersen et al., 2001).

The third complement pathway that differs from the upstream events of the classical and lectin pathways is the alternative pathway. There is a constant basal level of alternative pathway activation by the spontaneous hydrolysis of C3 into C3(H_2O) through a highly reactive thioester bond ('tick-over' theory) (Thurman and Holers, 2006). C3(H_2O) can bind the plasma protein, factor B (fB), and become susceptible to factor D (fD) cleavage to form the soluble C3 convertase, C3(H_2O)Bb (Dunkelberger and Song, 2010). This C3 convertase cleaves C3 into C3b and C3a. C3b binds to the cell surface via a thioester bond and can further bind to fB to form C3bB, which can then be cleaved by fD to form an additional C3 convertase (C3bBb) (Thurman and Holers, 2006). This C3 convertase can now cleave more C3 molecules to C3b. C3b generation from the classical and lectin pathway can also bind to factor B to eventually form C3 convertase, resulting in an 'amplification loop' (Merle et al., 2015).

All three pathways converge at the cleavage of the complement component C3 by the C3 convertase. In the classical and MBL pathways, C2a of the C3 convertase (C4b2a) cleaves C3 to C3a and C3b (Beltrame et al., 2015). C3b is deposited on the bacterial surface, by binding covalently to the surface. The pathogen is targeted for phagocytosis after being 'decorated' by the deposited C3b and C4b components (Dunkelberger and Song, 2010). For all three pathways, the addition of C3b to the C3 convertase forms C5 convertases (C4b2a3b and C3bBb3b), which then cleaves C5 to C5a and C5b. C5b binds to the bacterial surface, where it recruits and binds to C6, followed by C6 binding to C7 (Merle et al., 2015). Binding of C7 to C6 exposes C7's hydrophobic site, allowing C7 to be inserted into the lipid bilayer of the pathogen (Dunkelberger and Song, 2010). The complement component C8 is composed of C8β and C8α-γ. Binding of C8β to the C5b-7 complex allows C8α-γ to be inserted into the membrane and recruits C9 (Bubeck et al., 2011). Binding induces the polymerization of C9, which is about 10-16

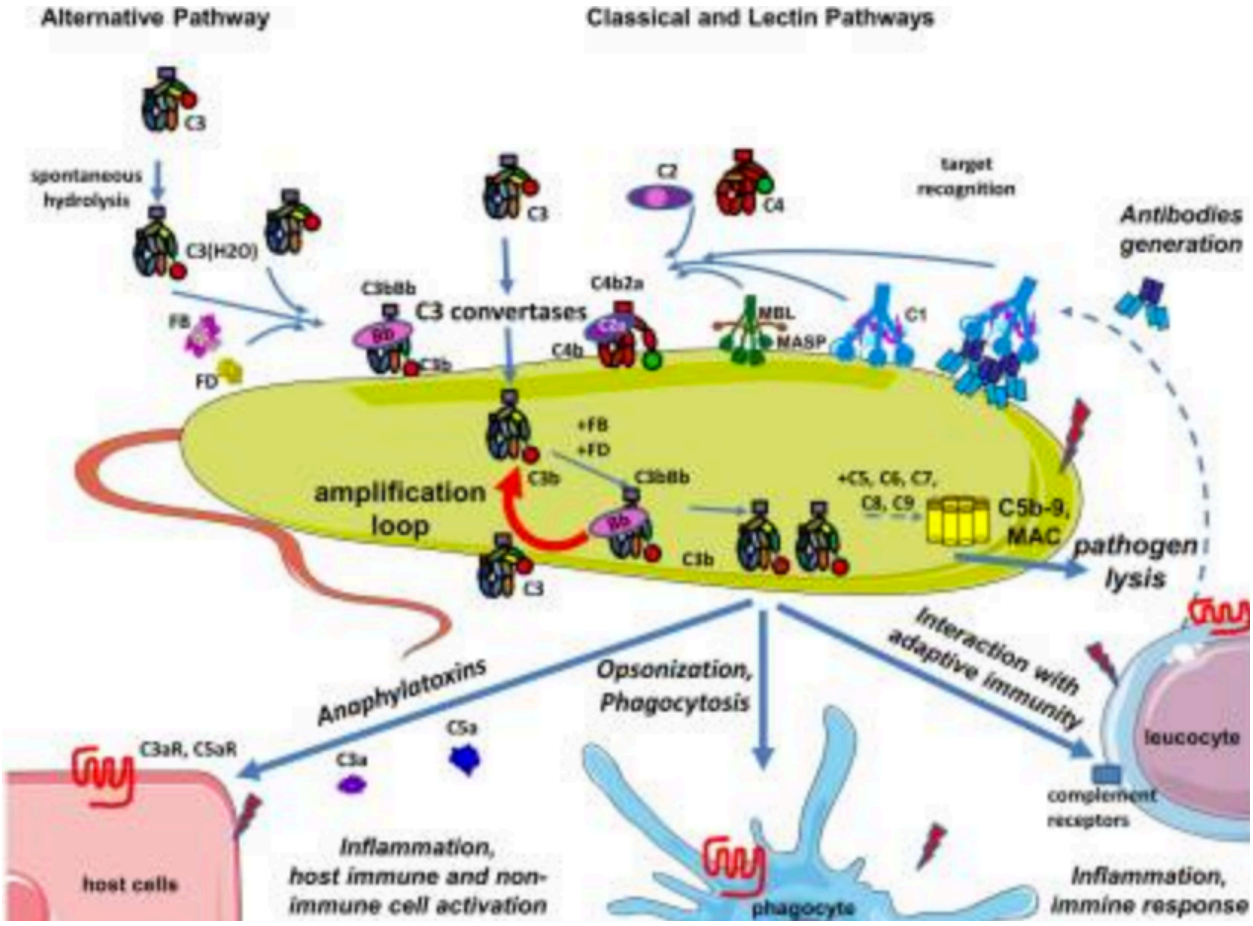

Figure 1. The complement system is composed of three pathways. (Reprinted with permission from Merle et al., 2015)

molecules that form a pore on the bacterial surface. This perturbs the integrity of the bacterial cell membrane, eventually leading to the lysis of the pathogen. This C5b-9 complex is termed the membrane attack complex (MAC) (Nesargikar et al., 2012). The complement fragments that were generated upstream of the pathway, C3a, C4a, and C5a, called anaphylatoxins, act as chemoattractants to recruit leukocytes to the site of infection (Haas and van Strijp, 2007).

Thus, with all pathways generating convertases and complement deposition, the immune response is amplified and propagated. Not only can more phagocytes be recruited to the opsonized pathogen, but also more pathogens can be lysed due to the MAC formation.

The coagulation cascade and fibrinolytic system

The hemostasis system facilitates the balance of the body by the interactions of the coagulation cascade and the fibrinolytic system (Fig 2; (Vadasz et al., 2015)). The coagulation cascade consists of the intrinsic and the extrinsic pathways (Fig 3; (Smith et al., 2015; Palta, et al., 2014; Peetermans et al., 2015)). Activation of the cascade is initiated by tissue damage, in which a series of serine protease zymogens are activated in a step-wise fashion to generate a blood clot to prevent excessive blood loss and to limit bacterial dissemination into the tissues (Fig 3; (Smith et al., 2015; De Luca et al., 2018; Peetermans et al., 2015)) (Table 1).

When the body incurs vascular injury, platelets, anucleated effector cells, are recruited to the site of injury (Palta, et al., 2014). Von Willebrand factor (vWF), a multimeric glycoprotein, serves as a bridging molecule between platelets and collagen, and is expressed on the damaged endothelial surface (Lenting et al., 2015; Deckmyn and Vanhoorelbeke, 2006). The platelets adhere to the damaged endothelial surface, forming a “platelet plug” to stop further bleeding (Palta, et al., 2014). The platelet plug provides as a surface on which coagulation factors can assemble (Palta, et al., 2014).

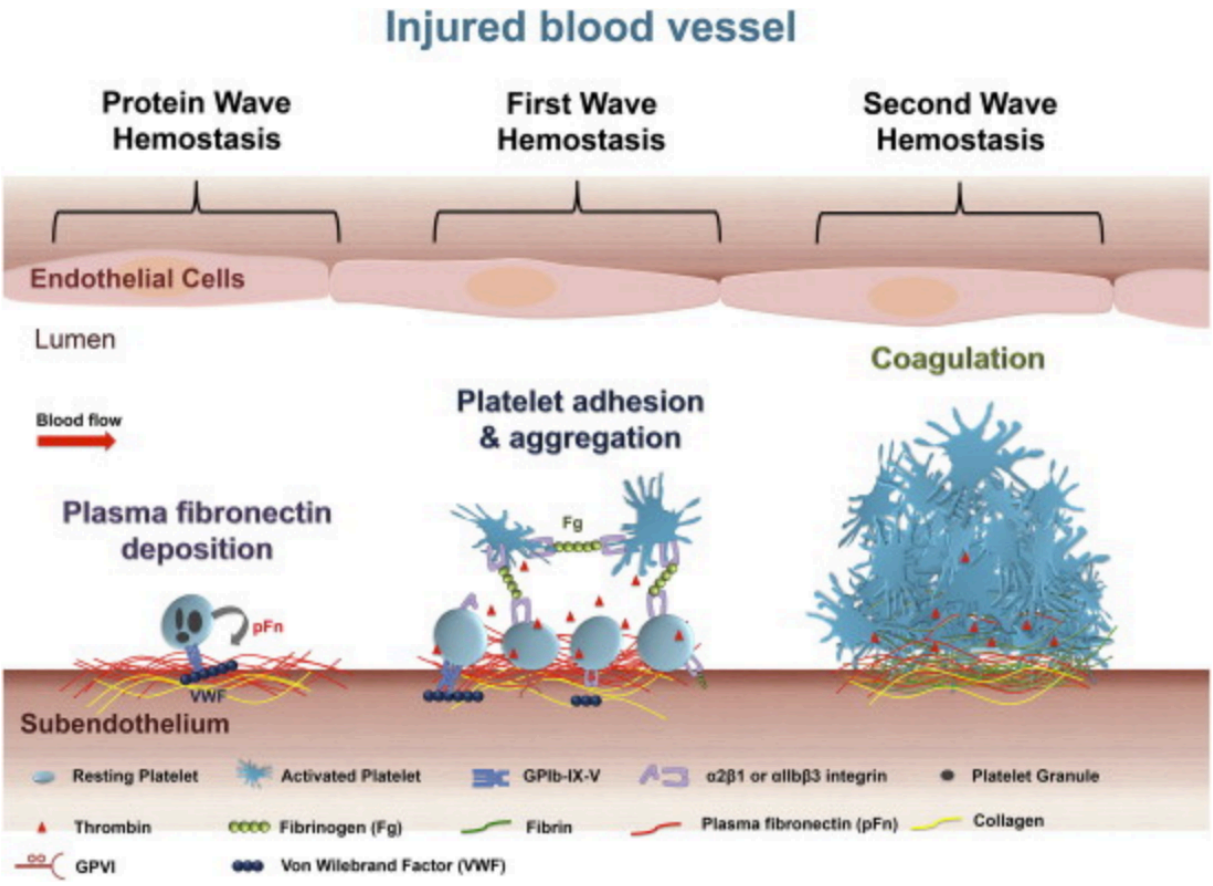

Figure 2. The hemostasis system prevents further bleeding upon vascular injury. (Reprinted with permission from Vadasz et al., 2015)

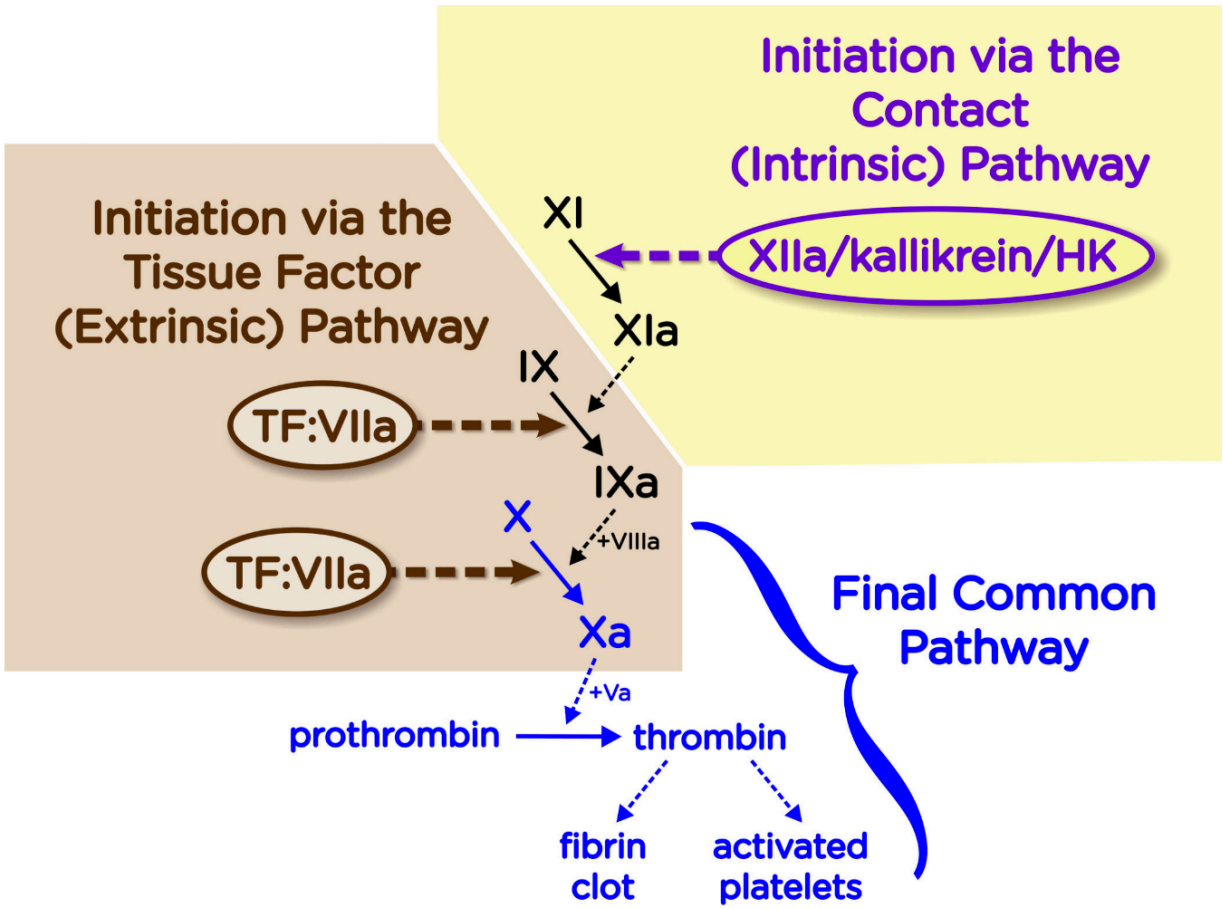

Figure 3. The coagulation cascade can be activated via the extrinsic or intrinsic pathway.

(Reprinted with permission from Smith et al., 2015)

The cascade can be initiated via the Extrinsic Pathway or the Intrinsic Pathway. The Extrinsic Pathway is activated by vascular injury, in which tissue factor is overexpressed in the perivascular tissues (Davalos and Akassoglou, 2012). Tissue factor a transmembrane glycoprotein, acts as a cofactor for the serine protease fVIIa (Factor VIIa) for the activation of fX, in which the complex cleaves the zymogen to fXa (Table 1) (Smith et al., 2015). The Intrinsic Pathway is initiated by surface damage and recognition of negatively charged bacterial surface structures (Davalos and Akassoglou, 2012; Peetermans et al., 2015). Activation of the pathway requires fXIIa, prekallikrein (PK), high-molecular-weight kininogen (HK), calcium ions and phospholipids, which are secreted from platelets (Davalos and Akassoglou, 2012; Smith et al., 2015). PK is converted to kallikrein, which activates fXII to fXIIa and fXIIa activates fXI to fXIa (Smith et al., 2015). Through proteolytic cleavage, fXIa activates fX to fXa (Smith et al., 2015; De Luca et al., 2018). The extrinsic and intrinsic pathways merge at the activation of fX, known as the common pathway (Smith et al., 2015). Factor Va binds to the receptors of activated platelets to form a prothrombinase complex (Smith et al., 2015). The prothrombinase complex consists of fVa, fXa, platelet phospholipids, phosphatidylinositol, phosphatidylserine, Ca^{2+} and prothrombin (Davalos and Akassoglou, 2012). The complex proteolytically cleaves prothrombin, in which the zymogen is converted to the active form, thrombin. Thrombin cleaves the coagulation factor, fibrinogen, which conformationally changes into fibrin (Weisel, 2005). Fibrin monomers laterally aggregate together eventually forming a fibrin clot with the involvement of fXIIIa (Weisel, 2005). The fibrin clot serves to further stabilize the platelet plug (Palta, et al., 2014).

The fibrinolytic system results in the dissolution of the fibrin clot, to allow for tissue healing (Davalos and Akassoglou, 2012; Urano et al., 2018). Damaged endothelial cells release a

serine protease, tissue plasminogen activator (tPA) (Urano et al., 2018). The fibrinolytic system is initiated when tPA cleaves plasminogen to its activate form plasmin. Plasmin then degrades fibrin, fibrinogen, fV and fVIII (Amara et al., 2008).

Table 1. Coagulation factors

Inactive	Active
Fibrinogen (Factor I)	Fibrin (Factor Ia)
Prothrombin (Factor II)	Thrombin (Factor IIa)
Factor V	Factor Va
Factor VI	Factor VIa
Factor VII	Factor VIIa
Factor VIII	Factor VIIIa
Factor IX	Factor IXa
Factor X	Factor Xa
Factor XI	Factor XIa
Factor XII	Factor XIIa
Factor XIIIa	Factor XIIIa

Fibrinogen a critical player of the host immune response

Fibrinogen (Fg) is a 340 kDa homodimeric glycoprotein that is expressed by hepatocytes in the liver (Weisel and Litvinov, 2017). The protein is composed of two sets of three polypeptide chains, Aα, Bβ and γ that are linked together via 29 disulfide bonds (Fig 4; (Köhler et al., 2015)). The expected size of the α-chain is 63.5 kDa, β-chain is 56 kDa and the γ-chain is 47 kDa (Seo and Sullam, 2011). An altered γ'-chain is present in approximately 10% of normal Fg (Cheung et al., 2015). The two Fg molecules are composed of the central E fragment that comprises the disordered fibrinopeptides A and B, and the γ-chains (Wolberg and Campbell,

2008). The fragment is linked by triple α-helical coiled-coil segments to two globular D fragments (Wolberg and Campbell, 2008). The γ and β nodules of the D-fragments have a and b "holes" that are required for fibrin polymerization (Riedel et al., 2011).

The coagulation factor is a highly abundant plasma protein in which 1.5-4 g/L circulates in the blood plasma (Weisel and Litvinov, 2017). As an acute phase protein, Fg is upregulated upon vascular injury (Weisel, 2005). In the coagulation cascade, thrombin cleaves Fg at positions Arg^{15}-Gly^{16} of the α-chain and Arg^{14}-Gly^{15} of the β-chain, releasing fibrinopeptides A and B, respectively (Weisel, 2005; Liesenborghs et al., 2018). Although cleavage occurs simultaneously, the release of fibrinopeptide B is slower than the release of fibrinopeptide A (Doolittle, 1984; Weisel, 2005). Cleaved fibrinopeptide B serves as a chemoattractant that recruits leukocytes for bacterial clearance (Davalos and Akassoglou, 2012; Ko and Flick, 2016). Cleavage of fibrinopeptide A, exposes the "knob" A of the α-chain of fragment E that is inserted into the complementary "hole" a in the C-terminal γ-chain of the D-fragment (Riedel et al., 2012; Wolberg and Campbell, 2008). Fibrinopeptide B cleavage results in the insertion of "knob" B of the β-chain of fragment E into the b "hole" in the β-chain of the D-fragment. These insertions result in a half-staggered alignment of the molecules, since the E-fragment of one Fg molecule is inserted into the D-fragment of an adjacent Fg molecule (Riedel et al., 2012). Half-staggered alignment of the soluble fibrin monomers forms a fibrin strand (Wolberg and Campbell, 2008; Weisel and Litvinov, 2017). Transglutaminase, also known as fXIIIa, cross-links the fibrin strands, creating a fibrin mesh (Riedel et al., 2012). Polymerization of the strands results in protofibrils and then fiber bundles, which all together make up the fibrin clot (Walker and Nesheim, 1999; Weisel and Litvinov, 2017) The fibrin clot is formed on the surface of the

platelet plug which stabilizes the clot (Palta, et al., 2014). Thereby, further bleeding is prevented at the site of injury.

Fg not only plays a crucial role in the coagulation cascade of the hemostasis system by being converted to fibrin to form the fibrin clot, but also in modulating innate immunity (Flick et al., 2004; Davalos and Akassoglou, 2012). The C-terminus of the Fg γ-chain, residues 390-396, interacts with the leukocyte integrin receptor, $\alpha_M\beta_2$ (also known as CD11b/CD18 receptor, Mac-1) (Rubel et al., 2001; Davalos and Akassoglou, 2012). The $\alpha_M\beta_2$-binding motif is not exposed when Fg is in its soluble form in the blood. However, immobilized Fg or insoluble fibrin allows the binding site to become accessible for binding to $\alpha_M\beta_2$ (Flick et al., 2004). The interaction mediates neutrophil adhesion to the endothelial surface (Flick et al., 2004). In addition, binding releases signals that activate many proinflammatory pathways such as NF-κB pathway (Davalos and Akassoglou, 2012). Activation of the proinflammatory pathways leads to the production and release of TNF- α and IL-1β (Davalos and Akassoglou, 2012; Flick et al., 2013). However, blocking the Fg-$\alpha_M\beta_2$ interaction, in which amino acid residues 390-396 of the Fg-γ chain were mutated, reduced clearance of *Staphylococcus aureus* in an acute peritonitis murine model compared to wild type mice (Flick et al., 2004). CD11c/CD18 integrin also binds to Fg. The receptor is expressed on dendritic cells, macrophages, neutrophils, and monocytes (Davalos and Akassoglou, 2012; Mazzone and Ricevuti, 1995). Fg also activates mast cells by binding to the intergrin, $\alpha_{IIb}\beta_3$ via $\gamma^{408\text{-}411}$ region of Fg (Oki et al., 2006). In addition, the C-terminal Fg-γ chain-$\alpha_{IIb}\beta_3$ interaction mediates platelet aggregation (Ko and Flick, 2016). Thereby, Fg is a versatile protein that not only is critical to the coagulation hemostasis system but is also essential in generating proinflammatory responses.

Cross-talk between the coagulation and complement pathways

Studies demonstrate that cross-talks exists between the coagulation cascade and the complement system (Markiewski et al., 2007). Proteins of the complement system can activate and cleave coagulation factors, and enzymatic coagulation factors can cleave complement components in place of convertases. Complement components such as C3 and C5 are cleaved by the C3 and C5 convertases. In a C3-deficient mice study, C5a components were detected (Oikonomopoulou et al., 2012). It was shown that thrombin could cleave C5 to C5a and C5b. The released C5a generated a strong chemotactic signal in recruiting neutrophils (Oikonomopoulou et al., 2012). In another study, thrombin was also able to cleave C3 molecules to generate C3b and C3a (Amara et al., 2008). Therefore, the host immune system can still provide an effective immune response in the absence of the C3 and C5 convertases.

Fibrin(ogen) can also enhance the activity of the mannan-binding lectin (MBL) pathway, by binding to ficolin or MBL (Endo et at., 2010). MBL binds to the α and β-chains of Fg. Ficolin also binds to both the α and β-chains of Fg and fibrin, but not the γ chain. Binding enhances C4b and C3b deposition (Endo et at., 2010). C1q of the classical pathway can also to bind to Fg and fibrin (Entwistle and Furcht, 1988). In another study, the binding of one of the heads of C1q to Fg impaired fibrin polymerization (Lu et al., 1999). This interaction may serve as a regulatory mechanism to prevent thrombosis formation (Lu et al., 1999).

The serine proteases of the MBL pathway can activate and cleave coagulation factors. MASP-1 and MASP-2 are part of the MBL complex that cleave C3 to generate C3b (Nesargikar et al., 2012). MASP-1 can also cleave Fg to generate fibrin monomers (Conway, 2015). MASP-2 can activate prothrombin to active thrombin and cleave Fg to fibrin (Conway, 2015).

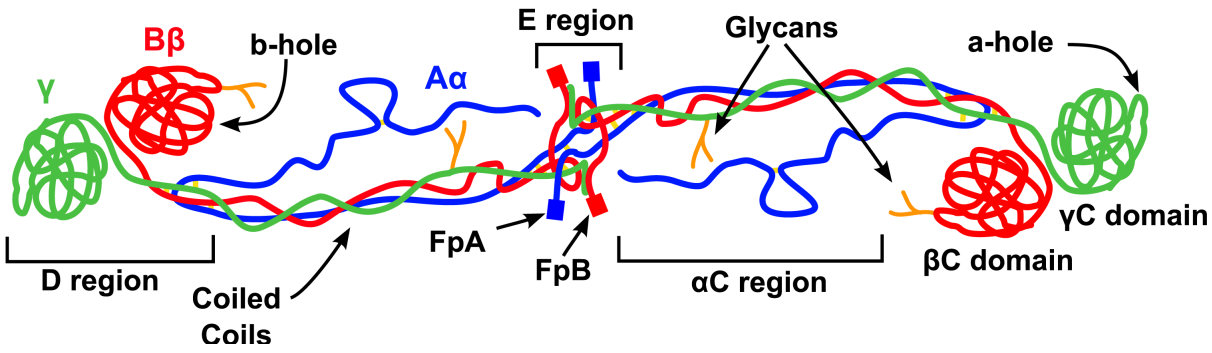

Figure 4. Fg is a homodimeric glycoprotein. (Reprinted with permission from Köhler et al., 2015)

Thus, the interplay between the coagulation and complement pathways can provide a robust and effective response towards bacterial invasion. In addition, cross-talk can function to regulate the pathways.

Mechanisms of bacterial clearance by leukocytes

Leukocytes use a wide range of mechanisms to overcome bacterial invasion. When the physical barrier of the host is breached, cytokines and chemokines are released from the damaged endothelium, signaling leukocytes to the site of infection (Sethi and Chakraborty, 2011). Two key leukocytes of the innate immune response are the neutrophils and macrophages (Foster, 2005). The leukocytes that play a critical role in the adaptive response are the lymphocytes. Both arms of the immune response system, innate and adaptive, serve to eliminate the invading microorganisms (Thammavongsa et al., 2015).

At the site of infection, complement opsonins, deposited on the bacterial surface, bind to receptors on the leukocytes (Dunkelberger and Song, 2010). Binding and clustering of the receptors, initiates invagination of the leukocyte cell membrane, resulting in bacterial engulfment, called phagocytosis (Spaan et al., 2013). Phagocytosis is carried out by the rearrangement of the actin cytoskeleton by an ATP-dependent process (May and Machesky, 2001). Non-professional phagocytes such as epithelial cells can also engulf pathogens using a 'trigger' and 'zipper' mechanism (Swanson and Baer, 1995; Lim et al., 2017).

Upon being engulfed by neutrophils and macrophages, the pathogens are trapped within a vesicle, a phagosome (Fig 5; (Perobelli et al., 2015)). The phagosome can be fused to a lysosome, resulting in a phagolysosome, where they encounter granules and reactive oxygen species. Granules contain antimicrobial peptides and proteases (Thammavongsa et al., 2015). The azurophilic granules consist of antimicrobial proteins and peptides including, lysozymes,

defensins, neutrophil elastase, and cathepsin G (Spaan et al., 2013). Defensins interfere with cell wall generation and lysozymes target bacterial walls (Spaan et al., 2013). Some proteases are found within specific leukocytes (Pham, 2006). Neutrophils carry neutrophil gelatinase-associated lipocalin (NGAL) and neutrophil elastase (Pham, 2006). NGAL binds to bacterial siderophores and interferes with iron acquisition (Spaan et al., 2013). Neutrophil elastase degrades bacterial toxins and cell wall-anchored proteins (Pham, 2006). For example, neutrophil elastase can degrade outer membrane protein A of *Escherichia coli* (Belaaouaj et al., 2000). This results in loss of bacterial membrane integrity, leading to cell death. Bactericidal permeability-increasing protein (BPI) also produced by neutrophils targets the bacterial membrane for degradation (Schultz and Weiss, 2007). The secondary granules contain lactoferrin, hCAP18 and lysozyme (Spaan et al., 2013; Lacy, 2006). Lactoferrin binds and sequesters away iron. Tertiary granules consist of metalloproteases, such as gelatinase B (Spaan et al., 2013; Lacy, 2006).

The pathogen can be also degraded by reactive oxygen and nitrogen species by a process called oxidative burst (Spaan et al., 2013; Robinson, 2008). High levels of superoxides and reduced oxygen are generated, in the space between the wall of the phagosome and the engulfed pathogen, due to the formation of the NADPH-dependent oxidase on the membrane of the phagosome (Spaan et al., 2013; Uribe-Querol and Rosales, 2017). These reactive oxygen species can damage DNA, proteins and lipids (Spaan et al., 2013). ATPase translocates cytosolic protons into the phagosolysosome, lowering the pH (Uribe-Querol and Rosales, 2017; Spaan et al., 2013; Belaaouaj et al., 2000). The protons cause the reduction of superoxide to hydrogen peroxide (Spaan et al., 2013). The electron pump on the phagolysosome pumps electrons in due to the inflow of protons and cations (Spaan et al., 2013). Myeloperoxidase (MPO) catalyzes the reaction between hydrogen peroxide and chloride to generate hypochlorous acid that kills the

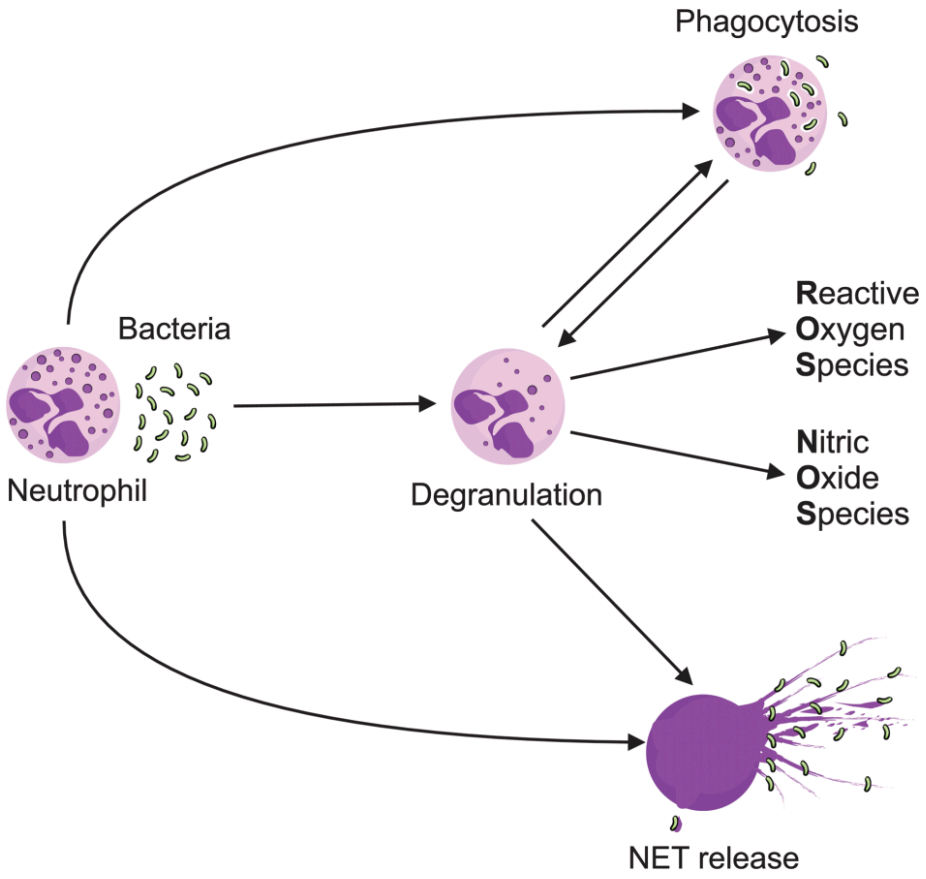

Figure 5. Neutrophils use different mechanisms for bacterial clearance. (Reprinted with permission from Perobelli et al., 2015)

pathogen (Spickett et al, 2000; Spaan et al., 2013). Release of cytokines by macrophages can recruit more leukocytes, amplifying bacterial clearance (Sethi and Chakraborty, 2011).

Upon lymphocyte activation via helper T-cells and antigen-presenting cells, cytotoxic T cells, as well as, natural killer (NK) cells can attack bacteria with the secretion of perforin and proteases, called granzymes (Alberts et al., 2002; Chen and Jensen, 2008; Walch et al., 2014; Jorgenson et al., 2017). Perforin works to form a pore on the bacterial surface, which perturbs the bacterial membrane integrity. Once the pore is formed, perforin can mediate delivery of granzymes into the bacterial cell (Chen et al., 2003). Granzymes are granules that secrete serine proteases that are similar to innate proteases, such as neutrophil elastase and cathepsin G (Walch et al., 2014). Cytotoxic T-cells and NK cells can also induce programmed cell death of infected cells, in which granzymes activate caspase-3 to trigger apoptosis (Chen et al., 2003; Jorgensen et al., 2017). In addition, since activation of these lymphocytes also causes proliferation, the attack responses are further amplified. The difference between the innate leukocytes and the adaptive cells is that the lymphocytes can develop into memory cells (Chen and Jensen, 2008). This proves as an advantage to the host, because a recurring infection can trigger a robust and rapid response from the lymphocytes (Chen and Jensen, 2008).

NETosis by neutrophils are considered to be the ‘the last resort’ for bacterial killing (Brinkmann and Zychlinsky, 2012). For entrapment and destruction of the pathogen, neutrophils sacrifice themselves by releasing neutrophil extracellular traps (NET). This formation is composed of decondensed chromatin that serves to capture bacteria and prevent dissemination (Sethi and Chakraborty, 2011; Lacy, 2006). Not only are bacteria trapped, but are also killed due to the bactericidal enzymes, such as neutrophil elastase and cathepsin G, that are embedded within the NET (Brinkmann and Zychlinsky, 2012; Lacy, 2006).

Due to being the first to encounter, as well as, responding immediately to bacterial invasion, the leukocytes of the innate immune response system, such as neutrophils and macrophages, have developed a wide array of ways to eliminate bacteria. The interplay, between leukocytes of the innate and adaptive immune response, work together to further amplify the response. Although the defense mechanism works in eliminating most bacteria, the method has not been as effective towards *Staphylococcus aureus* (Foster, 2005; Thammavongsa et al., 2015).

General characteristics of *S. aureus*

Staphylococcus aureus (*S. aureus*) from the family Staphylococcacae is a Gram-positive, facultative anaerobe that colonizes the inside of the gastrointestinal tract, nares and the skin (Thammavongsa et al., 2015; Thomer et al., 2016b; Ko and Flick, 2016). Approximately 30% of the population carries the microorganism in the anterior nares (Tong et al., 2015; Thammavongsa et al., 2015). *S. aureus* was first identified by Alexander Ogston, who isolated the microorganism from pus of abscesses (Ogston, 1881). Under the microscope, *S. aureus* appear as grape-like clusters and are non-motile. The distinguishing feature of the bacterium from another cocci-shaped bacterium, *Staphylococcus epidermidis,* is its golden-like pigment due to the expression of the carotenoid virulence factor, staphyloxanthin (Ogston, 1881). In addition, *S. aureus* colonies are large and spherical. The bacterium is a coagulase-positive and catalase-positive species (Foster, 1996).

S. aureus isolates are categorized in clonal groups by their sequence types (ST), which is done by Multi-Locus Sequence Typing (MLST) (Kovanen et al., 2014). MLST serves to distinguish closely related bacteria, which could be due to the exchange of genetic information via mobile genetic elements (Kovanen et al., 2014).

Virulence factors of *S. aureus*

Virulence factors are molecules that contribute to the pathogenicity of an organism, demonstrated in murine models (Table 2) (Foster, 2005; Thammavongsa et al., 2015; Thomer et al., 2016a; McAdow et al., 2011; Lim et al., 2012; Geraci et al., 2017). These molecules have been shown to interact and alter the pathways of the immune system in favor of bacterial survival and colonization (Foster, 2005; Thammavongsa et al., 2015; Ko and Flick, 2016). Staphyloxanthin, which produces the golden-like pigment appearance of *S. aureus* colonies, acts as an antioxidant towards reactive oxygen species from neutrophils (Zhang et al., 2018). The α- and β-hemolysins form pores in leukocytes, erythrocytes and platelets, causing the cells to lyse (Vandenesch et al., 2012).

S. aureus harbors many types of surface bound proteins, one being the MSCRAMMs (Foster et al., 2014). One of the groups of secreted proteins the bacterium expresses is the SERAMs (Crosby et al., 2016). Both the MSCRAMMs and SERAMs have been shown to contribute to the bacterium's ability to cause disease (Foster, 2005; Thammavongsa et al).

MSCRAMMs

Microbial Surface Components Recognizing Adhesive Matrix Molecules (MSCRAMMs) are covalently anchored surface-bound proteins, in which their N-terminal regions each harbor a signal sequence (Foster et al., 2014). Next to the signal sequence is the A domain which is composed of at least two tandemly linked IgG-like folded regions, that comprise of separately folded subdomains N_1, N_2, N_3 (Foster et al., 2014). At the C-terminus, is the cell wall spanning region and the sorting signal motif, LPXTG (X represents any amino acid) that serves to signal anchoring of the protein to the cell wall (Foster et al., 2014; Rivera et al., 2007).

The defining feature of the MSCRAMMs is not only its structure, but also the ligands they bind (Foster et al., 2014). The MSCRAMMs bind to the extracellular matrix proteins (ECM) of the host, such as collagen and fibronectin (Foster et al., 2014; Rivera et al., 2007). A common ECM protein that many of the MSCRAMMs bind to is Fg (Rivera et al., 2007; Ko and Flick, 2016). The Fg-binding MSCRAMMs include ClfA, ClfB, FnbpA, FnbB, Bbp, and SdrE. The A domain interacts with Fg by a dock-lock-latch mechanism (Foster et al., 2014; Rivera et al., 2007). ClfA and FnbpA bind Fg at the C-terminal γ-chain (Ko and Flick, 2016). In a murine septicemia model, mice, in which the binding motif for ClfA on the Fg γ-chain was deleted, showed an increase in survival when infected with *S. aureus* compared to wild type mice (Flick et al., 2013). This suggests that the Fg-binding activity of ClfA contributes to *S. aureus* pathogenicity.

SERAMs

The SERAMs (Secretable Expanded Repertoire Adhesive Molecules) are a group of small proteins that are secreted and adhere to molecules of the host (Foster and Hook, 1998; Harraghy et al., 2008). These secreted proteins include, Efb, Emp, Ecb, Eap, Coa, and vWbp (Rivera et al., 2007). Coa, vWbp and Efb harbor a predicted disordered segment within the protein (Fig 6; (Ko and Flick, 2016)). The flexibility of the disordered region allows the protein to occupy different conformations, resulting in the protein's ability to recognize and bind to multiple ligands (Thomer et al., 2013). One of the ligands that all three SERAMs bind to is Fg (Ko and Flick, 2016; Thomer et al., 2013).

Extracellular fibrinogen-binding protein

Extracellular fibrinogen-binding protein (Efb) is a 15.8 kDa virulence factor that is expressed in the post-exponential phase of *S. aureus* (Palma et al., 2001). The N-terminal region contains two Fg-binding domains, Efb-A and Efb-O, respectively, that are located in a predicted disordered region (Ko et al., 2016). The C-terminal half of the protein harbors the C3b-binding motif (Lee et al., 2004). Crystal structure of C-terminal Efb in complex with the C3b, demonstrated that the C-terminal half of Efb binds to C3d segment, in which residues R^{131} and N^{138} were critical for its function (Haspel et al., 2008). Efb contributes to *S. aureus* evasion of phagocytosis (Ko et al., 2013). The bacterial protein was shown to bind to both Fg and C3b, which impeded recognition of IgG by Fc receptors on neutrophils (Ko et al., 2013). Efb binding to C3b inhibited C3b binding to the complement receptor CR1 (Ko et al., 2013). Binding to Fg impeded Fg from binding to the integrin $\alpha_m\beta_2$ on neutrophils (Ko et al., 2011).

A secreted *S. aureus* protein that is homologous to the segment of Efb is Extracellular complement- binding protein (Ecb). Ecb lacks the two Fg-binding sequences of Efb. Both Efb and Ecb bind to C3b, in which Ecb shares a similar C3b-binding motif with the C-terminal region of Efb (Haspel et al., 2008; Amdahl et al., 2013). Similar to Efb, Ecb binds to C3d, which inhibits C3 convertase activity of the alternative pathway and the C5 convertases of the classical, lectin and alternative pathways (Jongerius et al., 2010). Thus, both secreted proteins binding to C3d contribute to *S. aureus* immune evasion (Amdahl et al., 2013).

Coagulase

Coagulase (Coa) coagulates plasma and blood (Tager, 1974). Its function is often used as a determining factor of whether a species is coagulase-positive or negative (Tager, 1974; Ko et

al., 2016). The *coa* gene is located between *geh*, a lipase gene and *spa*, which encodes for Protein A (Savini, 2018). Coa is expressed in the exponential phase, but its expression is downregulated by the *agr* system in the stationary phase (Savini, 2018).

The signature feature of Coa is its ability to non-proteolytically activate the zymogen, prothrombin (Thomer et al., 2016b). The protein structure and its interactions with prothrombin and Fg are characterized in some detail for Coa (Panizzi et al., 2006a, b; Ko et al., 2016). The 2.2-Å crystal structure of the N-terminal half of Coa in complex with prothrombin revealed that the N-terminal half of Coa is composed of a D_1D_2 domain in which each D unit forms a three-helix bundle (Panizzi et al., 2006a, b; Friedrich et al., 2003). The D_1D_2 domain binds directly to the inactive zymogen (Friedrich et al., 2003). Activation of prothrombin requires the insertion of the two N-terminal amino acid residues of Coa; Ile^1-Val^2, into the Ile^{16} pocket of prothrombin (Friedrich et al., 2003; Panizzi et al., 2006a, b; Kawabata et al., 1985). Subsequently, the complex undergoes a conformational change, resulting in an active Coa-prothrombin complex, staphylothrombin that is capable of cleaving Fg (Panizzi et al., 2006b).

The C-terminal region of Coa, which is predicted to be disordered, harbors a linker region and a tandem repeat domain (Ko and Flick, 2016). The major Fg-binding motif is located at the tandem repeat domain, in which a high affinity 27 amino acid long binding motif was identified (Ko et al., 2016). The Fg-binding region of Efb shares a common motif with that of the Fg-binding motif of Coa (Ko and Flick, 2016; Ko et al., 2016). The number of repeat units varies from 5-7 repeats amongst different *S. aureus* isolates (Ko et al., 2016). Deletion of the Fg-binding motif of Coa improved the survival of mice infected with *S. aureus* compared to wild mice, suggesting that the Fg-binding activity of Coa plays a role in pathogenicity (Thomer et al., 2016a).

von Willebrand factor-binding protein

von Willebrand factor-binding protein (vWbp) is the second coagulase of *S. aureus*. Bjerketorp and colleagues first identified the bacterial protein via phage display in which the DNA library of *S. aureus* Newman was screened against von Willebrand factor (Bjerketorp et al., 2002; Bjerketorp et al., 2004). The gene *vwb* is located between genes *clfa* and *emp*, the latter encodes for Extracellular matrix-binding protein (Harraghy et al., 2008; Geraci et al., 2017). Expression of *vwb* is regulated by a conserved octanucleotide sequence that is located within the promoter region of the gene (Harraghy et al., 2008). The protein has a theoretical molecular weight of 56 kDa that is 508 amino acid residues long, including the signal sequence (Bjerketorp et al., 2004). The protein is expressed during the early part of the exponential phase and decreases at the stationary phase (Bjerketorp et al., 2002).

High-resolution crystal structures of vWbp as an apo-protein or in complex with prothrombin are not available. However, structure prediction programs suggest that the N-terminal half of vWbp, which shares a 30% amino acid identity to that of the N-terminal region of Coa (Bjerketorp et al., 2004), forms a structure similar to that of the D_1D_2 domain of Coa (Kroh et al., 2009). Activation of prothrombin by vWbp is similar to the Coa mechanism in that the first two N-terminal residues, Val^1-Val^2 of vWbp, are required (Kroh et al., 2009). Thus, vWbp and Coa demonstrate multiple similarities in their coagulation induction function.

The two *S. aureus* coagulases may give the impression that the two proteins are indistinguishable. However, closer examination reveals significant differences. Although the C-terminal halves of Coa and vWbp are both predicted to be unordered (Friedrich et al., 2003; Kroh and Bock, 2012), there are substantial differences at the amino acid sequence level (Kroh and

Bock, 2012; Liesenborghs et al., 2018; McAdow et al., 2012b; Ko and Flick, 2016). The C-terminal part of Coa is comprised of a linker region and a tandemly repeated Fg-binding motif (Ko and Flick, 2016). This Fg-binding motif is not present in vWbp (McAdow et al., 2012b; Ko and Flick, 2016). Instead, the C-terminal region of vWbp harbors a unique von Willebrand factor-binding motif of 26 amino acid residues (Bjerketorp et al., 2002) that enables vWbp to bind to von Willebrand factor (vWF) and mediate *S. aureus* adherence to the vessel wall of activated endothelial cells (Claes et al., 2014; Claes et al., 2017; Claes et al., 2018). These differences demonstrate that the C-terminal halves of Coa and vWbp have distinct functions (Ko and Flick, 2016).

The coagulases also differ from each other in their affinities to prothrombin and Fg. Intact Coa appears to have a higher affinity for both prothrombin (5 nM) and Fg (33 nM) than that observed for vWbp (98 nM; 271 nM, respectively) (Cheng et al., 2010; Liesenborghs et al., 2018; McAdow et al., 2012b). Activation of prothrombin by Coa is independent of Fg, whereas, the N-terminal region of vWbp activates prothrombin by a "hysteretic conformational" mechanism (Kroh et al., 2009), where Fg is required for full activation. The C-terminal half of vWbp was suggested to contribute to prothrombin activation as well since full-length vWbp showed an increase in the rate of prothrombin activation (Kroh and Bock, 2012). These observations indicate that vWbp and Coa interact with Fg by different mechanisms.

Attempts to locate the Fg-binding activity of vWbp gave apparently contradicting results (McAdow et al., 2012a; Thomer et al., 2013). Using an ELISA-type binding assay, McAdow and colleagues showed that the immobilized C-terminal region of vWbp bound to soluble Fg, suggesting that the C-terminal half of vWbp harbors Fg-binding activity (McAdow et al., 2012a). However, affinity chromatography, in which vWbp was coupled to a Strep-Tactin column and

human plasma was passed over the column, revealed that the Fg-binding region was within the D_1D_2 domain and not at the C-terminal half (Thomer et al., 2013). Thus, the Fg interaction with vWbp remains unclear.

S. aureus an opportunistic pathogen

S. aureus is a commensal organism, however, the pathogen can enter into the tissues via an open wound site, triggering activation of the immune response system (Gordon and Lowy,

Table 2. Virulence factors

Virulence Factors	Ligands	Virulence Factors	Ligands
α, β-Hemolysin	Leukocytes, erythrocytes	**IsdA IsdB IsdC**	Heme
Adenosine synthase	Ado, dAdo synthesis	**Nuclease (Nuc)**	Nucleic acids of NETs
Aureolysin	C3	**Lipoprotein diacyl-glyceride transferase**	Lipoproteins
Bone sialo-binding protein (Bbp)	Fg, bone sialoprotien	**Protein A (SpA)**	Igs, vWF, platelets
Capsule	-	**Phenol soluble modulins α1, 2, 3, 4, β1**	FPR2
CHIPS	FPR1, C5aR	**Panton-Valentinleucocidin (PVL)**	C5aR
Clumping factor A (ClfA)	Fg, Factor I, platelets	**Staphylokinase (Sak)**	Plasminogen, Fn, C3, IgG
Clumping factor B (ClfB)	Fg, keratin 10, loricrin, platelets	**Staphylococcal inhibitor of IgG (Sbi)**	IgG Fcγ, C3, FH
Can	C1q, collagen	**SCIN**	C3bBb
Coagulase (Coa)	Prothrombin, Fg	**SCIN-B**	C3bBb
δ-toxin	-	**SCIN-C**	C3bBb

Table 2. Continued

Virulence Factors	Ligands	Virulence Factors	Ligands
Extracellular adherence-binding protein (Eap)	ICAM1, C4b, elastase,cathepsin G, proteinase 3	**HlgAB**	CXCR1, CXCR2, CCR2
EapH1	elastase, cathepsin G,proteinase 3	**Serine-aspartate-repeat- C, D (SdrC, SdrD)**	β-neurexin (SdrC) Desquamated epithelial cels
EapH2	elastase, cathepsin G,proteinase 3	**Serine-aspartate-repeat- E (SdrE)**	Fg, Factor I
Enterotoxin B	Vβ _TCR	**SSL3**	TLR2
Enterotoxin C	Vβ _TCR	**SSL5**	PSGL-1, GPCRs, GPIbα, GPVI
Enterotoxin like IX	PSGL-1	**SSL6**	PSGL-1
Extracellular complement-binding protein (Ecb)	C3d	**SSL7**	IgA, C5
Extracellular fibrinogen-binding protein (Efb)	C3d, αMβ2	**SSL10**	IgG, Fg, Fn, FIIa, FXa
Extracellular matrix-binding protein (Emp)	Fg, Fn, collagen	**SSL11**	PSGL-1
FLIPr	FPR2	**Staphyopain**	CXCR2
FLIPr-L	FPR1, FPR2	**Staphyloxanthin**	Superoxides, radicals, hydrogen peroxide
Fibronectin-binding protein-A (FnbpA)	Fg, Fn, elastin, platelets	**TSST1**	Vβ2 TCR, αMHC class II
Fibronectin-binding protein-B (FnbpB)	Fg, Fn, platelets, elastin	**von Willebrand factor-binding protein (vWbp)**	Fg. Prothrombin, FXIII, Fn

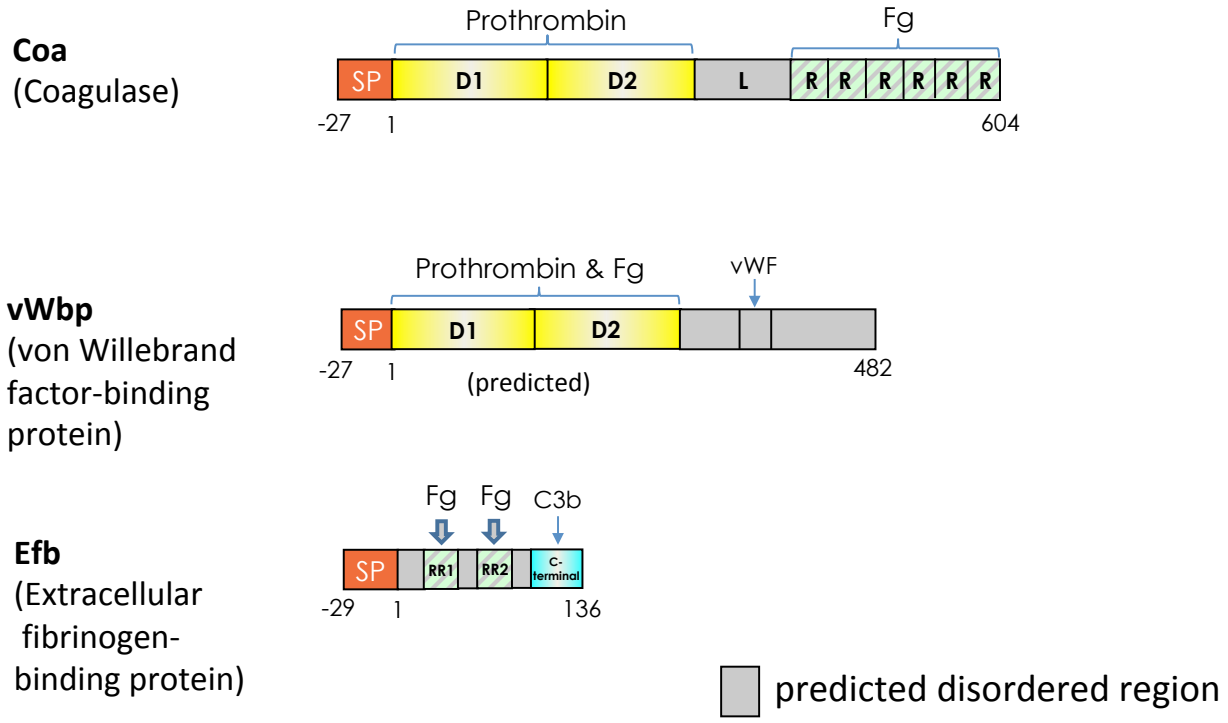

Figure 6. Coa, vWbp, and Efb are Fg-binding SERAMs of *S. aureus*. Cartoon of the domain organizations of Coa, vWbp, and Efb. SP, Signal peptide, orange; D_1D_2, prothrombin-binding and fibrinogen-binding domain. R, repeat domain, light green; L, linker region. vWF indicates vWF-binding motif. C3b indicates the C3b-binding motif. RR1, RR2, fibrinogen-binding motifs, light green. 2, 3 α-helix bundle, yellow; 3 α-helix, blue. D_1D_2, structure of vWbp, predicted. Gray represents the predicted unordered region.

2008). *S. aureus* is equipped with an arsenal of virulence factors that work to mask itself from immune response cells. Immune evasion allows *S. aureus* to cause a wide range of infections from endocarditis, septic arthritis, osteomyelitis to skin and soft tissue infections (Foster, 1996; Gordon and Lowy, 2008).

Certain types of MRSA can be responsible for different types of infection. Health-care associated MRSA predominately cause infections of surgical wounds (Gordon and Lowy, 2008). Skin and soft tissue infections including abscesses, furuncles, carbuncles and folliculitis are commonly caused by community-associated MRSA isolates that are observed in adults and children (Miller and Kaplan, 2009).

Abscesses are considered the hallmark of *S. aureus* infections (Ogston, 1881; Cheng et al., 2011). An abscess is a structure that contains live bacteria at the center of the lesion, in which phagocytes are incapable of clearing (Cheng et al., 2011). At the core of an abscess is the nidus, composed of the *S. aureus* bacterial community, which is encased by a layer of fibrin. Adjacent to this region is a layer of dead leukocytes, which separates the viable leukocytes from clearing the bacterial community (Thomer et al., 2016b). At the periphery of the abscess is another layer of Fg/fibrin. Once the abscess ruptures, *S. aureus* can enter into the bloodstream or tissues and spread to distant organs, where it will generate multiple abscesses in the tissues and propagate its expansion (Cheng et al., 2011; Thomer et al., 2016b).

Mobile genetic elements

Bacteria are able to acquire genes encoding for bacterial defense mechanisms and virulence factors via mobile genetic elements (MGE) (Malachowa and Deleo, 2010). MGE are segments of DNA that can be transferred within or between genomes in eukaryotes and prokaryotes (Fig 7; (Malachowa and Deleo, 2010; Frost et al., 2005)). Bacteria are able to uptake

genetic information by three ways, transduction, transformation or conjugation (Malachowa and Deleo, 2010). Transduction involves the transfer of genetic information via bacteriophages and conjugation involves cell contact (Sun, 2018). Transformation is the uptake of free DNA material by bacteria. Transfer of genetic material between cells is called horizontal gene transfer (HGT) or from parent to progeny is vertical gene transfer (Frost et al., 2005; Malachowa and Deleo, 2010). MGEs that can be horizontally transferred include plasmids, transposons, bacteriophages, insertion sequences, pathogenicity islands and chromosome cassettes (Malachowa and Deleo, 2010). Some of the MGEs of *S. aureus* are pathogenicity islands, chromosome cassettes and three genomic islands, νSaα, νSaβ and νSaγ (Malachowa and Deleo, 2010; Hanssen and Ericson Sollid, 2006).

The νSaγ island contains a variety of genes that encode for toxins and other virulence factors (Aswani et al., 2019). Present on the island is a cluster of *ssl* genes that encode for enterotoxins called Staphylococcal superantigen-like proteins, as well as, β-type phenol soluble modulin genes (Malachowa and Deleo, 2010; Smyth et al., 2007). In addition, the island consists of an immune evasion cluster (IEC-2) that comprises of the genes that encode for Ecb, Efb and α- hemolysin (Jongerius et al., 2007). Another gene present towards the 3' end of the island is the household gene *argF*, encoding for ornithine carbamoyltransferase subunit F (Malachowa and Deleo, 2010; Jongerius et al., 2007). The gene that flanks the 3' end of vSaγ encodes for acetyltransferase, which is part of the GCN5-related *N*-acetyltransferases (GNAT) family (Favrot et al., 2016).

The genes encoding for the two coagulases are also found on pathogenicity islands (Foster and Geoghegan, 2015; Tulinski et al., 2014). Both Coa and vWbp are unable to coagulate equine, bovine, nor ovine plasma. However, *S. aureus* strains isolated from infected livestock

were shown that the genes encoding for Coa and vWbp are present on the pathogenicity islands that include SaPIbov4, SaPIbov5, SaPLeq1 and SaPIov2 (Viana et al., 2010). Strains isolated from ruminants carried two genes of vWbp, a chromosomal *vwb* and a *vwb* variant on the pathogenicity island, such as SaPIbov2 (Viana et al., 2010). vWbp encoded from SaPI, could clot ruminant plasma. However, this was not the case for the chromosomal encoded vWbp, which failed to clot ruminant plasma (Viana et al., 2010). In addition, regulation of the *vwb* variant expression was suggested to be different compared to how chromosomal *vwb* is regulated, since the promoter region of variant *vwb* lacked the conserved octanucleotide sequence (COS), but COS was present for chromosomal *vwb* (Viana et al., 2010; Harraghy et al., 2008).

Thus, *S. aureus* strains acquiring genes from MGE gives the pathogen the ability to ward off immune response cell attacks by expressing various proteins that can target different parts of the immune response system. In addition, this can also allow the microorganism to adapt and survive within different hosts.

Mechanisms of immune evasion

S. aureus expresses a wide range of proteins that alter and inhibit the activation of the complement system and manipulate the coagulation and fibrinolytic pathways, allowing the bacterium to evade the innate immune response and survive within the host (Foster, 2005; Thammavongsa et al., 2015).

Staphylococcal complement inhibition

Given the critical and central role of C3 in complement activation, it is not surprising that many *S. aureus* proteins, both secreted and cell wall-anchored, target this complement component (Fig 8; (Foster, 2005; Thammavongsa et al., 2015)). Inhibiting C3 convertase formation appears to be a common target in all three pathways (Thammavongsa et al., 2015).

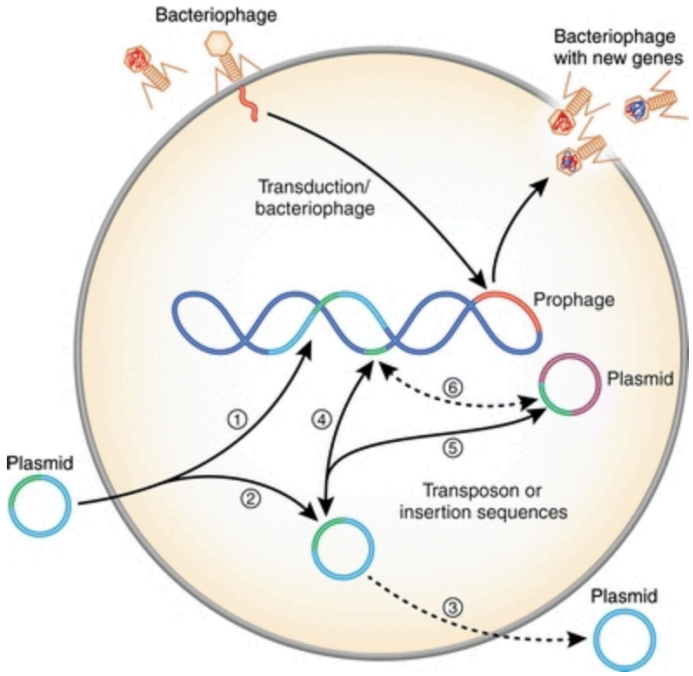

Figure 7. DNA can be transferred via mobile genetic elements. (Reprinted with permission from Malachowa and Deleo, 2010)

Physiologically, in the alternative pathway, Factor H serves as a cofactor for the serine protease regulator, factor I, to prevent MAC formation on host cells (Dunkelberger and Song, 2010). Aureolysin (Aur), a secreted *S. aureus* zinc-dependent metalloprotease, cleaves C3 to C3a and C3b and recruits factor H and factor I to degrade C3b to iC3b, which is inactive in forming C3 convertase (Laarman et al., 2011; Thammavongsa et al., 2015). This reduces C3b deposition on the bacterial surface. Cell wall-anchored proteins, SdrE and ClfA are shown to inhibit phagocytosis by blocking C3b deposition on the bacterial surface (Foster et al., 2014). SdrE binds to factor H and enhances factor I cleavage of C3b. ClfA can bind to factor I directly and promote degradation of C3b (Thomer et al., 2016b). Degradation of C3b hampers the ability to form the C3bBb complex. Staphylococcal complement inhibitor (SCIN) inhibits C3 convertase (C3bBb), which blocks C3 from being cleaved to C3b and C3a (Thammavongsa et al., 2015). Its homologues, SCIN-B and SCIN-C also block C3 convertase formation. Efb and Ecb can bind to C3d (Haspel et al., 2008; Amdahl et al., 2013). C3d is a cleavage product of C3b that activates both the innate and adaptive immune response via binding to complement receptor 2 (CR2) on B-cells, macrophages and neutrophils (Thammavongsa et al., 2015). Efb and Ecb binding to C3d inhibit formation and activation of C3b containing convertases, as well as, recruitment and activation of innate and adaptive immune response players (Jongerius et al., 2010; Amdahl et al., 2013). Ecb can also recruit factor H to bind to C3b, to inhibit alternative pathway activity (Amdahl et al., 2013). Staphylococcal inhibitor of IgG (Sbi) forms a tripartite complex with C3d and factor H, inhibiting C3 convertase formation (Haupt et al., 2008). Extracellular adherence protein (Eap) binds to C4b, prohibiting C2 from binding and forming the C3 proconvertase (Thammavongsa et al., 2015). Therefore, *S. aureus* has developed the ability to inhibit formation

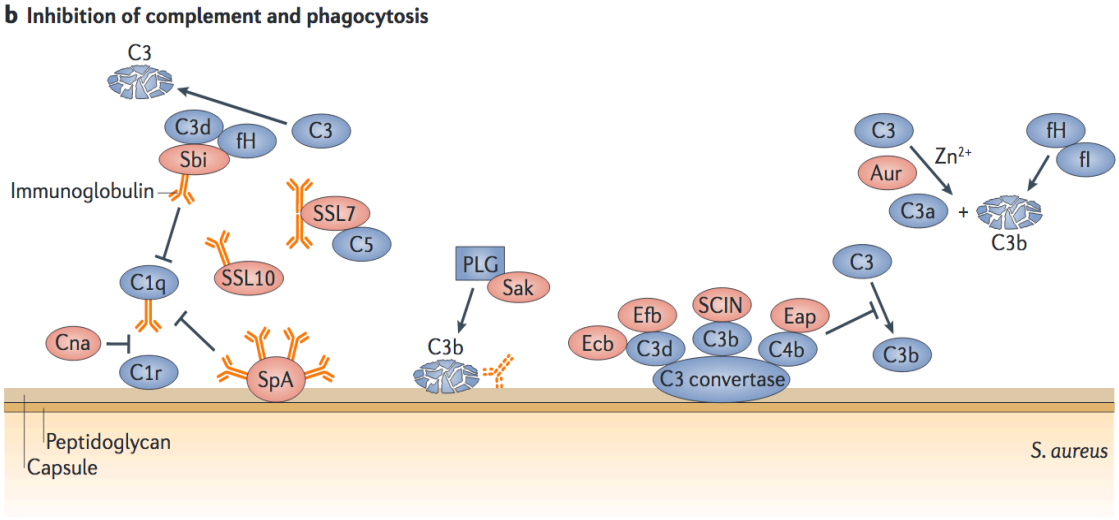

Figure 8. *S. aureus* expresses a wide range of proteins that target the complement system.

(Reprinted with permission from Thammavongsa et al., 2015)

of the C3 and C5 convertases, and block C3b deposition in all three pathways, especially the alternative pathway.

Besides targeting C3, *S. aureus* targets other complement components. Another common theme is the inhibition of the classical pathway. Collagen adhesin (Cna) interferes with the interaction between C1q and C1r/ C1s (Kang et al., 2013). As a result, C1r/C1s is displaced from C1q $(C1r:C1s)_2$, inactivating the C1 complex. The staphylococcal proteins, protein A (Spa), Sbi and staphylococcal superantigen-like 10 (SSL10) bind to the Fcγ region of IgG that plays a role in antibody opsonization (Laarman et al., 2011; Thammavongsa et al., 2015). These staphylococcal proteins then sequester away these immunoglobins from binding to C1q, inhibiting classical pathway activation. Staphylokinase (Sak) can activate plasminogen to plasmin (Peetermans et al., 2014; Thammavongsa et al., 2015). Sak forms a 1:1 complex with plasminogen (Bhattacharya et al., 2012). Within the complex, the peptide bond between K^{10}- K^{11} is cleaved, which converts Sak-plasminogen to an active Sak-plasmin complex (Bhattacharya et al., 2012). This complex can then degrade C3b bound to immunoglobulin, inhibiting immunoglobulin opsonization, and; thus, blocking classical pathway activity.

S. aureus is also able to use other mechanisms of inhibiting the complement system. For example, the exterior and the composition of the cell wall provide *S. aureus* with protection against the complement system (Foster, 2005; Thammavongsa et al., 2015). Despite the presence of opsonins, the bacterial capsule prevents phagocytosis by neutrophils and macrophages (Foster, 2005). The thick peptidoglycan layer makes it difficult for the membrane attack complex (MAC) to lyse the cell (Thammavongsa et al., 2015). Staphylococcal superantigen-like 7 (SSL7) can bind to C5 and the Fc receptor of IgA (Lorenz et al., 2013). This interaction prohibits generation of C5b and C5a, as well as, interferes with IgA from binding to FcrRI, which are expressed on

neutrophils and macrophages (Lorenz et al., 2013). Thus, this interaction interferes with leukocyte recruitment. In addition, the chemotaxis inhibitory protein of *S. aureus* (CHIPS) can bind to the complement C5a receptor (C5aR), blocking C5a from recruiting phagocytes (Foster, 2005; Thammavongsa et al., 2015).

Although the complement system is able to target and eliminate most bacteria, *S. aureus* is able to express a number of proteins that serve a wide variety of functions to inhibit cell lysis by MAC formation and impede leukocyte recruitment, allowing the bacterium to survive within the host.

Manipulation of the coagulation and fibrinolytic system

S. aureus uses its proteins to also manipulate the coagulation system with its capability to clot murine and human blood (Cheng et al., 2010). In the physiological condition, prothrombin is activated to thrombin by being cleaved by the prothrombinase complex (Liesenborghs et al., 2018). However, *S. aureus* secretes two proteins, Coa and vWbp, that can non-proteolytically activate prothrombin (Fig 9; (McAdow et al., 2012b; Liesenborghs et al., 2018)). Activation of prothrombin by either coagulases, occurs when the zymogen in complex with the bacterial protein is conformationally changed to its active state, termed as staphylothrombin, that can cleave Fg to eventually generate fibrin clots (Cheng et al., 2010). In contrast to thrombin, staphylothrombin is unable to interact and cleave other thrombin substrates, such as factors V and VIII (Panizzi et al., 2006b). Another inhibitor of prothrombin and fXa is SSL10, which binds weakly to the γ-carboxyglutamic acid domain of the two coagulation factors (Thammavongsa et al., 2015; Itoh et al., 2013).

S. aureus also uses the mechanism, agglutination, to hide bacteria from being targeted by neutrophils and other leukocytes (Fig 9; (Thammavongsa et al., 2015; McAdow et al., 2011)).

The mechanism involves ClfA, FnbpA, prothrombin and Fg (Thammavongsa et al., 2015). Agglutination is not to be considered the same as "clumping", which is also carried out by ClfA (Crosby et al., 2016).

The fibrinolytic system is also altered by *S. aureus* virulence factor, Sak (Thammavongsa et al., 2015). Sak forms a complex with plasminogen, becoming active plasmin (Thammavongsa et al., 2015). Thereby, Sak can sequester away plasminogen. Sak expression has been shown to be proportional to bacterial density in that as the bacterial density increases, the Sak expression increases (Peetermans et al., 2015). Thereby, the Sak-plasmin complex can play a role in breaking down the Fg/fibrin barriers, releasing *S. aureus* from an abscess to then disseminate into other tissues and amplify itself (Thammavongsa et al., 2015).

The Fg shield

One of the common ligands for many of the MSCRAMMs and SERAMs is Fg (Ko and Flick, 2016). The Fg-binding activity of many of the MSCRAMMs and SERAMs has been shown to contribute to the pathogenicity of the bacterium (Flick et al., 2004; Flick et al., 2013; Cheng et al., 2010; Ko et al., 2016; Thomer et al., 2016a). One of the immune evasion mechanisms of *S. aureus* is the generation of the Fg/fibrin shield (Ko et al., 2013; Guggenberger et al., 2012; Thomer et al., 2016b). The Fg shield is a two-layered structure composed of Fg and fibrin. *S. aureus* is found at the center of the structure. Due to the abundance of Fg that is recruited at the site of injury, it is of no surprise that *S. aureus* expresses at least a dozen proteins that bind to Fg (Foster and Hook, 1998; Harraghy et al., 2008). These two groups, the Fg-binding MSCRAMMs and SERAMs are likely to work in concert to assemble the Fg/fibrin shield (Ko et al., 2013; Guggenberger et al., 2012; Thomer et al., 2016a).

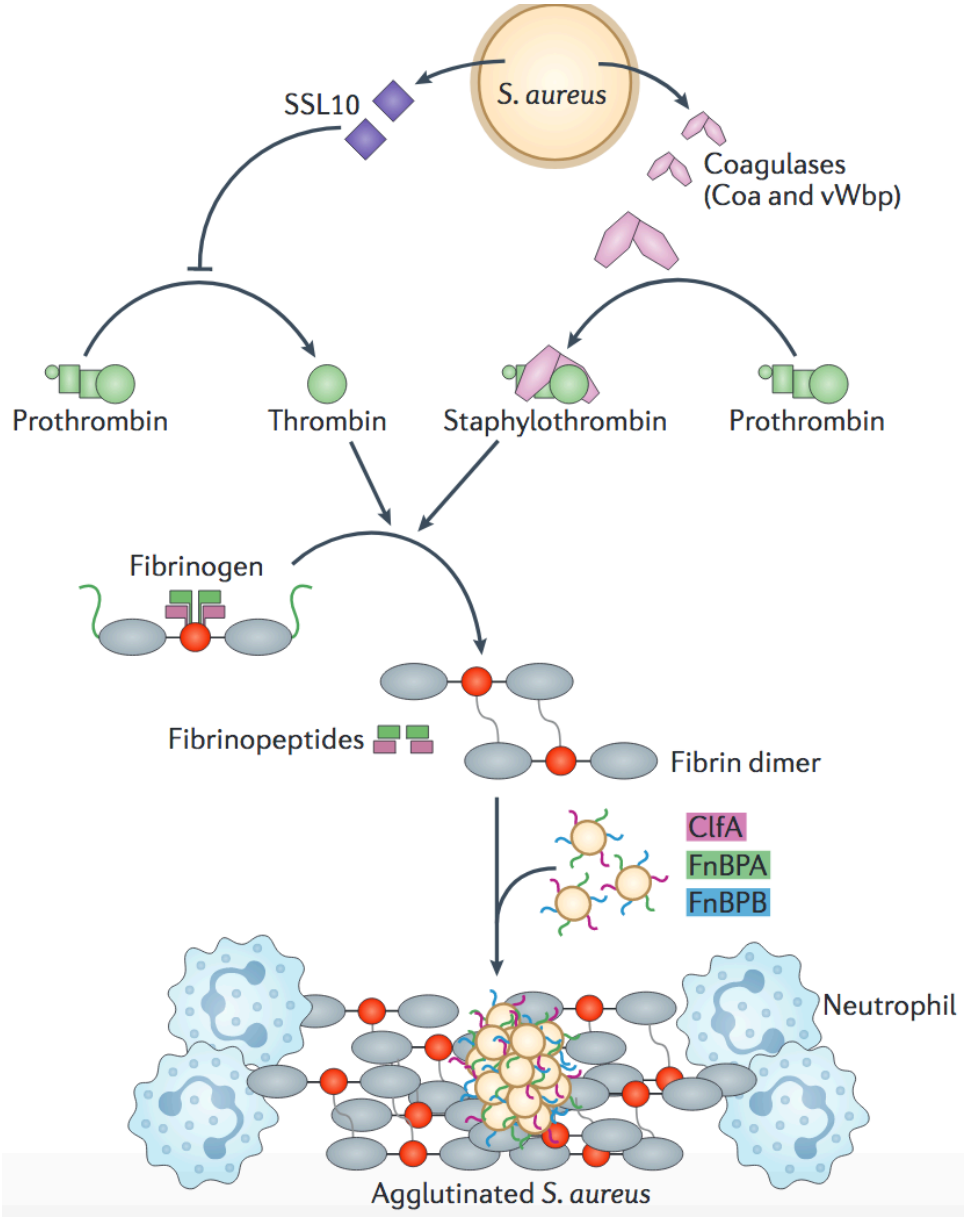

Figure 9. Manipulation of the coagulation cascade allows *S. aureus* to evade immune response cells. (Reprinted with permission from Thammavongsa et al., 2015)

MSCRAMMs role in Fg shield

ClfA, ClfB, FnbpA, FnbpB, SdrE, and Bbp, are all cell wall anchored proteins that bind Fg. Bound Fg coats the bacterial surface and protects the bacterium from immune detection (Crosby et al., 2016, Ko and Flick, 2016). Thereby, binding to Fg, allows each individual cocci an initial layer of protection (Ko and Flick, 2016).

Two MSCRAMMs that play a role in causing bacterial clumping are ClfA and ClfB. ClfA has been shown to play a major role in clumping (Crosby et al., 2016). The bacterial protein can bind to soluble Fg by binding to the 27 residues of the C-terminal of the Fg-γ chain (Crosby et al., 2016; McDevitt et al., 1997). Bound Fg acts a bridge to nearby *S. aureus* cells, resulting in the cells to clump together. Clumping protects *S. aureus* cells from being phagocytized (Crosby et al., 2016). In addition, the immune response cells were not able to penetrate through the clumped cells. Clumping has been suggested to play a role in Fg/fibrin shield assembly (Crosby et al., 2016). At the center of the shield, is a nidus of *S. aureus* microcolonies (Cheng et al., 2010). Clumping may serve as part of the initial stages of Fg/fibrin shield formation in forming the nidus (Crosby et al., 2016).

Another mechanism that may also play a role in shield formation is agglutination (McAdow et al., 2012b; Crosby et al., 2016). Coa and vWbp activate prothrombin to generate staphylothrombin (McAdow et al., 2012b). Staphylothrombin that is in complex with either Coa or vWbp is suggested to be capable of cleaving Fg to generate fibrin monomers (McAdow et al., 2011; McAdow et al., 2012b). Fibrin monomers laterally aggregate to become fibrin cables (Crosby et al, 2016). ClfA can then bind to the fibrin cables, tethering *S. aureus* to the polymerized fibrin (Crosby et al, 2016; McAdow et al., 2011). The pathogen can then be hidden

within the polymerized fibrin cables from phagocytes and other immune response cells (Crosby et al, 2016).

SERAMs role in Fg shield

A study by Ko and colleagues showed that *S. aureus* pre-opsonized with serum and supplemented with Fg, in the presence of Efb, forms a thick layer of Fg that covers the bacterial surface (Fig 10; (Ko et al., 2013)). Efb can bind simultaneously to Fg and C3b in that the N-terminal region of Efb binds Fg and at its C-terminal half interacts with C3d region of C3. The Fg layer was shown to block antibody recognition of the Fc region of IgG and impede the recognition and binding of C3b to complement receptor-1 (CR1) (Ko et al., 2013). Recognition of these targets is critical for phagocytosis. Using an *in vivo* murine peritonitis model, neutrophils were not able to uptake fluorescently labeled *S. aureus* in the presence of Efb, further supporting that that the shield blocks phagocytosis of the pathogen (Ko et al., 2013).

One form of the Fg/fibrin shield is manifested in murine abscess models (Cheng et al., 2009). *S. aureus* microcolonies, found at the nidus of an abscess, are surrounded by a pseudocapsule (McAdow et al., 2011; Cheng et al., 2009), a layer of Fg/fibrin that also contains Coa and prothrombin as revealed by antibody staining (Cheng et al., 2010). The periphery of the pseudocapsule is composed of another layer of Fg/fibrin that exhibits a pronounced staining of vWbp. This suggested that vWbp predominantly co-localizes with Fg, as well as prothrombin, at this second Fg/fibrin layer. The two distinct layers of Fg/fibrin structure observed in the murine abscess model is re-established in the 3D-Collagen-Fg system, in which *S. aureus* microcolonies assemble two concentric Fg/fibrin barriers (Guggenberger et al., 2012).

Guggenberger and colleagues showed in a 3D-Collagen-Fg gel model that the two coagulases assemble two distinct concentric Fg/fibrin structures that surround and protect *S.*

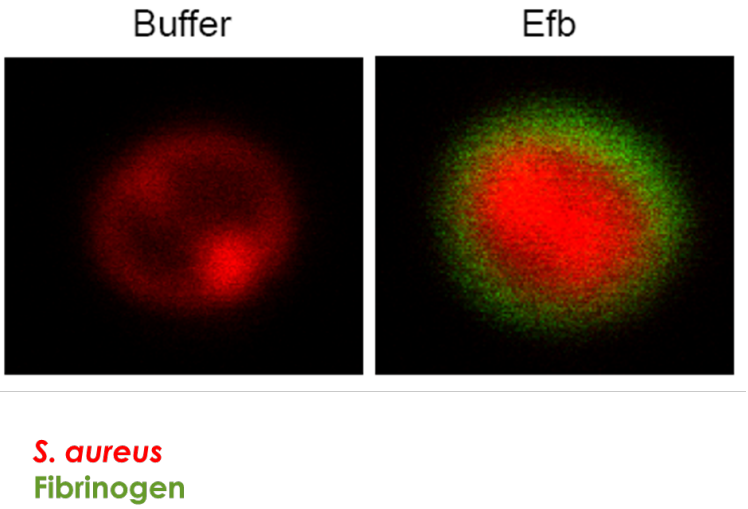

Figure 10. *S. aureus* uses Efb to form the Fg shield. (Reprinted with permission from Ko et al., 2013)

aureus microcolonies from being phagocytized by neutrophils (Fig 11; (Guggenberger et al., 2012)). By analyzing coagulase mutants, they demonstrated that Coa contributes to the formation and integrity of the pseudocapsule, the layer of Fg/fibrin that encapsulates the bacterial microcolony; whereas, vWbp contributes to the microcolony associated meshwork, an outside layer of Fg that surrounds the pseudocapsule structure (Guggenberger et al., 2012). vWbp was identified as playing a predominant role in creating the meshwork. These observations suggest that vWbp and Coa contribute differently in Fg shield assembly.

Medical problem

Antibiotics, such as penicillin, that serve to eliminate bacterial infections have contributed to bacteria rapidly developing resistance mechanisms towards antibacterial drugs (Fletcher, 2015; Lobanovska and Pilla, 2017). However, this is not a new concept, evolution has shown that environmental pressures will cause an organism to develop an alternative mechanism for survival (Fletcher, 2015). *S. aureus* development of resistance to pencillin led to the introduction of the semisynthetic compound, methicillin, for treatment (Stapleton and Taylor, 2002; Lobanovska and Pilla, 2017). Eventually the bacterium became resistance towards the drug. Methicillin-resistant *S. aureus* (MRSA) was soon labeled as a multi-drug resistant microorganism (Stapleton and Taylor, 2002). In 2017, the World Health Organization listed *S. aureus,* methicillin-resistant, vancomycin-intermediate and resistant strains as organisms for which novel strategies are desperately needed (Tacconelli and Magrini, 2017). Antibiotics currently used for treatment of skin and soft tissue infections are clindamycin, tetracycline, linezolid and rifampin that are used in combination with other antimicrobial agents (Lambert, 2011).

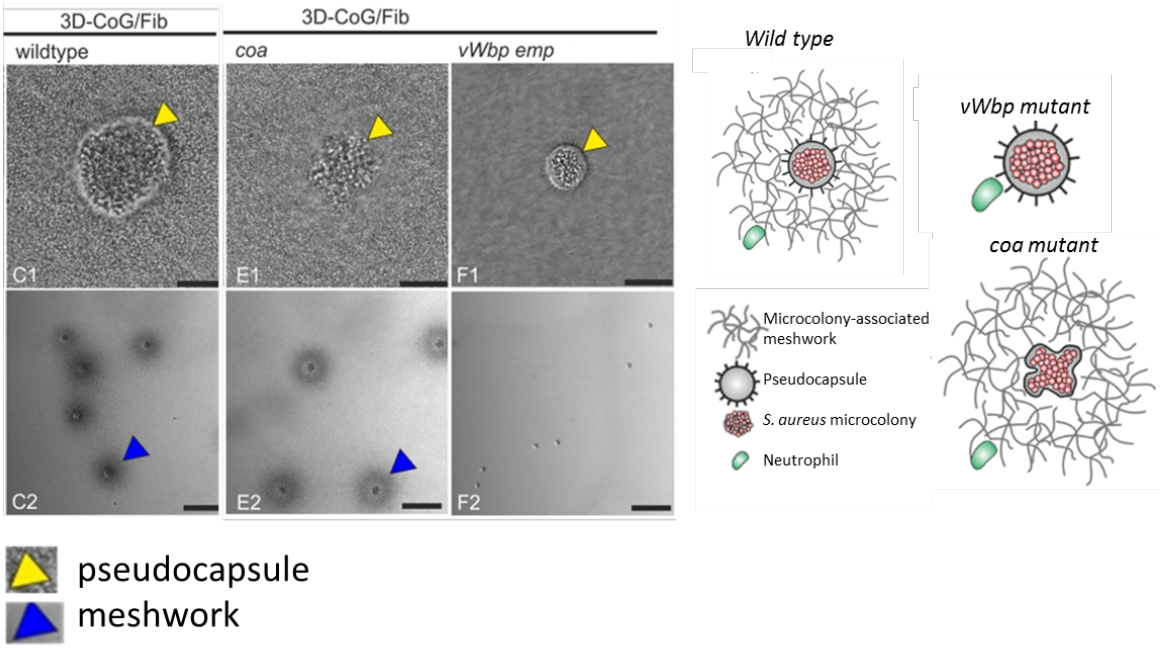

Figure 11. Coa and vWbp contribute to form the Fg shield in a 3-D-Collagen-Fg gel model.

(Reprinted and modified with permission from Guggenberger et al., 2012)

Targeting critical staphylococcal virulence factors in the design of new therapeutics represents a strategy currently being explored by investigators in the field (Fig 12; (Mohamed et al., 2017; Redi et al., 2018). Passive and active immunization attempts have been proven successful in animal models and phase I clinical trials, but many have failed at phase II and III clinical trials. Due to the broad range of types of infections, some of the vaccine candidates demonstrated failed protective effects toward different staphylococcal infections (Fowler and Proctor, 2014). Most of the vaccine designs aim at targeting surface antigens (Fowler and Proctor, 2014). Unfortunately, *S. aureus* expresses many virulence factors that show redundant function (Ko and Flick, 2016; Liesenborghs et al., 2018). Currently, the vaccine approach is to target multiple antigens, which have shown to be successful in phase I clinical trials. So far, NDV-3A has entered into phase II and is presently ongoing (Mohamed et al., 2017; Alqarihi et al., 2019). The lack of effective vaccines and treatment options make infections caused by antibiotic resistant *S. aureus* a worldwide health concern (Fowler and Proctor, 2014).

Investigational vaccines	Developer	Target antigen(s)	Composition	Development phase
SA4Ag[123–126]	Pfizer (Pearl River, New York, USA)	CP5, CP8, ClfA, MntC	CP5 and CP8 conjugated to CRM197; mutated recombinant ClfA (*rm*ClfA), MntC Adjuvant: none	Phase I/IIa, completed Phase IIb ongoing
Four-component *S. aureus* vaccine[127]	GSK (Rixensart, Belgium)	CP5, CP8, AT, ClfA	CP5 and CP8 conjugated to tetanus toxoid, with mutant forms of AT and ClfA Adjuvant: with or without adjuvant $AS03_B$	Phase I, completed
NDV-3A (formerly NDV-3)[128]	NovaDigm Therapeutics (Grand Forks, North Dakota, USA)	A single candidal surface glycoprotein antigen (Als3p), which is predicted to have three-dimensional structural similarity to ClfA	Recombinant version of N-terminal region (416 amino acids) of Als3p with the addition of a six-His tag and linker sequences Adjuvant: aluminium hydroxide	Phase I/Ib, completed
4C-Staph[129,130]	GSK (Novartis) (Siena, Italy)	Five *S. aureus* antigens, two surface-exposed antigens, FhuD2 and Csa1A, and EsxAB, a protein fusion of two secreted proteins, EsxA and EsxB	Genetically detoxified derivative of the secreted AT, FhuD2 and Csa1A, EsxAB Adjuvant: aluminium hydroxide	Phase I, completed
STEBVax[131]	IBT/NIAID (Rockville, Maryland, USA)	SEB	Recombinant rSEB with three point mutations that render SEB non-toxic	Phase I, completed
S. aureus toxoids[132,133]	Nabi Biopharmaceuticals (Rockville, Maryland, USA)	AT, PVL	Recombinant AT, recombinant subunit of PVL (rLukS-PV) Adjuvant: aluminium hydroxide	Phase I/II, completed
Bioconjugate vaccine[134]	GSK (GlycoVaxyn) (Schlieren, Switzerland)	CP5, CP8, AT	CP5-Epa, CP8-Epa and CP5-AT Bioconjugate vaccines prepared using glycoengineering technology	Preclinical

Figure 12. Various clinical trials are tested for the prevention of *S. aureus* infections.

(Reprinted with permission from Mohamed et al., 2017)

CHAPTER II

MATERIALS AND METHODS[1]

Bacterial plasmids, strains, culture conditions

Escherichia coli strain TG1(Zymo Research) was used as the host for plasmid cloning. *E. coli* strains containing pLysS i.e. BL21 (DE3) (GE Healthcare) or *E. coli* BL21 (DE3)-derivative, with the deletions of the *endA* and *recA* genes (Acella^{TM}, Edge Bio), were used for the production of the His_6-tagged and glutathione-S-tranferase (GST)-tagged fusion proteins, respectively. Chromosomal DNA from *S. aureus* strain Newman was used to amplify *vwb* and *coa* genes. *E. coli* strain TG1 was grown on LB medium supplemented with ampicillin (100 μg/ml). *E. coli* BL21 (DE3)pLysS and Acella strains were grown on Terrific Broth medium (Invitrogen) supplemented with ampicillin (100 μg/ml) and chloramphenicol (35 μg/ml).

Cloning of vWbp and Coa constructs

Genomic DNA isolated from *S. aureus* strain Newman was used as the template for all PCR experiments with oligonucleotide primers described in the supplementary figure (A-6), restriction enzyme cleavage sites are underlined. For His-vWbp and Coa, PCR products were digested with BamHI and PstI (New England BioLabs) and then ligated into pRSET-A vector (Invitrogen). For GST-vWbp, PCR products were digested with BamHl and EcoRI and ligated into pGEX-5x-1 (GE Healthcare). The ligation mixture for vWbp was transformed in *E. coli* strain TG1 cells (Zymo Research).

[1] Part of this chapter is reprinted with permission from "The Complex Fibrinogen Interactions of the Staphylococcus aureus Coagulases" by Thomas, S., Liu, W., Arora, S., Vannakambodi, G., Ko, Y-P., and Höök, M. 2019. Front. Cell. Infect. Microbiol. 9:106. Copyright © 2019 Thomas, Liu, Arora, Ganesh, Ko and Höök.

Cloning of GST-Coa was described previously (Ko et al., 2016). These were grown on LB agar plates containing 100 μg/ml ampicillin to select for transformants. Insertions were confirmed by DNA sequencing.

Expression and purification of recombinant proteins

E. coli strains containing plasmids pRSET-A-vWbp/Coa or pGEX-5x-1-vWbp/Coa were grown overnight at 37°C in Terrific Broth medium containing 100 μg/ml ampicillin and 35 μg/ml chloramphenicol. The overnight cultures were then diluted 1:50 into fresh Terrific Broth medium, and grown to an OD_{600} of 0.8-1. Recombinant expression was then induced with 0.2 mM isopropyl β-D-1-thiogalactopyranoside (Gold Biotechnology, Inc.) for 3 h at 37°C. Bacteria were then harvested, centrifuged and lysed using the French press (SLM Aminco). Soluble recombinant proteins were purified by nickel chelate chromatography (GE Healthcare) and anion exchange chromatography (GE Healthcare) or through a glutathione -Sepharose 4B column (GE Healthcare) according to the manufacturer's manual.

Gel permeation chromatography

The peak fractions of each recombinant protein from either affinity or ion exchange chromatography were pooled, concentrated and then further purified by gel permeation chromatography, using a HiLoad 16/600 Superdex 200 pg column (GE Healthcare) equilibrated in 1.2x Phosphate Buffered Saline (PBS; Gibco, pH 7.4). The recombinant proteins were then stored at -20°C. Protein concentration was determined by the Bradford assay (Pierce). Protein size and purity were analyzed on SDS-PAGE gels and stained with Coomassie Blue R-250 (Sigma Aldrich).

Fibrinogen (Fg)

Human fibrinogen (Catalog # FIB3, Enzyme Research Laboratories) was used in all experiments.

Circular dichroism spectroscopy (CD)

CD spectra were measured in far UV (185 nm- 260 nm) to measure secondary structure composition. The instrument used was Jasco J720 spectropolarimeter that was calibrated with d-10-camphorsulfonic acid, with a band pass of 1 nm and integrated for 1 s at 0.2-nm intervals. His-vWbp or -Coa was measured at a concentration of 0.6-0.3 mg/ml in PBS, pH 7.4. Spectra were recorded at an ambient temperature in cylindrical 0.5 mm path length cuvettes. Ten scans were averaged for each spectrum and the contribution from the buffer was subtracted. Deconvolution software programs, BeStSel and CAPITO, were used to quantify the secondary structures (Micsonai et al., 2018; Wiedemann et al., 2013).

ELISA type binding assay

96-well immulon 4HBX (Thermo Fisher Scientific) microtiter plates were used. Wells were coated with 100 µl of 5 µg/ml of either Fg (diluted in phosphate-buffered saline [PBS]; Gibco, pH 7.4) or GST-vWbp or -Coa ot His-vWbp-$C_{(386-482)}$ (diluted in PBS), for overnight at 4°C. Plates were blocked with 3% BSA in TBS (25 mM Tris, pH 7.4, 3 mM KCl, and 140 mM NaCl). For immobilized Fg binding, diluted recombinant vWbp or Coa proteins (in 1% BSA, 0.05% Tween 20, TBS) were added to the Fg- coated wells and incubated for 1 h at room temperature. Bound vWbp or Coa proteins were detected using Horseradish Peroxidase (HRP)- conjugated anti-GST polyclonal antibodies (6,000X dilution) (Abcam). For soluble Fg binding, diluted Fg (in 1% BSA, 0.05% Tween 20, TBS) was added to vWbp- or Coa- coated wells. Bound Fg was detected using HRP-conjugated Human Fg polyclonal antibodies (1,000X dilution) (Rockland Immunochemicals, Inc.). Binding was quantified by the addition of substrate o-

phenylenediamine dihydrochloride (Sigma-Aldrich) and the absorbance was measured at 450 nm using the ELISA microtiter plate reader (ThermoMax). Raw data was fitted using the one-site binding equation, apparent K_D values and goodness of fit (R^2) were obtained from GraphPad Prism software version 4.0. Apparent K_D values represent averages of three independent experiments.

ELISA-based competition assay

96-well immunlon 4HBX microtiter plate was coated with full-length Fg (5 μg/ml) or vWbp-$C_{(386-482)}$ (10 ug/ml). Various concentrations of the GST-vWbp or -Coa were mixed with a fixed concentration of His- vWbp (200 nM) or -Coa (1 nM); Peptide Coa-RI or Efb-O (Shanghai Hanhong Scientific Co., Ltd.) (Ko et al., 2016) was mixed with a fixed concentration of GST-vWbp-C (500 nM) or -Coa-C (0.6 nM); Fg β-chain peptides (1-QGVNDNEEGFFSARGHRPLDKKREE-25); (13- ARGHRPLDKKREEAPSLRPAPPPISG-38); (26- APSLRPAPPPISGGGYRARPAKAAAT-51); (39-GGYRARPAKAAATQKKVERKAPDAGG-64) or scrambled Fg β-chain peptide (1-FSERKDLHQGEGNPREFVENDAKGR-25) (Shanghai Hanhong Scientific Co., Ltd.) (Ponnuraj et al., 2003) was mixed with a fixed concentration of His-SdrG (50 nM), GST-vWbp-N (6 nM) or -Coa-N (400 nM); soluble vWbp-$C_{(386-482)}$ was mixed with a fixed concentration of Fg (10 nM). All proteins and peptides were diluted (in 1% BSA, 0.05% Tween 20, and TBS) and were added to coated wells. Binding was detected using the HRP-conjugated rabbit-anti-His polyclonal antibodies (5000X dilution) (Alpha Diagnostic Intl. Inc.) or HRP- conjugated anti-GST polyclonal antibodies (6,000X dilution) or HRP-conjugated anti-Fibrinogen polyclonal antibodies (1,000X dilution)(Rockland Immuno Chemicals Inc). Results were presented as percentage of binding to Fg and 100% binding Fg was defined as the absorbance measured in the

absence of the inhibitor. Data was normalized to the % of binding Fg in the presence of the inhibitor. The data was then fitted using the one-phase exponential decay equation from GraphPad Prism software version 4.0. The competition experiments were carried out three times.

Far western

Fg (5 μg/lane) was reduced in Laemmli buffer (Bio-Rad) and separated on 10% SDS-PAGE gel. Reduced Fg was then stained with Coomassie Blue or electro transferred to a nitrocellulose membrane (Bio-Rad). Nitrocellulose membrane was blocked with 5% non-fat milk in TBS. Upon rinsing with blocking reagent, the membrane was probed with either recombinant vWbp-N (5 μg/ml), Coa-N (5 μg/ml), SdrG (2.5 μg/ml) or ClfA (15 μg/ml) (Vazquez et al., 2011). Membrane was incubated with proteins for 1 h at room temperature. After washing with TBST (0.1% Tween 20 and TBS), bound protein was detected with HRP-conjugated GST polyclonal antibodies (6000X dilution) or HRP-conjugated Rabbit-anti-His polyclonal antibodies (5000X dilution) (used for SdrG and ClfA), for 1 h at room temperature. Detection was developed using HyGLO Chemiluminescent reagent (Denville), according to manufacturer's manual.

Protein structure prediction

Protein structures of N- and C-terminal regions of vWbp were determined using Phyre^2 (Protein Homology/analogY Recognition Engine V 2.0) (Kelley et al., 2015).

Comparative genomics and protein homology

Comparison of the genomes was generated by Easyfig 2.2.2 (Sullivan et al., 2011) for the visualization of BLASTN between the genomes. Identification of homologous proteins were identified by BLASTP using databases from PATRIC and NCBI. Sequences were chosen based on amino acid identity of below 90% to above 30% to the amino acid, and were from complete

genomes. Signal sequence was predicted using SignalP-5.0 Server. Alignment of protein sequences was done by using Clustal Omega (Sievers et al., 2011).

Accession numbers

N315 (BA000018.3); NTCT8325 (CP000253.1); DSM20231 (CP011526.1); Newman (AP009351.1); FPR3757 (CP000255.1); JH1 (CP000736.1); Mu3 (AP009324.1); Mu50 (BA000017.4); N315-Ecb (BAB42250), SHPA (BAB41978); NTCT8325-Ecb (ABD30224.1), SHPB (ABD29944.1); DSM20231-Ecb (AKJ17012.1), SHPB (AKJ16668.1); CN1-Ecb (AGU61216.1), SHPA (AGU60934.1); JKD6159-SHPA (ADL22693.1); N315-Coa (BAB41444.1), vWbp (BAB41976.1), Efb (BAB42253.1), NTCT8325-Coa (ABD29370.1), vWbp (ABD29942.1), Efb (ABD30228.1); DSM20231-Coa (AKJ16095.1), vWbp (AKJ18593.1), Efb (AKJ17015.1); CN1-Coa (AGU60340.1), vWbp (AGU60931.1), Efb (AGU61219.1); JKD6159-Coa (ADL22160.1), vWbp (ADL22691.1), Efb (ADL22957.1); TCH1516- Ecb (ABX29109.1), SHPB (ABX28843.1); Newman- Ecb (BAF67338.1), SHPB (BAF67031.1); FPR3757-Ecb (ABD21122.1), SHPB (ABD21761.1); Mu50-Ecb (BAB57317.1), SHPA (BAB56976.1); JH1-Ecb (ABR52089.1), SHPA (ABR51687.1); Mu3-Ecb (BAF78028.1), SHPA (BAF77693.1); ED98-Ecb (ACY11030.1), SHPA (ACY10678.1) are available from Genbank/ EMBL under the accession numbers listed.

CHAPTER III

CHARACTERIZATION OF THE FIBRINOGEN-BINDING ACTIVITY OF N-TERMINAL VWBP[1]

Recombinant vWbp and Coa have similar secondary structure compositions

In order to characterize vWbp and Coa and their interactions with Fg, I expressed and purified recombinant versions of the full-length proteins, as well as, the N- and C-terminal halves with a His_6-or a glutathione-S-transferase (GST) tag fused to the N-terminus (Fig 13). The protein purities were analyzed by SDS-PAGE after the gels were stained with Coomassie Blue (Fig A-1a, b). The secondary structure compositions of the His-vWbp and Coa proteins were analyzed by circular dichroism (CD) (Fig 14A, B; (Kelly et al., 2005)). The spectra for the vWbp proteins and the corresponding Coa proteins are similar (Fig 14A, B). This is also shown from the secondary structure composition data using deconvolution programs (A-2a, b). The spectra of full-length vWbp and Coa show two negative bands at approximately 220 nm and 206 nm (Fig 14A, B, orange). The data suggests that the N-terminal regions for both vWbp and Coa are dominated by alpha helices, as shown by the signature alpha helical spectra of two negative bands near 222 nm and 208 nm (Fig 14A, B, purple; (Kelly et al., 2005)). These results are in line with the crystal structure of Coa-N in complex with prothrombin, where the staphylococcal protein domain is composed of two, three-helix bundles (67% alpha helical, 13 helices) (Friedrich et al., 2003) and support the predicted structure of vWbp-N, which is proposed to be

[1] Part of this chapter is reprinted with permission from "The Complex Fibrinogen Interactions of the Staphylococcus aureus Coagulases" by Thomas, S., Liu, W., Arora, S., Vannakambodi, G., Ko, Y-P., and Höök, M. 2019. *Front. Cell. Infect. Microbiol.* 9:106.

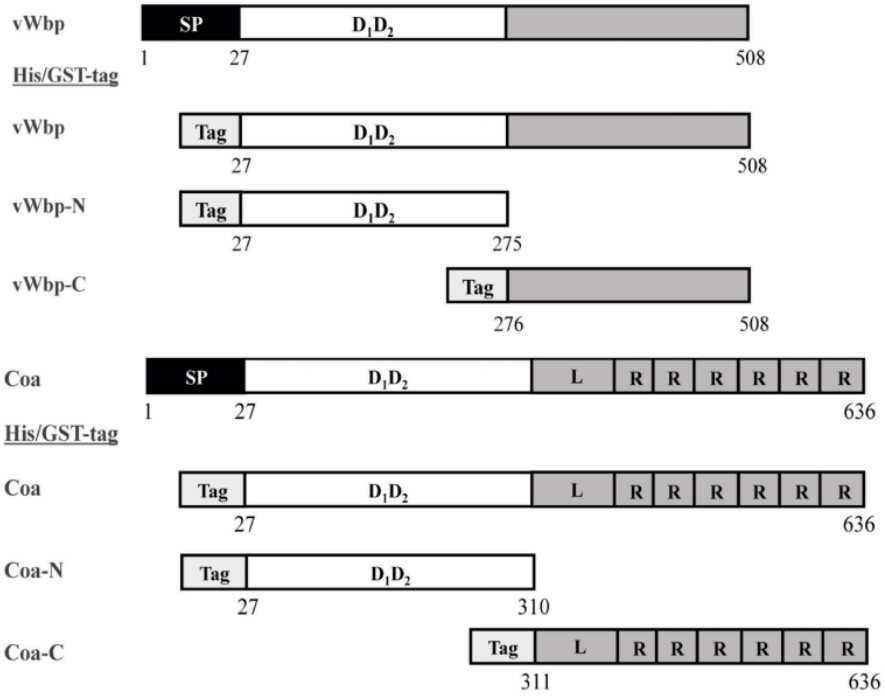

Figure 13. Constructs of the recombinant coagulases. Schematic overview of the vWbp and Coa constructs generated in this study. Gray represents the predicted unordered region. SP, Signal peptide; D_1D_2, prothrombin-binding domain. R, repeat domain; L, linker region. Tag box, His or GST-tag at N-terminal. (Reprinted with permission from Thomas et al., 2019)

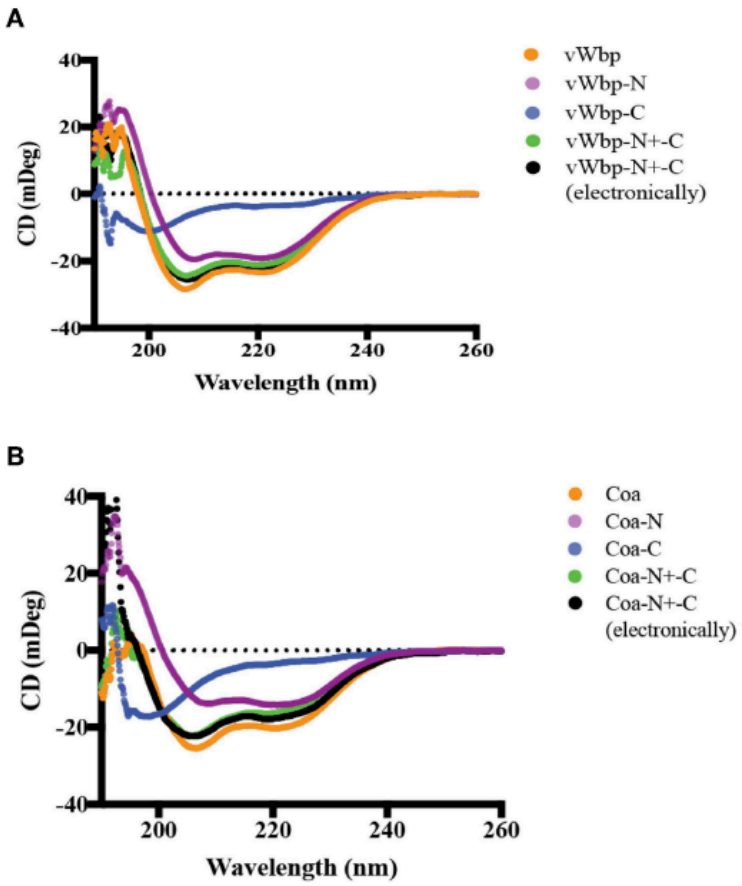

Figure 14. Circular dichroism analyses of secondary structures of vWbp and Coa. (A) vWbp (10 µM; orange), vWbp-N (9 µM; purple), vWbp-C (10 µM; blue). vWbp-N mixed with vWbp-C (5 µM; vWbp-N+-C, green). Sum of CD spectra of vWbp-N and vWbp-C using Excel (vWbp-N+-C electronically, black). **(B)** Coa (8 µM; orange), Coa-N (8 µM; purple), Coa-C (8 µM; blue). Coa-N mixed with Coa-C (4 µM; vWbp-N+-C, green). Sum of CD spectra of Coa-N and Coa-C using Excel (Coa-N+-C electronically, black). mDeg, millidegrees. The graphs are representative of the three independent experiments. (Reprinted with permission from Thomas et al., 2019)

similar to that of Coa-N (Fig 14A, B; (Kroh et al., 2009)). The spectra for both vWbp-C and Coa-C show that the proteins harbor unordered regions (Fig 14A, B, blue; A-3). The overall CD spectra signatures of full-length vWbp and Coa (Fig 14A, B, orange) are very similar to those of their N-terminal halves (Fig 14A, B, purple). The spectra of the mixture of vWbp-N with vWbp-C, and the sum of the spectra of the two proteins (vWbp-N+-C; green and black, respectively) are similar to the spectra of full-length vWbp and vWbp-N (Fig 14A). This is also observed for Coa (Fig 14B). Together, the data demonstrate that the recombinant intact proteins and the two subdomains of vWbp and Coa are similar in secondary structure composition as determined by CD.

vWbp and Coa differ in their relative binding to immobilized and soluble Fg

Under physiological conditions, Fg exists in multiple conformations, including a soluble form, which dominates when the protein is circulating in the blood, and an "immobilized" form, which Fg adopts when the protein is absorbed on the surface of an implanted device (Ugarova et al., 1993; Entenza et al., 2000; Moreillon et al., 1995). To explore how the coagulases interact with immobilized and soluble Fg, I used ELISA-type binding experiments. The binding results for Coa confirmed and extended earlier observations that the protein binds the two forms of Fg in a dose-dependent manner (Fig 15A, B; (Ko et al., 2016)). Coa bound preferably to soluble Fg with almost a 30-fold higher apparent affinity compared to immobilized Fg (0.09 nM vs. 2.4 nM, Table 3) (Ko et al., 2016). vWbp also bound immobilized and soluble Fg, but did not show preference in affinity for either of the two forms of Fg (apparent K_D = 9.9 nM and 5.3 nM, respectively) (Fig 15A, B). As a negative control, neither vWbp nor Coa showed binding to wells coated with bovine serum albumin (BSA) (data not shown).

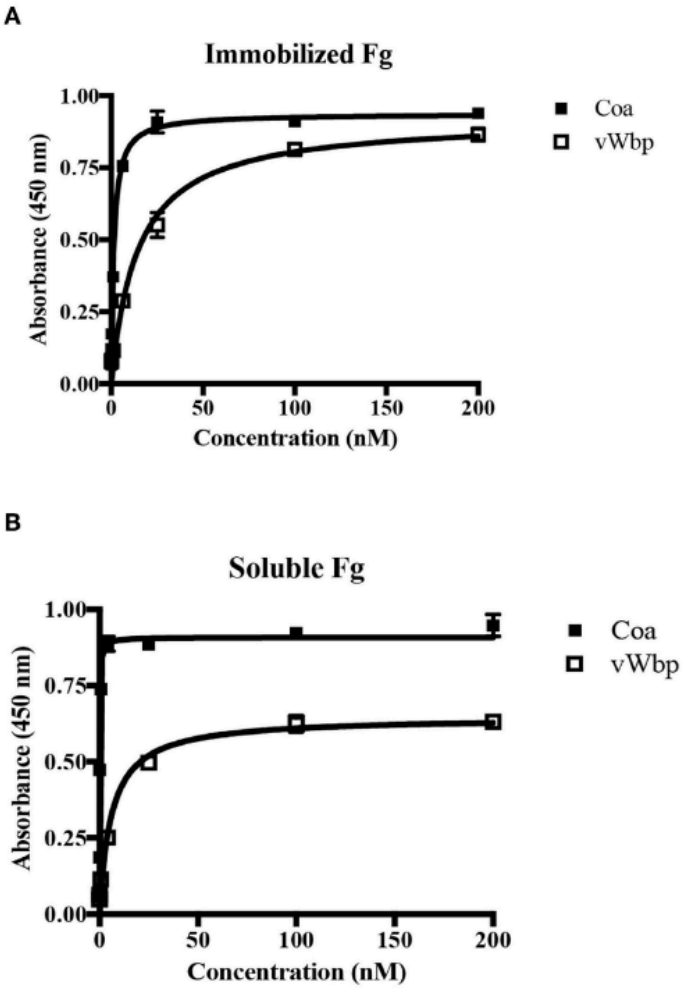

Figure 15. vWbp and Coa differ in their relative binding to immobilized and soluble Fg. **(A)** ELISA binding of GST-Coa or -vWbp to immobilized Fg (0.5 μg/well). **(B)** ELISA binding of Fg to immobilized GST-Coa or -vWbp (0.5 μg/well). Error bars, standard error of the mean (SEM). The graphs are representative of three independent experiments. (Reprinted with permission from Thomas et al., 2019)

vWbp and Coa do not target the same binding sites in Fg

Since both coagulases interact with Fg, I determined if vWbp and Coa target the same sites on Fg. To this end, I used an ELISA-based competition binding assay in which Fg was coated in a microtiter plate. The binding of His-vWbp or -Coa to immobilized Fg was evaluated in the presence of various concentrations of either GST-vWbp or -Coa. vWbp and Coa inhibited their respective selves from binding to Fg (Fig 16A, B). However, vWbp did not inhibit Coa from binding to immobilized Fg (Fig 16A), and Coa did not interfere with the binding of vWbp to Fg (Fig 16B, A-4). Thus, these results suggest that vWbp and Coa bind Fg at different, non-overlapping sites.

Both the N-terminal and C-terminal halves of vWbp and Coa bind Fg

Although vWbp has been shown to bind Fg, the actual location of Fg-binding site(s) in vWbp remains to be defined (McAdow et al., 2012a; Thomer et al., 2013). To locate the Fg-binding site, I determined the Fg-binding activity of the N- and C-terminal regions of vWbp in detail and compared their binding activities to that of full-length vWbp, using ELISA-type binding assays. Full-length vWbp, vWbp-N and vWbp-C bound to immobilized Fg, exhibiting dose-dependent binding and saturation kinetics with apparent K_Ds of 9.9 nM, 3.2 nM, and 38 nM, respectively (Fig 17A; Table 3). Interestingly, vWbp-N appeared to bind Fg with an approximately ten-fold higher affinity than vWbp-C. I also analyzed Fg binding to intact Coa and its subdomains (Fig 17B; Table 3). In accordance with our earlier data, both the N- and C-terminal halves of Coa harbor Fg-binding activities, with the N-terminal region having a lower affinity to Fg than its C-terminal part (reported apparent K_D = 200 nM and 7.5 nM, respectively; Ko et al., 2016). The apparent K_D determined for the C-terminal region of Coa showed a significantly higher affinity for Fg compared to that determined for the C-terminal half of vWbp

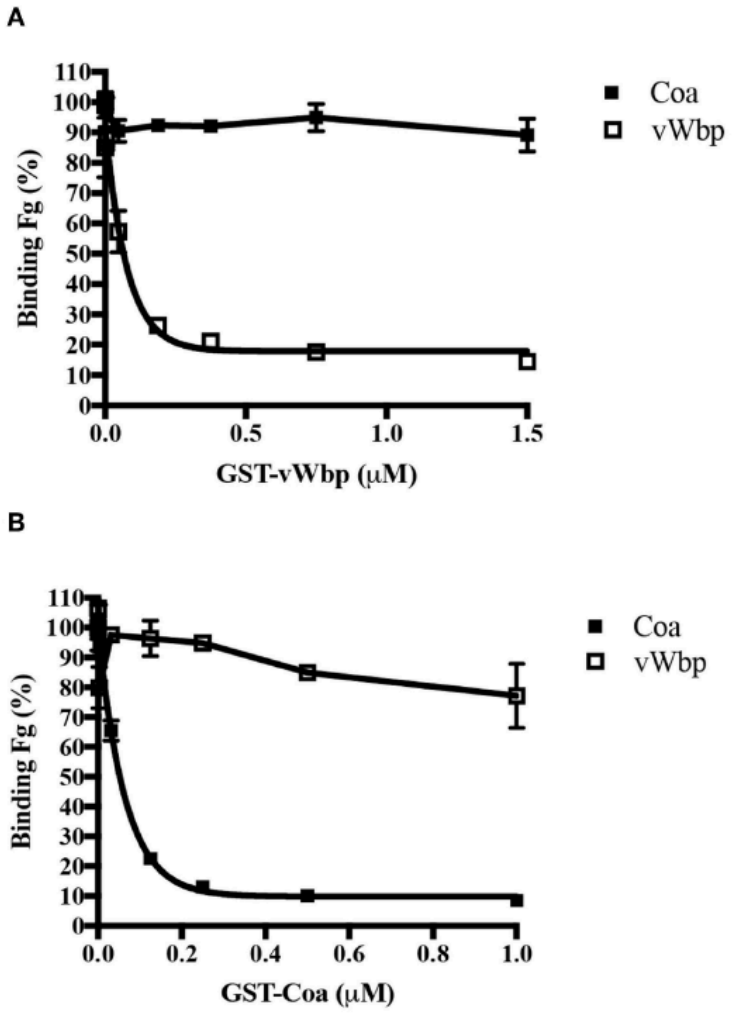

Figure 16. vWbp and Coa do not target the same binding sites in Fg. Competition ELISA of His-Coa (1 nM) or His-vWbp (200 nM) binding to immobilized Fg (0.5 μg/well) by **(A)** GST-vWbp and **(B)** GST-Coa. Error bars, standard error of the mean (SEM). The graphs are representative of three independent experiments. (Reprinted with permission from Thomas et al., 2019)

(apparent K_D = 0.46 nM vs. 38 nM, respectively). Thus, both Coa and vWbp harbor at least two Fg-binding sites located at their N- and C-terminal sections. However, the relative potencies of these sites seem to differ between the two coagulases. The N-terminal half of vWbp contains the predominant Fg-binding activity, whereas, the C-terminal half is the major Fg-binding region of Coa.

Table 3. Half-maximal binding concentrations (Apparent K_D)

Proteins	Constructs	vWbp	Coa
Soluble Fg	**Full-length**	5.3×10^{-9} M ± 8.9×10^{-10} M	9.0×10^{-11} M ± 6.1×10^{-11} M
Immobilized Fg	**Full-length**	9.9×10^{-9} M ± 5.0×10^{-9} M	2.4×10^{-9} M ± 1.9×10^{-9} M
	N-terminal	3.2×10^{-9} M ± 1.3×10^{-9} M	2.0×10^{-8} M ± 1.4×10^{-8} M
	C-terminal	3.8×10^{-8} M ± 2.9×10^{-8} M	4.6×10^{-10} M ± 6.3×10^{-11} M

(Reprinted with permission from Thomas et al., 2019)

The N-terminal region of vWbp binds to the N-terminal of the Fg β-chain

I next wanted to characterize how vWbp-N interacts with Fg. In an attempt to identify the Fg polypeptide(s) targeted by the recombinant vWbp-N and Coa-N, I used far western analysis. The three Fg polypeptide chains were separated by SDS-PAGE and transferred to a supporting membrane to be probed with vWbp-N and Coa-N, respectively (Fig 18A). ClfA and SdrG of

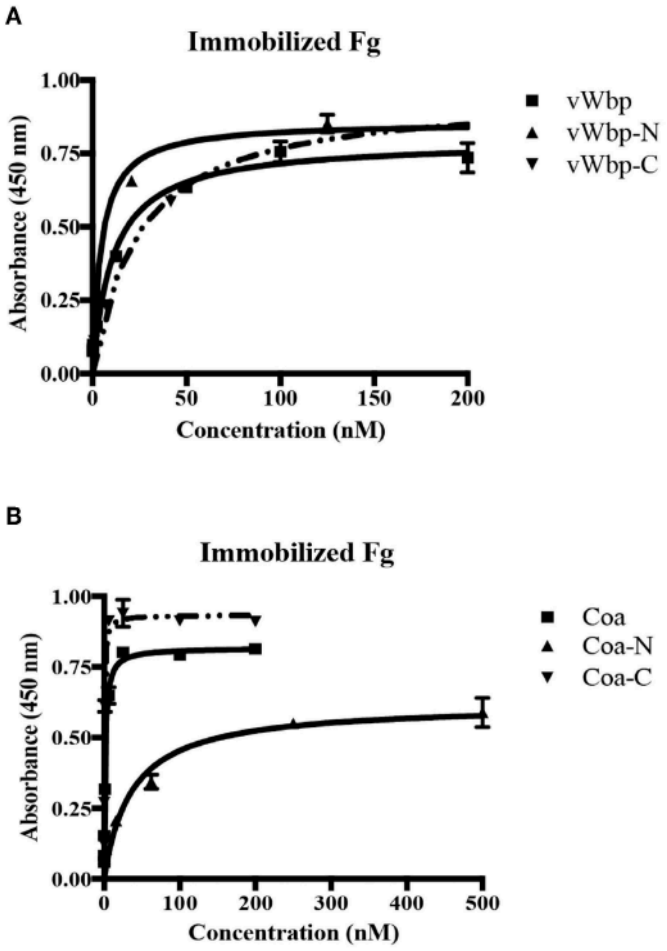

Figure 17. Both the N-terminal and C-terminal halves of vWbp and Coa bind Fg. (A) ELISA binding of GST-vWbp, -N, or -C to immobilized Fg (0.5 μg/well). **(B)** ELISA binding of GST-Coa, -N or –C to immobilized Fg (0.5 μg/well). vWbp or Coa (full-length), vWbp-N or Coa-N (N-terminal), vWbp-C or Coa-C (C-terminal). Error bars, standard error of the mean (SEM). The graphs are representative of three independent experiments. (Reprinted with permission from Thomas et al., 2019)

Staphylococcus epidermidis, two staphylococcal Fg-binding MSCRAMMs known to bind to the C-terminus of the γ- chain (ClfA) and the N-terminal of the β-chain (SdrG), served as controls (McDevitt et al., 1997; Ganesh et al., 2008; Ponnuraj et al., 2003). The results revealed that both vWbp-N and Coa-N bound to the β-chain of Fg, but Coa-N also bound weakly to the α-chain. Since vWbp-N binds to the denatured form of the Fg β-chain, it is likely that vWbp-N binds to a specific linear sequence of the β-chain. SdrG was previously shown by our laboratory to bind to the first 25 amino acid residues of the Fg β-chain, which is unordered (Ponnuraj et al., 2003). I, therefore, examined if vWbp-N binds to this region by using a synthetic peptide corresponding to the Fg β-chain 1-25 residues (Fg β (1-25)) in an ELISA- based competition assay, where Fg was coated in a microtiter plate. Binding of vWbp-N to immobilized Fg was evaluated in the presence of increasing concentrations of the peptide Fg β (1-25). As expected, SdrG, which served as the positive control, was effectively inhibited by the peptide Fg β (1-25) from binding to full-length Fg (Fig 18B). A scrambled 25-residues peptide did not inhibit vWbp-N nor SdrG binding, and served as a negative control (Fig A-5). The results showed that the Fg β (1-25) peptide only partially inhibited vWbp-N from binding to Fg, suggesting that Fg β (1-25) constitutes a part of the binding site and that additional Fg residues beyond the Fg β (1-25) are likely involved in the interaction. In contrast, binding of Coa-N to full-length Fg was not affected by the Fg β (1-25) peptide, suggesting that Coa recognizes a different region in the Fg β-chain.

To further determine the binding site, I used various synthetic Fg β-chain peptides that covered the first 64 amino acid residues in an ELISA- based competition assay, with Fg immobilized to the microtiter plate (Fig 19A, B). Each peptide overlapped with each other by about 13 amino acid residues. Inhibition was evaluated in the presence of increasing concentrations of peptides, Fg β (13-38), Fg β (26-51), or Fg β (39-64). Fg β (1-25) was used as

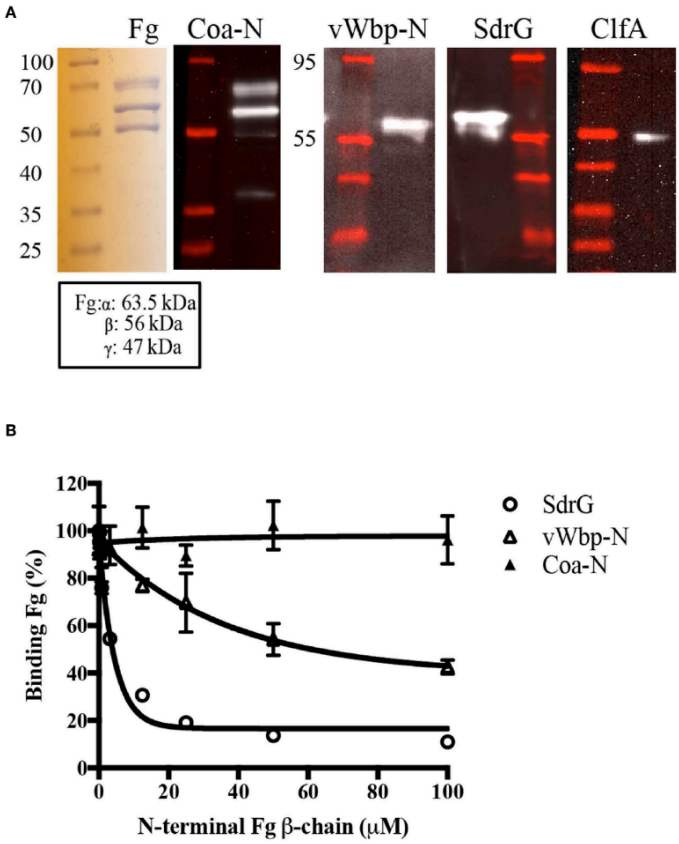

Figure 18. The N-terminal region of vWbp binds to the N-terminal of the Fg β-chain. (A) Far Western, Fg (5 μg/ lane) was separated on a SDS-PAGE gel and probed with vWbp-N (15 μg/ml) or Coa-N (5 μg/ml). ClfA (15 μg/ml) and SdrG (2.5 μg/ml) were used as controls. **(B)** Competition ELISA of SdrG (50 nM), vWbp-N (6 nM) or Coa-N (400 nM) binding to immobilized Fg (0.5 μg/well) by Fg β-chain (1-25) peptide. Error bars, standard error of the mean (SEM). The graphs are representative of three independent experiments. (Reprinted with permission from Thomas et al., 2019)

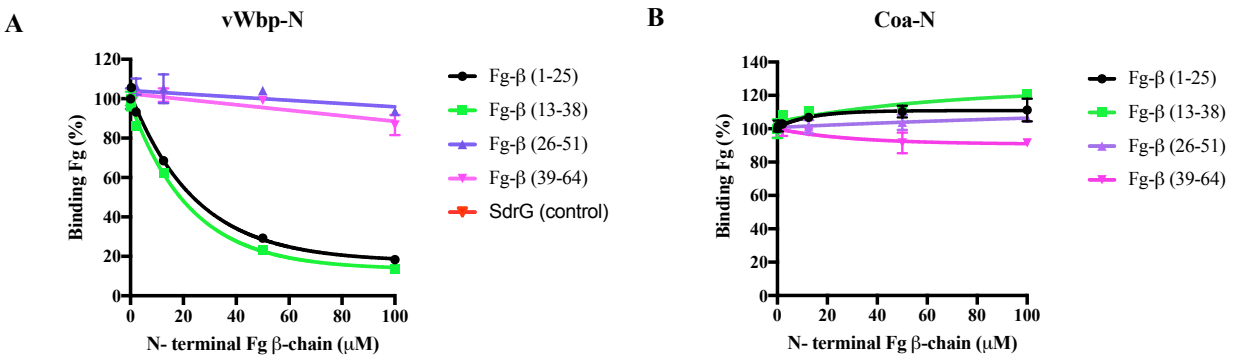

Figure 19. The N-terminal region of vWbp binds to the N-terminal of the Fg β-chain (1-38). Competition ELISA of **(A)** vWbp-N (6 nM) or **(B)** Coa-N (400 nM) binding to immobilized Fg (0.5 μg/well) by peptides Fg β (1-25; black), Fg β (13-38; green), Fg β (26-51; magenta), Fg β (39-64; purple). Error bars, standard error of the mean (SEM).

a positive control. As expected, vWbp-N was inhibited from binding to full-length Fg by the Fg β (1-25) peptide (Fig 19A). Interestingly, the Fg β (13-38) also showed inhibition of vWbp-N. However, both peptides Fg β (26-51) and Fg β (39-64) failed to inhibit vWbp-N. Thus, the data suggests that the binding site is located within the N-terminal Fg β-chain (1-38). On the other hand, Coa-N binding to Fg was not impeded by any of the peptides, suggesting that the N-terminal half of Coa does not bind to this region of the N-terminal Fg β-chain (Figure 19B).

CHAPTER IV

CHARACTERIZATION OF THE FIBRINOGEN-BINDING ACTIVITY OF C-TERMINAL VWBP[1]

vWbp-C and Coa-C do not share similar Fg-binding motifs

Our earlier studies have shown that Coa and Efb contain a common Fg-binding motif within their predicted disordered domains (Ko et al., 2016; Ko et al., 2011). Since vWbp-C is also predicted to be disordered, I wanted to determine if the Fg-binding site in vWbp-C is related to the Fg-binding motif in Coa or Efb. Using the synthetic peptides corresponding to the Fg-binding motif of Coa (Coa-RI; (Ko et al., 2016)) and Efb (Efb-O; (Ko et al., 2016)), I performed an ELISA- based competition assay, using these peptides as potential inhibitors. I determined the binding of vWbp-C and Coa-C to immobilized Fg in the presence of various concentrations of Coa-RI or Efb-O (Fig 20A, B). As expected, Coa-C was inhibited from binding to Fg by both peptides. However, the Coa peptide (Fig 20A) and the Efb peptide (Fig 20B) did not inhibit vWbp-C binding to Fg, suggesting that vWbp does not harbor the Fg-binding motif found in Coa and Efb. Intriguingly, the increasing amount of peptide added enhanced vWbp-C binding to immobilized Fg. Since these peptides also bind Fg, it is possible that this binding results in a structural change to the protein, which accommodates more favorable vWbp-C binding. I, therefore, conclude that the disordered C-terminal halves of vWbp and Coa contain different Fg-

[1] Part of this chapter is reprinted with permission from "The Complex Fibrinogen Interactions of the Staphylococcus aureus Coagulases" by Thomas, S., Liu, W., Arora, S., Vannakambodi, G., Ko, Y-P., and Höök, M. 2019. *Front. Cell. Infect. Microbiol.* 9:106. Copyright © 2019 Thomas, Liu, Arora, Ganesh, Ko and Höök.

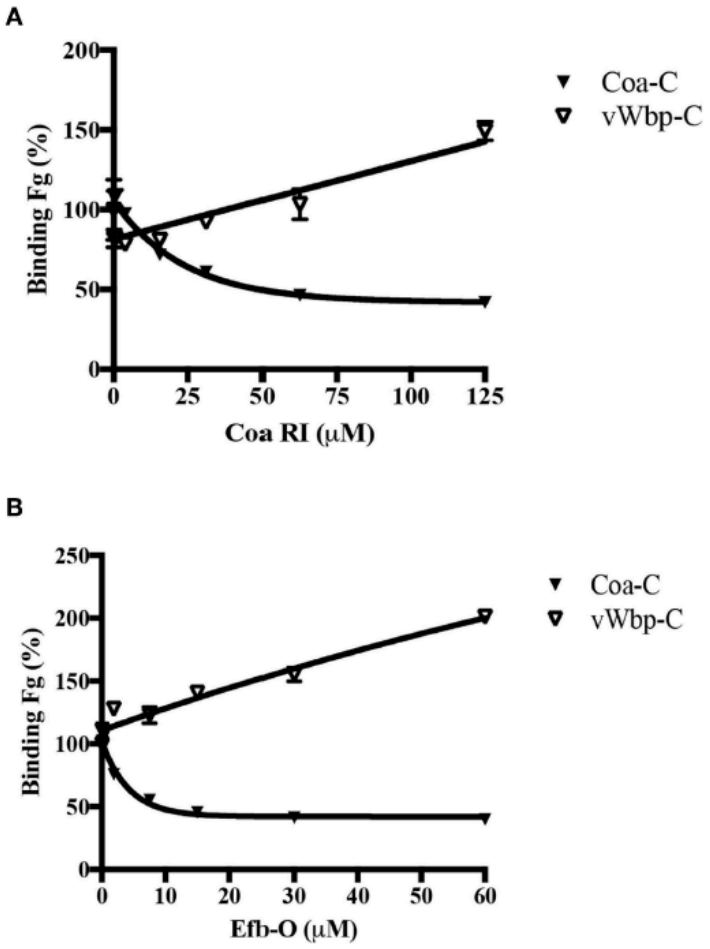

Figure 20. vWbp-C and Coa-C do not share similar Fg-binding motifs. Competition ELISA of Coa-C (0.6 nM) or vWbp-C (500 nM) binding to immobilized Fg (0.5 μg/well) by peptide **(A)** Coa RI and peptide **(B)** Efb-O. Error bars, standard error of the mean (SEM). The graphs are representative of three independent experiments. (Reprinted with permission from Thomas et al., 2019)

binding motifs. Specifically, Coa contains the Efb-O type of binding motif, and vWbp contains a distinct and unidentified Fg-binding motif.

Predicted structure of vWbp-C$_{(386-482)}$ is similar to the C3b-binding motif of Efb

Our CD data have suggested that the C-terminal half of vWbp is disordered. However, using a structure prediction program, Phyre2 (Kelley et al., 2015), the predicted structure of the C- terminal region of vWbp was shown to be similar to the crystal structure of the C-terminal half of Efb that harbors the C3b-binding motif, since both C-terminal regions are composed of three α-helices (Fig 21A; (Haspel et al., 2008)). In addition, amino acid sequence alignment of full-lengths Efb and vWbp showed sequence similarity at their C-terminal sections (Figure 21B). The amino acid region 386-482 of vWbp showed more similarity to the C-terminal sequence of Efb. Furthermore, vWbp-C$_{(386-482)}$ is the minimum region that retains the predicted ordered structure of being composed of three α-helices. Thereby, the C-terminal half of vWbp harbors not only a disordered region, but also an alpha helical region that covers residues 386-482.

C-terminal Fg-binding motif of vWbp binds to soluble Fg

I wanted to then test whether if the predicted ordered portion of the C-terminal of vWbp has Fg-binding activity. With Fg coated to the plastic surface in an ELISA assay, vWbp-C$_{(386-482)}$ was not able to bind well to immobilized Fg (Fig 22A). However, vWbp-C$_{(386-482)}$ bound to soluble Fg with a half-maximal binding affinity similar to the half-maximal binding affinity of intact vWbp-C (4.5 nM vs 1.8 nM, respectively) (Fig 22B). Thus, the data suggests that the Fg-binding motif of the C-terminal half of vWbp encompasses 386-482. In addition, the motif seems to prefer binding to the soluble form of Fg than immobilized Fg.

Since vWbp-C$_{(386-482)}$ exhibited weaker binding to immobilized Fg, I determined whether if this region of vWbp prefers a certain conformation for binding to Fg. In a competition ELISA

A

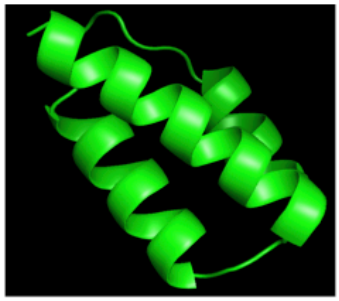

B

```
efb     ----------------------------------------------------SEGYGPR  7
vWbp    KKDNPELKDFNEEEQLKCDLELNKLENQILMLGKTFYQNYRDDVESLYSKLDLIMGYKDE  180
                                                             **  .

efb     ------------------------------------------------------------  7
vWbp    ERANKKAVNKRMLENKKEDLETIIDEFFSDIDKTRPNNIPVLEDEKQEEKNHKNMAQLKS  240

efb     ----------------------EKKPVSIN---HNIVEYNDGT----FKYQSRPKFNST  37
vWbp    DTEAAKSDESKRSKRSKRSLNTQNHKPASQEVSEQQKAEYDKRAEERKARFLDNQKIKKT  300
                               ::**.* :   :: .**:. :     :: .. *::.*

efb     PK---YIKFKHD----------------------------------------------  46
vWbp    PVVSLEYDFEHKQRIDNENDKKLVVSAPTKKPTSPTTYTETTTQVPMPTVERQTQQQIIY  360
        *      .*:*.

efb     ------------------------------YNILEFNDGTFEYGARPQ-------FNK-P  68
vWbp    NAPKQLAGLNGESHDFTTTHQSPTTSNHTHNNVVEFEETSALPGRKSGSLVGISQIDSSH  420
                                       *::**:: :   * :         ::.

efb     AAKTDATIKKEQKLIQAQNLVREFEKTHTVSAHRKAQKAVNLVSFEYKVKKMVLQERIDN  128
vWbp    LTEREKRVIKREHVREAQKLVDNYKDTHSYKDRINAQQKVNTLSEGHQK---RFNKQINK  477
         :: :  : *.::: :**:** :::.**: . : :**: ** :*  ::     ::::*::

efb     VLKQGLVK      136
vWbp    VYNGK---      482
        * :
```

Figure 21. Predicted structure of vWbp-C$_{(386-482)}$ is similar to the C3b-binding motif of Efb. **(A)** Predicted structure of vWbp-C (386-482). **(B)** Amino acid sequence alignment of full-lengths Efb and vWbp.

assay, various concentrations of soluble vWbp-$C_{(386-482)}$ were added as a potential inhibitor to block the binding of immobilized vWbp-$C_{(386-482)}$ from binding to soluble Fg (Fig 22C). The data showed that soluble vWbp-$C_{(386- 482)}$ was unable to inhibit its immobilized form from binding to Fg, suggesting that vWbp-$C_{(386-482)}$ binding to a plastic surface induces an optimal conformational change of the protein that allows for Fg binding.

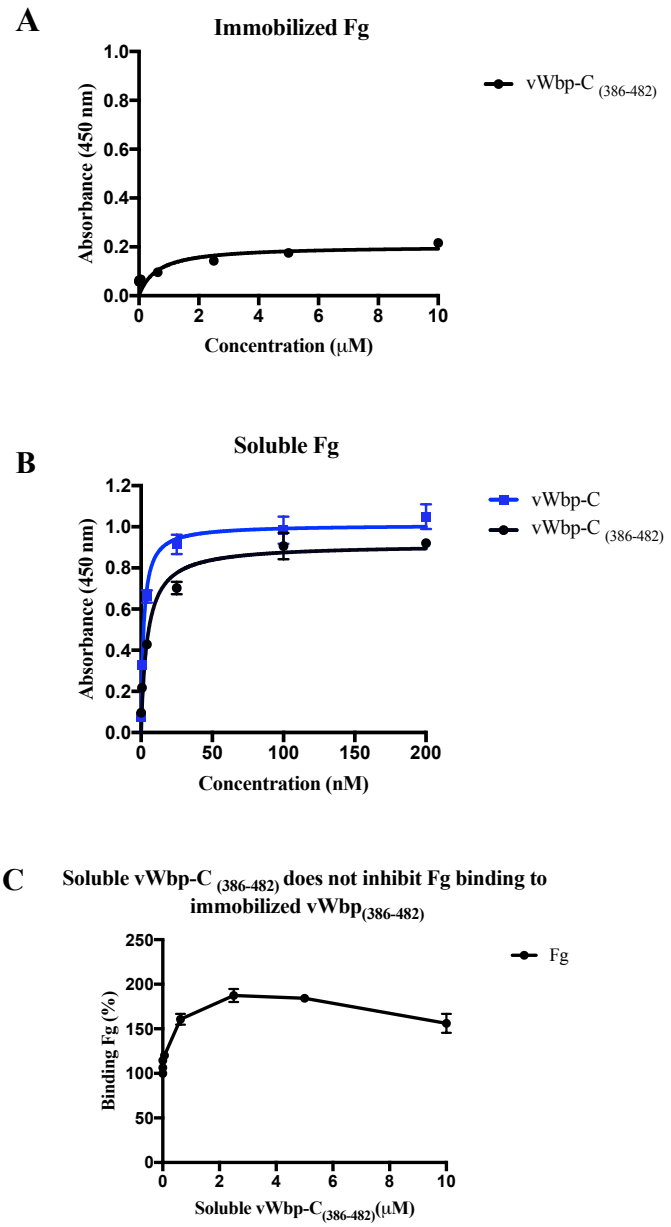

Figure 22. The Fg-binding motif of the C-terminal region of vWbp is located at 386-482. ELISA binding of His-vWbp–C (386-482) to immobilized Fg (0.5 μg/well). **(B)** ELISA binding of Fg to immobilized His-vWbp–C (386-482; black) or His-vWbp-C (250-482; blue) (1.0 μg/well). vWbp-C (C-terminal). **(C)** Competition ELISA of Fg (10 nM) binding to immobilized

CHAPTER V

IDENTIFICATION OF ADDITIONAL SECRETED PROTEINS STRUCTURALLY RELATED TO VWBP

Homologs of the C3b-binding or C-terminal Fg-binding motif are found in different *S. aureus* isolates

Since the structural prediction of vWbp-$C_{(386-482)}$ suggested that the C-terminal halves of both Efb and vWbp are related, I wanted to identify other secreted proteins that harbor the α-helical C3b-binding motif of Efb or the predicted α-helical C-terminal Fg-binding motif of vWbp. Using Basic Local Alignment Search Tool (BLAST), five *S. aureus* isolates, N315, NTCT8325, DSM20231, CN1 and JKD6159 were identified to have protein sequences with similar motifs (Table 4) (Altschul et al., 1990).

From the strains listed above, I identified three proteins. One protein was homologous to C3b-binding motif of Efb. Further analysis of the protein showed that it had been discovered and is named Extracellular complement-binding protein (Ecb) (Amdahl et al., 2013). The other two proteins were homologous to the C-terminal Fg-binding motif of vWbp. The two proteins both have an N-terminal signal sequence of 26 amino acid residues and lack the cell wall-anchoring motif, suggesting that they may be secreted proteins. The two homologs share a 65% amino acid identity with each other, indicating they are two different proteins (Fig 23). Since the two uncharacterized proteins are homologous to the predicted α-helical Fg-binding motif, I named the proteins, Secreted helix protein A (SHPA), which is from a sequence type 5 isolate and Secreted helix protein B (SHPB) from a sequence type 8 isolate. Analysis of the five strains

identified showed that Ecb and either SHPA or SHPB were present. In addition, the isolates have all three secreted Fg-binding proteins, Efb, Coa and vWbp.

Table 4. Homologous proteins harboring C3b-binding or C-terminal Fg-binding motif

Strain	Ecb	Secreted helix protein A	Secreted helix protein B	Origin	ST	Coa	vWbp	Efb
N315	Y	Y	-	Human	5	Y	Y	Y
NTCT8325	Y	-	Y	Human	8	Y	Y	Y
DSM20231	Y	-	Y	Human	8	Y	Y	Y
CN1	Y	Y	-	Human	72	Y	Y	Y
JKD6159	Y	Y	-	Human	93	Y	Y	Y

SHPA is found in ST 5 and SHPB is present in ST 8 isolates

I then expanded our list of isolates, solely focusing on strains that were of sequence type (ST) 5 or 8, since these strains are associated with *S. aureus* infections, such as skin and soft tissue infections (Table 5) (Pardos de la Gandara et al., 2015; Uhlemann et al., 2014). Similar to Table 4, Ecb was present in the 10 isolates (data not shown). Of the 10, five isolates have SHPA and SHPB was identified in the other five.

Ecb is structurally related to the C-terminal Fg-binding motif of vWbp (Amdahl et al., 2013). In addition, the gene is located in the genomic island, vSaγ (A-8, red arrow; (Gill et al., 2005)). My data supports the technique I used for identifying homologs, since both our data and studies on Ecb, show that the protein is homologous to the C-terminal region of Efb and that the gene is located in a MGE (A-8; (Amdahl et al., 2013; Gills et al., 2005; Jongerius et al., 2007)).

The protein homologous to the C-terminal Fg-binding motif of vWbp, SHPA was present in ST 5 isolates, but were absent in ST 8 isolates. Amino acid alignment of the protein showed 49% sequence similarity to the Fg-binding motif and 39% similarity to full-length vWbp. I compared the amino acid sequence of SHPA from the different isolates that were of ST 5, and they were found to be 100% identical. The protein is smaller compared to full-length vWbp, in that it is 173 amino acid residues long, including the signal sequence. The protein lacks the two domains characteristic of vWbp, the prothrombin-binding domain and the vWF-binding motif. This suggests that SHPA is not vWbp, but is a different protein that harbors a motif that is similar to the C-terminal Fg-binding motif of vWbp.

The second protein homologous to the C-terminal Fg-binding motif of vWbp, SHPB was present in ST 8 isolates, but were absent in ST 5 isolates. Amino acid alignment of the protein showed 58% sequence similarity to the Fg-binding motif and 46% similarity to full-length vWbp. I compared the amino acid sequence of SHPB from the different isolates that were of ST 8 and they were found to be 100% identical. The protein is also smaller compared to full-length vWbp, in that it is 156 amino acid residues long, including the signal sequence. The protein lacks the prothrombin-binding domain and the vWF-binding motif, suggesting that SHPB is not vWbp, but is a different protein that also has a motif that is similar to the C-terminal Fg-binding motif of vWbp.

C-terminal regions of SHPA and SHPB are predicted to be α- helical

I then determined the predicted structure of SHPA and SHPB. Structure predictions of SHPA and SHPB showed that both proteins were composed of three-α-helices, which was similar to the predicted structure of the C-terminal Fg-binding motif of vWbp (Fig 23). The template used was the crystal structure of the C3b-binding motif of Efb in complex with C3b

(Haspel et al., 2008). The percent of confidence for full-lengths SHPA and SHPB were 85.7% and 84.6%, respectively. I then determined which region was more likely to be α- helical. Residues 111-173 of SHPA and residues 98-156 of SHPB were the minimum regions that retained the predicted ordered structure of being 95% α-helical (data not shown). Thus, the C-terminal regions for both SHPA and SHPB were predicted to be composed of α-helices.

Table 5. Presence of SHPA or SHPB in sequence type 5 or 8 isolates

Strain	SHPA	SHPB	Origin	ST
N315	Y	-	Human	5
Mu50	Y	-	Human	5
JH1	Y	-	Human	5
Mu3	Y	-	Human	5
ED98	Y	-	Animal	5
NTCT8325	-	Y	Human	8
DSM20231	-	Y	Human	8
TCH1516	-	Y	Human	8
Newman	-	Y	Human	8
FPR3757	-	Y	Human	8

A

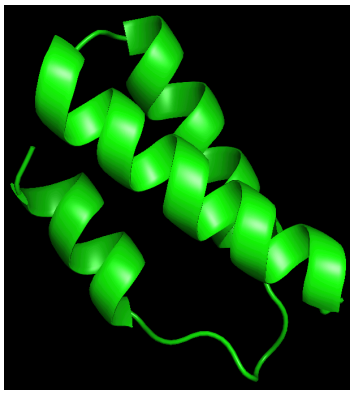

B

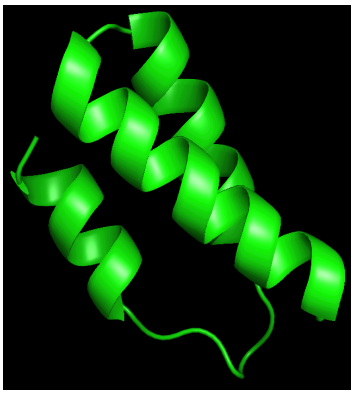

C

```
vWbp      QQKAEYDKRAEERKARFLDNQKIKKTPVVSLEYDFEHKQRIDNENDKK-L---------V  350
SHPA      ----------------------MKRKVLVLTMGVICATQLWHSNHANALVTESVETNFV  37
SHPB      ----------------------MKRKVLVLTMGVICATQLWHSNHANALVTESGAND--  35
                                 *  *: *  ..    :: :.*. : *

vWbp      VSAPTKKPTSPTTYTETTTQVPMPTVERQTQQQIIYNAPKQLAGLNGESHDFTTTHQSPT  410
SHPA      VKDSD-NKNILQTHTEITTEEKFSIV--------------------------EKSQLNK  69
SHPB      ----------TKQFTEIVSEEKVITV--------------------------EHAQINI  58
                    .** .::  .  *                                *

vWbp      TSNHTHNNVVEFEETSALPGRKSGSLVGISQIDSSHLTEREKRVIKREHVREAQKLVDNY  470
SHPA      LKALSNDNYIEYDLHTNQTGIKKGWLYGYSEIDSSHFTDRDKRVIRRDHVKEAQSLINDY  129
SHPB      FQSNSNSNLMEFNIL--TMGGKSGAMVGYSEIDSSHFTDRDKRVIRRDHVKEAQSLVENY  116
           .  ::.* :*::      * *.* : * *:*****:*:*:****:*:**:***.*:::*

vWbp      KDTHSYKDRINAQQKVNTLSEGHQKRFNKQINKVYNGK------  508
SHPA      KDTQSYEDLAKATAKVSTLSQSHQNYLNKQIDKVNNKIEKTEKR  173
SHPB      KDTQSADARMKAKQKVNTLSKPHQNYFNKQIDKVYNGLQR----  156
          ***:* .   :*  **.***: **: :****:** *
```

Figure 23. Predicted structures of SHPA and SHPB. (A) Predicted structure of full-length SHPA. **(B)** Predicted structure of full-length SHPB. **(C)** Amino acid sequence alignment of full-lengths vWbp, SHPA and SHPB, including signal sequences.

CHAPTER VI

CONCLUSIONS AND FUTURE WORK[1]

Conclusions and discussions

In this study, I have compared the secondary structure compositions and the Fg binding of the *S. aureus* coagulases vWbp and Coa. The similarity in the circular dichroism (CD) spectra of the N-terminal halves of the two coagulases support earlier sequence analyses and molecular modeling studies (Friedrich et al., 2003; Kroh et al., 2009; Kroh and Bock, 2012; Liesenborghs et al., 2018; Ko et al., 2016). This suggests that it is likely that the D_1D_2 domain of vWbp-N, composed primarily of alpha helices, resembles the structure of the corresponding Coa segment (Friedrich et al., 2003), despite the fact that these segments only have 30% amino acid sequence identity (Bjerketorp et al., 2004). In addition, our CD data showed that substantial sections of the C-terminal regions of both vWbp and Coa have an intrinsically disordered character (Fig 14A, B; A-3).

vWbp and Coa fall into the zymogen activator and adhesin protein (ZAAP) family since they activate prothrombin non-proteolytically (Panizzi et al., 2004; Friedrich et al., 2003; McAdow et al., 2012b). Both coagulases can induce clotting of murine blood (Bjerketorp et al., 2004; Cheng et al., 2010) and the observed effects of vWbp and Coa in mouse infection models therefore seems clinically relevant. At the nidus of a murine abscess model, *S. aureus* is surrounded by a pseudocapsule (McAdow et al., 2011; Cheng et al., 2009), a layer of Fg that also contains Coa and prothrombin as revealed by antibody staining (Cheng et al., 2010). The

[1] Part of this chapter is reprinted with permission from "The Complex Fibrinogen Interactions of the Staphylococcus aureus Coagulases" by Thomas, S., Liu, W., Arora, S., Vannakambodi, G., Ko, Y-P., and Höök, M. 2019. *Front. Cell. Infect. Microbiol.* 9:106.

periphery of the pseudocapsule is composed of another layer of Fg/fibrin that exhibits a pronounced staining of vWbp. This suggested that vWbp predominantly co-localizes with Fg, as well as prothrombin, at this second fibrin layer. The distinct two layers of Fg structure observed in the murine abscess model is re-established in the 3D-Collagen-Fg system, in which *S. aureus* microcolonies assemble two concentric Fg/fibrin barriers (Guggenberger et al., 2012). In this *in vitro* culture model, Coa is found to contribute to the formation of the pseudocapsule that encloses the microcolonies; whereas, vWbp is critical to the formation of the Fg/fibrin meshwork, which lies immediately adjacent to the pseudocapsule (Guggenberger et al., 2012). These observations suggest that despite sharing similar secondary structures and interacting with Fg and prothrombin, the coagulases contribute differently in assembling Fg/fibrin shield structures. Furthermore, the two coagulases reportedly differ in the role that Fg-binding plays in prothrombin activation. Fg enhances vWbp but not Coa-mediated prothrombin activation (Kroh et al., 2009).

Our study reports significant differences both in the Fg-binding affinities of these two coagulases and in the sites of interaction between the coagulases and Fg. I showed that both bacterial proteins recognize both soluble and adsorbed Fg, which represent two different conformations of the host protein, yet only Coa seems to prefer the soluble over the immobilized form of Fg (Fig 15A, B, Table 3). The observed difference could be the consequence of a conformational change in Fg induced on binding to Coa. Restricted mobility for the adsorbed form of Fg could limit this flexibility. In this scenario, soluble Fg but not adsorbed Fg could undergo a hypothetical conformational shift associated with high affinity binding of Coa to Fg. On the other hand, full-length vWbp showed essentially no preference for either form of Fg,

indicating that a similar hypothetical conformational restriction issue does not apply to Fg in its interaction with full-length vWbp (Table 3).

The two coagulases each harbor at least two distinct Fg-binding sites located at the N-and C-termini segments of the proteins (17A, B). Under the experimental conditions used, the N-terminal domain (vWbp-N) is the predominant Fg-binding region in vWbp, and the C-terminal section (Coa-C) is the major Fg-binding region in Coa. Our lab has previously identified a Fg-binding repeated linear motif in Coa-C (Ko and Flick, 2016; Ko et al., 2016), which is also present in the Fg-binding protein Efb (Ko et al., 2016). Sequence analysis indicates that vWbp does not contain this motif and consistent with this observation, synthetic peptides corresponding to the Coa and Efb versions of the motif, respectively, did not inhibit vWbp-C from binding to Fg (Fig 20A, B). I identified that the Fg-binding motif of vWbp-C was located at amino acid residues 386-482 (Fig 22B). In addition, the Fg-binding motif of vWbp exhibits preference in binding to soluble Fg when vWbp-$C_{(386-482)}$ is in its immobilized form than its soluble form (Fig 22A, B, C). Previously, I saw that intact vWbp-C was able to bind to immobilized Fg, however truncation of the region upstream of residues 386-482 shows that binding is nearly abolished (Fig 17A, 22A, respectively). Thereby, a certain type of conformational restriction may be imposed on Fg that does not allow vWbp-$C_{(386-482)}$ to bind to Fg. Amino acid residues upstream of the 386-482 region may be required to induce a conformational change to allow the C-terminal region of vWbp to bind to immobilized Fg.

Furthermore, I noticed that the presence of either of the previously identified Coa or Efb Fg-binding peptides enhanced Fg binding to vWbp-C (Fig 20A, B). It is possible that the binding of the peptides to Fg induces a conformational change in the host protein resulting in an increased number and/or affinity of vWbp binding sites in Fg. Earlier studies suggest that vWbp

undergoes a conformational change upon the binding to prothrombin (Kroh et al., 2009; Pozzi et al., 2013). These authors speculate that vWbp exhibits a certain degree of conformational plasticity. Our data appears to support this concept and also extends it to Coa. Our CD spectra analyses suggest that large sections of the C-terminal halves of both vWbp and Coa are intrinsically disordered (Fig 14A, B; A-3). Intrinsically disordered regions exist in various conformational states and contribute to the structural flexibility of the protein (van der Lee et al., 2014; Portman, 2010). I also noticed significant batch-to-batch variations for both coagulases in the inhibition experiments, which are consistent with a mixture of conformational forms with different properties. Thus, it appears that the conformations of both Fg and the coagulases can be affected through their interactions. To fully understand how these virulence factors activate prothrombin, a detailed understanding of the conformational isoforms of the proteins involved and their transitions are needed.

Although the structure of the C-terminal Fg-binding motif of vWbp is predicted to be composed of three α-helices, the disordered region could possibly be upstream of the Fg-binding site (Fig 21A, 24). The 27 amino acid long vWF-binding motif may lie in this disordered region, meaning that the vWF-binding site could be a linear motif. Since vWF is a multimeric protein, binding of a bulky molecule to a linear motif may be favorable, whereas, if the motif was ordered, this may cause steric hinderance and thus, unfavorable binding to vWF. In a study by Claes and colleagues, vWbp was shown to mediate *S. aureus* adherence to the endothelial surface via its interactions with vWF under shear stress (Claes et al., 2014). Due to its conformational plasticity nature, it is tempting to speculate that vWbp may bind to vWF that could induce a conformational change to the bacterial protein, allowing vWbp to also bind soluble Fg that is recruited to the site of injury.

Earlier studies on the interaction between vWbp and Fg, apparently gave conflicting results. McAdow et al. showed, using an ELISA-based approach, that the Fg-binding activity was located in the C-terminal half of vWbp (McAdow et al., 2012a). The N-terminal half of vWbp binding to Fg was not determined in their study. Later, the same group used affinity chromatography (Thomer et al., 2013) where they found that the N-terminal region of vWbp, but not the C-terminal half, bound Fg. Our ELISA data presented here provides a potential explanation for the earlier published results. Both the N-and C-terminal regions of vWbp harbor Fg-binding sites. These observations paired with the different methods used in the earlier binding studies could possibly explain the contradicting results. In addition, coupling the disordered C-terminal segment of vWbp to the column may have reduced its conformational freedom; thereby, the Fg-binding region may be buried within the protein and not accessible for Fg to bind (van der Lee et al., 2014; Chang et al., 2007). Utilizing the ELISA based approach as a common method allowed us to analyze the binding of vWbp and Coa to both Fg adsorbed to a surface and Fg in a soluble state, and to compare the Fg-interaction with the subdomains of the two bacterial proteins.

The interactive sites in Fg targeted by the two coagulases are not shared. I demonstrated that vWbp-N binds to a synthetic peptide corresponding to the N-terminus of the Fg β-chain (Fig 18A, B, 19A). Although Coa-N also appears to target the Fg β-chain, the protein appears to bind to a different site since the Fg β peptides that cover the first 64 amino acid residues do not affect Fg binding to this segment of Coa (Fig 18B, 19B). Thus, I conclude that the two coagulases make multiple connections with Fg but the interactive sites in both the host protein and the bacterial binding partner differ for vWbp and Coa, respectively.

The two coagulases of *S. aureus* have a similar structural organization and are able to activate prothrombin without cleaving the zymogen, but our data shows that in terms of their Fg interactions, the two proteins behave differently. Their interactions with Fg are complex, engage multiple contact sites, and appear to involve significant conformational changes in the interacting proteins, which may be essential for how they can act as critical virulence factors in different steps of the pathogenic process of *S. aureus* infections. Due to the differences noted between Coa and vWbp in their interaction with Fg, targeting one coagulase alone may not be an effective strategy for drug development. However, inhibiting the interactions of both coagulases could effectively block the protective Fg/fibrin shield assembly and serve as a preventive measure.

The three structurally related proteins, Efb, Coa and vWbp contribute to Fg/fibrin shield formation; however, their role and at what stage in creating the shield may be different from each other (Fig 24, 25). *S. aureus* expresses Coa and vWbp during the early and mid-exponential phase (Bjerketorp et al., 2002; Savini, 2018). I propose in our Fg/fibrin shield model that in the early stages of assembly both vWbp and Coa interact with prothrombin, activating the zymogen. Coa forms a complex with prothrombin becoming active staphylothrombin (McAdow et al., 2012b; Ko and Flick, 2016). Staphylothrombin can then cleave Fg to generate fibrin monomers. The fibrin monomers aggregate together forming a layer fibrin over the *S. aureus* microcolonies (Cheng et al., 2010). vWbp binds to Fg and prothrombin, activating prothrombin and generating fibrin that also contributes to the layer covering the microcolonies. Under shear stress in the blood vessels, secreted vWbp binds to vWF that is located at the damaged endothelial surface (Claes et al., 2014). vWF bound to vWbp induces a conformational change to vWbp in which soluble Fg binds to tethered vWbp. The MSCRAMMs of *S. aureus* also bind Fg, especially ClfA (Foster et al., 2014). vWbp also binds to the bound Fg that is captured by ClfA. ClfA forms a

complex with vWbp, vWF, and Fg (Claes et al., 2014; Claes et al., 2017; Claes et al., 2018). This allows the pathogen to adhere to the endothelial surface (Claes et al., 2014). In addition, ClfA can bind to Fg/fibrin tethering *S. aureus* to polymerized fibrin cables (McAdow et al., 2011; Thammavongsa et al., 2015). An increase in Fg concentration also results in Fg binding to other Fg molecules (Mosesson, 2005). Complement proteins also arrive at the site of injury in which C3b and C3 convertases bind to the bacterial surface (Foster, 2005). Efb and Ecb can bind to C3b that is bound to the bacterial surface (Haspel et al., 2008; Amdahl et al., 2013). Efb can also bind to soluble Fg; thus, bringing Fg to the bacterial surface to contribute to shield formation during the post-exponential phase. With vWbp being the key player, a Fg/fibrin mesh begins to form at the periphery of the Fg/fibrin composed pseudocapsule that was created by Coa, vWbp, Efb and the Fg-binding MSCRAMMs (Guggenberger et al., 2012; Rivera et al., 2007). Neutrophils and other immune response cells are not able to come in contact with the Fg/fibrin pseudocapsule due to the presence of the Fg/fibrin mesh (Ko et al., 2013; Guggenberger et al., 2012; Cheng et al., 2010). Therefore, the Fg shield protects *S. aureus* from bacterial clearance.

Structural mosaic proteins are defined as proteins comprising of different functional domains, giving the protein multiple functions (Patthy, 1988). vWbp, Coa and Efb belong to a family of structurally related mosaic proteins that are composed of different functional binding sites (Fig 24; (Thomer et al., 2016b)). The N-terminal region of vWbp shows predicted structural similarity to the N-terminal half of Coa, that is composed of 2, 3 α-helical bundles (Friedrich et al., 2003). Both N-terminal regions encompass the prothrombin-binding domain, D_1D_2. The C-terminal half of Coa and the N-terminal region of Efb harbor the predicted disordered, Fg-binding motif (Ko et al., 2016; Ko and Flick, 2016). The motifs for both Efb and Coa share sequence similarity. Some proteins may appear to be distantly related, due to sharing a similar

structure but not having the same function. The predicted structure of the C-terminal half vWbp is similar to that of the 3- α-helical structure of the C-terminal region of Efb. However, both regions do not share the same function since the ordered the C-terminal half of Efb harbors the C3b-binding site and the predicted ordered C-terminal section of vWbp binds Fg. Structural mosaic proteins can be used as a helpful tool in gaining a better understanding of a particular function, such as generating a chimeric protein composed of the same functional domain from two different proteins (Campbell et al., 1997). In addition, functions of mosaic proteins can be useful to study homologous proteins that are uncharacterized (Patthy, 1988).

S. aureus expresses three additional proteins that also belong to the structurally related family of secreted proteins, Ecb, SHPA, and SHPB (Table 4, 5). Our data showed that *ecb* is located in immune evasion cluster-2 (IEC-2) along with *efb*, in the vSaγ island (A-8; (Jongerius et al., 2007)). SHPA and SHPB are predicted to be structurally homologous to the C-terminal Fg-binding region of vWbp (Fig 23). The two proteins are functionally uncharacterized. Our data provides insight into identifying additional proteins of *S. aureus* that may be structurally and functionally similar to other well-characterized proteins of the pathogen (Table 4, 5). Some genes that encode for proteins that are homologous to the MSCRAMMs or other SERAMs may have been possibly acquired from other unidentified isolates or from different bacterial species via MGE. Nonetheless, Ecb, SHPA and SHPB may play a role in Fg/fibrin shield formation, especially if they have a similar function to that of Efb, vWbp or Coa, or they may play an entirely different role in one of the immune evasion mechanisms of *S. aureus*.

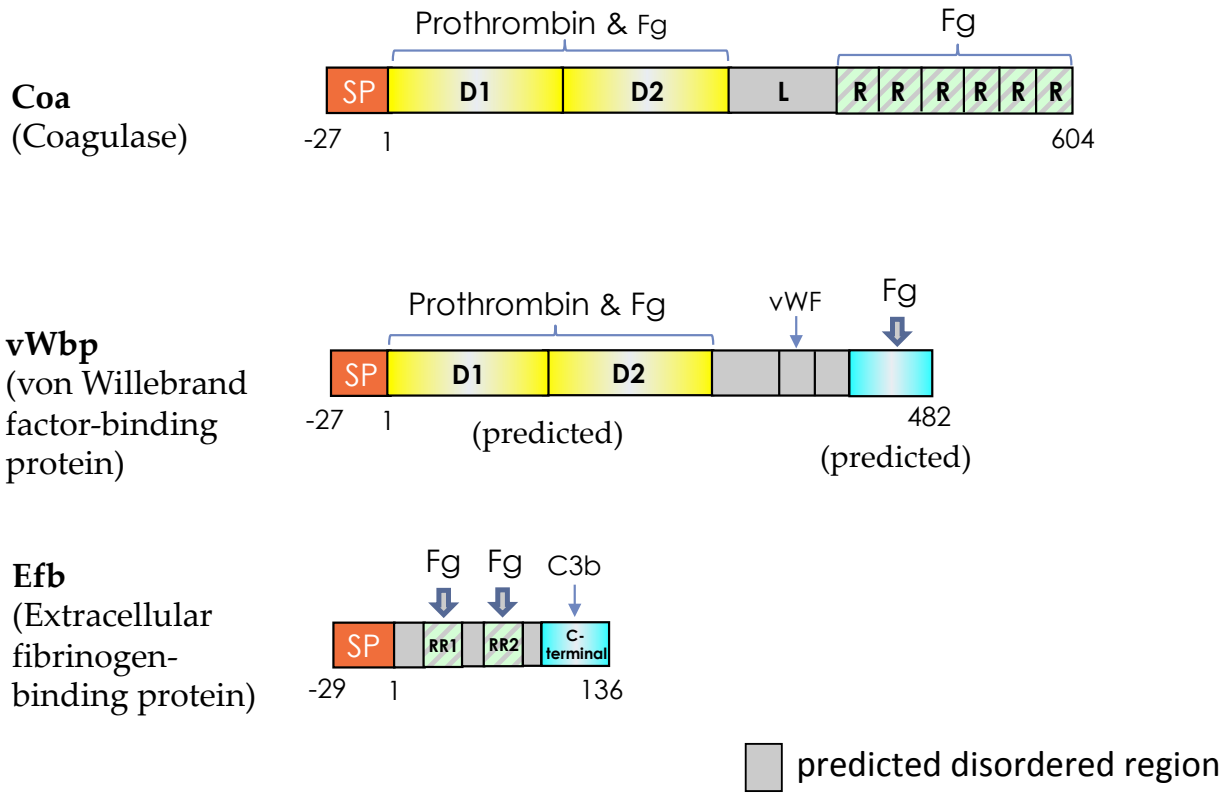

Figure 24. Family of secreted structurally related proteins. Model of the domain organizations of Coa, vWbp, and Efb. SP, Signal peptide, orange; D_1D_2, prothrombin-binding and fibrinogen-binding domains. R, repeat domain, light green; L, linker region. vWF indicates vWF-binding motif. Fg of the C-terminal region of vWbp represents the Fg-binding site. C3b indicates the C3b-binding motif. RR1, RR2, fibrinogen-binding motifs, light green. 2, 3 α-helix bundle, yellow; 3 α-helix, blue. Structures of domains of vWbp are predictions. Gray represents the predicted unordered region.

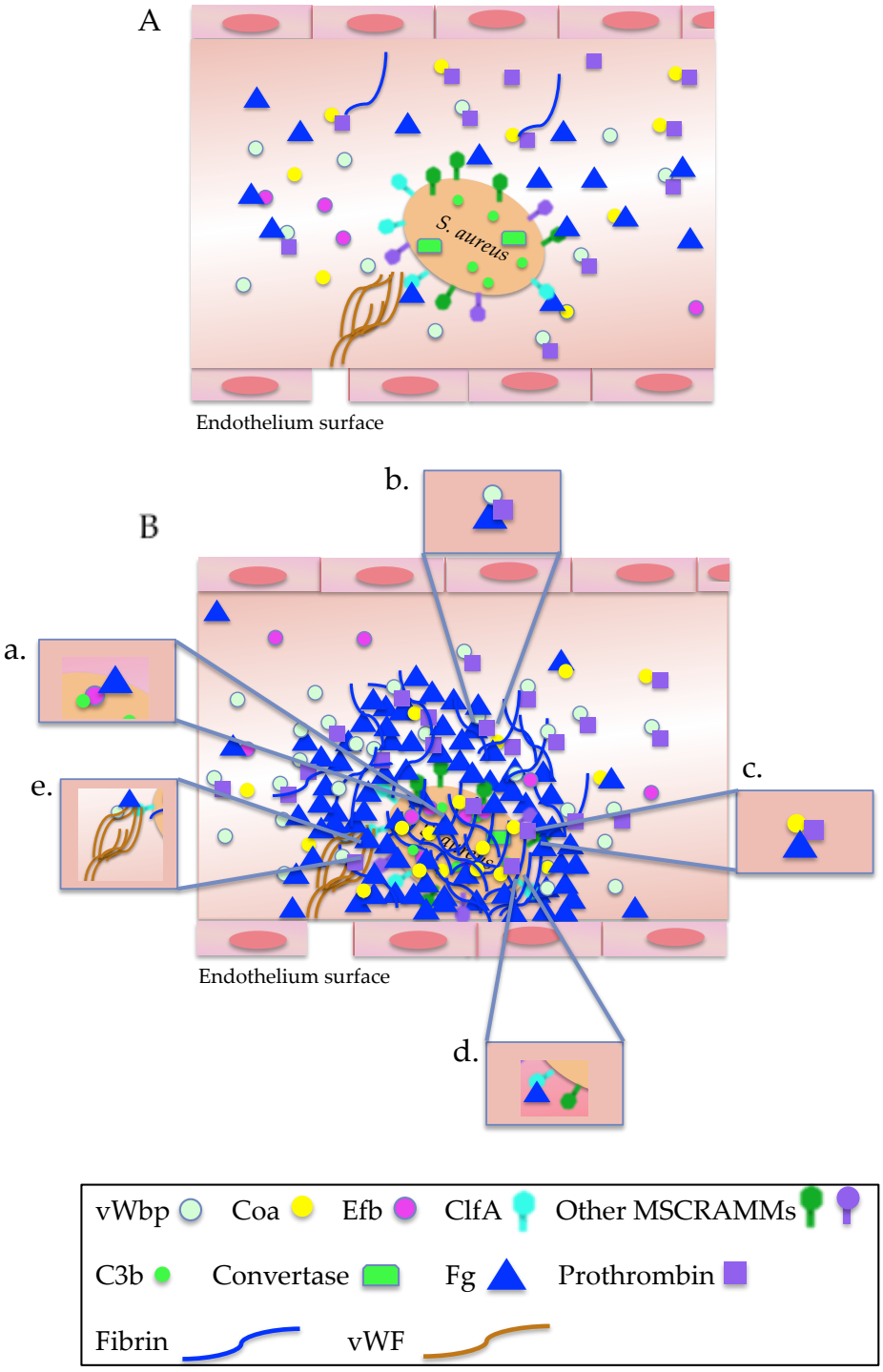

Figure 25. Efb, Coa and vWbp's role in Fg/fibrin shield formation.

Figure 25. Efb, Coa and vWbp's role in Fg/fibrin shield formation. Cartoon model of Fg/fibrin shield assembly of *S. aureus* by Efb, Coa and vWbp. Gap at the endothelial surface indicates breach of vessel wall barrier. **(A)** *S. aureus* enters into the blood vessel. Fibrinogen, blue triangle. Prothrombin, purple, square. Fibrin, blue. vWF, brown. C3b, light green, circle. Convertase, light green, rectangle. vWbp, light blue. Coa, yellow. Efb, magnenta. ClfA, turquoise. Other MSCRAMMs, dark green and purple. **(B)** *S. aureus* is covered by a layer of aggregated fibrin cables. A mesh of Fg/fibrin lies periphery to the first layer. a. Efb binds both C3b and Fg on the bacterial surface. b. vWbp in complex with prothrombin and Fg. c. Coa in complex with prothrombin and Fg. d. ClfA and other MSCRAMMs bind Fg. e. Ultra large vWF in complex with vWbp, Fg and ClfA.

Future work

Our data showed that the N-terminal prothrombin-binding domain of vWbp binds to the N-terminal Fg-β chain that harbors the thrombin cleavage site (Fig 18A, B, 19A). Both Fg and prothrombin are bulky molecules, yet prothrombin activation mediated by vWbp requires Fg. I would determine what role does Fg-binding play on the vWbp-prothrombin activation. One method to test this is by deleting the Fg-binding motifs of vWbp. First, I would determine the binding affinity of vWbp-N to the N-terminal Fg β-chain peptides (1-25) and (13-25) to see if there are additional residues required in the interaction using isothermal titration calorimetry (ITC) (Pierce et al., 1999; Du et al., 2016). To determine the amino acid residues involved in binding, crystallization of vWbp-N in complex with the N-terminal Fg β-chain would be done. To eliminate the Fg-binding motif for the C-terminal region of vWbp, I would delete the amino acid region 386-482. To determine the effect Fg-binding has on prothrombin activation mediated by vWbp, I would use recombinant constructs that lack the Fg-binding motif(s) and test their prothrombin activity using a chromogenic substrate assay. If the vWbp-prothrombin complex is activated, the complex can cleave the substrate, releasing a color in which its absorbance can be measured. Since vWbp binds to the region that contains the thrombin cleavage site on fibrinopeptide B, I would test if the vWbp-prothrombin complex cleaves the of N-terminal Fg-β chain. I would measure if fibrinopeptide B is released upon cleavage by incubating vWbp with prothrombin and Fg and use an antibody against fibrinopeptide B.

Since the C-terminal Fg-binding region of vWbp showed preference in binding to soluble Fg than the immobilized form (Fig 22A, B, C), I would test whether if vWbp binds to another ligand to induce a conformational change that allows its C-terminal half to bind immobilized Fg. vWbp has been suggested to bind to the A1 domain of vWF (Claes et al., 2014; Emsley et al.,

1998). To determine whether if binding causes a conformational change, crystallization of the apo-form of vWbp-C would be compared with vWbp-C in complex with vWF-A1 domain protein (Emsley et al., 1998; Moree et al., 2015). I would test if vWbp-C binding to immobilized Fg is enhanced in the presence of vWF or vWF-A1 domain using an ELISA type binding assay. In addition, using surface plasmon resonance (SPR) would be helpful in determining whether if there is an increase in vWbp binding to immobilized Fg in the presence vWF or vWF-A1 domain (Claes et al., 2014).

From our BLAST results (Table 4, 5), I identified two uncharacterized proteins, SHPA and SHPB that are homologous to the C-terminal Fg-binding motif of vWbp. I would characterize the function of the two proteins by determining whether if they can bind to immobilized or soluble Fg using an ELISA-type binding assay. I would identify which Fg polypeptide chain(s) do the proteins bind by doing a far western. In addition, I would test whether if SHPA and SHPB bind to complement proteins, such as C3b, since both homologs are predicted to be structurally related to the C3b-binding motif of Efb.

Clinical relevance

To date, most of the *S. aureus* clinical trials have not proceeded to phase II nor phase III (Mohamed et al., 2017; Redi et al., 2018). In addition, many of the vaccine candidates target surface bound proteins than secreted proteins (Mohamed et al., 2017). Three proteins that are structurally and functionally related in that they all bind to Fg and contribute to Fg/fibrin shield formation are Efb, Coa and vWbp, which are potential targets to use in creating a multi-target vaccine. A multi-target vaccine recognizing antigens that are both MSCRAMMs as well as SERAMs would be an effective therapeutic strategy as well as protective against *S. aureus* infections.

REFERENCES

Alberts, B., Johnson, A., Lewis, J., Raff, M., Roberts, K., and Walter, P. (2002). *Molecular Biology of the Cell*. 4th edition. New York: Garland Science; Innate Immunity.

Alqarihi, A., Singh, S., Edwards, J. E., Jr., Ibrahim, A. S., and Uppuluri, P. (2019). NDV-3A vaccination prevents C. albicans colonization of jugular vein catheters in mice. *Sci Rep, 9*(1), 6194. doi:10.1038/s41598-019-42517-y

Altschul, S.F., Gish, W., Miller, W., Myers, E.W. and Lipman, D.J. (1990) "Basic local alignment search tool." J. Mol. Biol. 215:403-410.

Amara, U., Rittirsch, D., Flierl, M., Bruckner, U., Klos, A., et al. (2008). Interaction between the coagulation and complement system. *Adv Exp Med Biol, 632*, 71-79.

Amdahl, H., Jongerius, I., Meri, T., Pasanen, T., Hyvarinen, S., et al. (2013). Staphylococcal Ecb protein and host complement regulator factor H enhance functions of each other in bacterial immune evasion. *J Immunol, 191*(4), 1775-1784. doi:10.4049/jimmunol.1300638

Aswani, V., Najar, F., Pantrangi, M., Mau, B., Schwan, W. R., and Shukla, S. K. (2019). Virulence factor landscape of a Staphylococcus aureus sequence type 45 strain, MCRF184. *BMC Genomics, 20*(1), 123. doi:10.1186/s12864-018-5394-2

Belaaouaj, A., Kim, K. S., and Shapiro, S. D. (2000). Degradation of outer membrane protein A in Escherichia coli killing by neutrophil elastase. *Science, 289*(5482), 1185-1188.

Beltrame, M. H., Catarino, S. J., Goeldner, I., Boldt, A. B., and de Messias-Reason, I. J. (2014). The lectin pathway of complement and rheumatic heart disease. *Front Pediatr, 2*, 148. doi:10.3389/fped.2014.00148

Bhattacharya, S., Ploplis, V. A., and Castellino, F. J. (2012). Bacterial plasminogen receptors utilize host plasminogen system for effective invasion and dissemination. *J Biomed Biotechnol, 2012*, 482096. doi:10.1155/2012/482096

Bjerketorp, J., Nilsson, M., Ljungh, A., Flock, J.I., Jacobsson, K., and Frykberg, L. (2002) A novel von Willebrand factor binding protein expressed by *Staphylococcus aureus*. *Microbiology.* 148, 2037-2044. doi:10.1099/00221287-148-7-2037

Bjerketorp, J., Jacobsson, K., and Frykberg, L. (2004). The von Willebrand factor-binding protein (vWbp) of Staphylococcus aureus is a coagulase. *FEMS Microbiol Lett.* 234, 309-314. doi:10.1016/j.femsle.2004.03.040

Brinkmann, V., and Zychlinsky, A. (2012). Neutrophil extracellular traps: is immunity the second function of chromatin? *J Cell Biol, 198*(5), 773-783. doi:10.1083/jcb.201203170

Bubeck, D., Roversi, P., Donev, R., Morgan, B. P., Llorca, O., and Lea, S. M. (2011). Structure of human complement C8, a precursor to membrane attack. *J Mol Biol, 405*(2), 325-330. doi:10.1016/j.jmb.2010.10.031

Campbell, R. K., Bergert, E. R., Wang, Y., Morris, J. C., and Moyle, W. R. (1997). Chimeric proteins can exceed the sum of their parts: implications for evolution and protein design. *Nat Biotechnol, 15*(5), 439-443. doi:10.1038/nbt0597-439

Centers for Disease Control and Prevention. (2013). Antibiotic resistant threats in the United States, 2013.

Chaplin, D. D. (2010). Overview of the immune response. J Allergy Clin Immunol, 125(2 Suppl 2), S3-23. doi:10.1016/j.jaci.2009.12.980

Chang, C. E., Chen, W., and Gilson, M. K. (2007). Ligand configurational entropy and protein binding. *Proc Natl Acad Sci U S A* 104, 1534-1539. doi:10.1073/pnas.0610494104

Chen, X., and Jensen, P. E. (2008). The role of B lymphocytes as antigen-presenting cells. *Arch Immunol Ther Exp (Warsz), 56*(2), 77-83. doi:10.1007/s00005-008-0014-5

Chen, L., Woo, M., Hakem, R., and Miller, R. G. (2003). Perforin-dependent activation-induced cell death acts through caspase 3 but not through caspases 8 or 9. *Eur J Immunol, 33*(3), 769-778. doi:10.1002/eji.200323783

Cheng, A. G., Kim, H. K., Burts, M. L., Krausz, T., Schneewind, O., and Missiakas, D. M.

(2009). Genetic requirements for *Staphylococcus aureus* abscess formation and persistence in host tissues. *FASEB J.* 23, 3393-3404. doi:10.1096/fj.09-135467

Cheng, A.G., McAdow, M., Kim, H.K., Bae, T., Missiakas, D.M., and Schneewind, O. (2010) Contribution of coagulases towards *Staphylococcus aureus* disease and protective immunity. *Plos Pathog.* 6:8. doi: 10.1371/journal.ppat.1001036

Cheng, A. G., DeDent, A. C., Schneewind, O., and Missiakas, D. (2011). A play in four acts: Staphylococcus aureus abscess formation. *Trends Microbiol, 19*(5), 225-232. doi:10.1016/j.tim.2011.01.007

Cheung, E. Y., Weijers, E. M., Tuk, B., Scheffer, R., Leebeek, F. W., et al. (2015). Specific effects of fibrinogen and the gammaA and gamma'-chain fibrinogen variants on angiogenesis and wound healing. *Tissue Eng Part A, 21*(1-2), 106-114. doi:10.1089/ten.TEA.2014.0020

Claes, J., Vanassche, T., Peetermans, M., Liesenborghs, L., Vandenbriele, C., et al. (2014). Adhesion of Staphylococcus aureus to the vessel wall under flow is mediated by von Willebrand factor-binding protein. *Blood, 124*(10), 1669-1676. doi:10.1182/blood-2014-02-558890

Claes, J., Liesenborghs, L., Peetermans, M., Veloso, T. R., Missiakas, D., et al. (2017). Clumping factor A, von Willebrand factor-binding protein and von Willebrand factor anchor Staphylococcus aureus to the vessel wall. *J Thromb Haemost, 15*(5), 1009-1019. doi:10.1111/jth.13653

Claes, J., Ditkowski, B., Liesenborghs, L., Veloso, T. R., Entenza, J. M., et al. (2018). Assessment of the Dual Role of Clumping Factor A in S. Aureus Adhesion to Endothelium in Absence and Presence of Plasma. *Thromb Haemost, 118*(7), 1230-1241. doi:10.1055/s-0038-1660435

Conway, E. M. (2015). Reincarnation of ancient links between coagulation and complement. *J Thromb Haemost, 13 Suppl 1*, S121-132. doi:10.1111/jth.12950

Crosby, H. A., Kwiecinski, J., and Horswill, A. R. (2016). Staphylococcus aureus Aggregation and Coagulation Mechanisms, and Their Function in Host-Pathogen Interactions. Adv Appl Microbiol, 96, 1-41. doi:10.1016/bs.aambs.2016.07.018

Davalos, D., and Akassoglou, K. (2012). Fibrinogen as a key regulator of inflammation in disease. *Semin Immunopathol, 34*(1), 43-62. doi:10.1007/s00281-011-0290-8

Deckmyn, H., and Vanhoorelbeke, K. (2006). When collagen meets VWF. Blood, 08(12), 3628. Accessed May 06, 2019. doi.org/10.1182/blood-2006-09-046540.

De Luca, C., Colangelo, A. M., Alberghina, L., and Papa, M. (2018). Neuro-Immune Hemostasis: Homeostasis and Diseases in the Central Nervous System. *Frontiers in cellular neuroscience*, *12*, 459. doi:10.3389/fncel.2018.00459

Doolittle, R. F. (1984). Fibrinogen and fibrin. *Annu Rev Biochem, 53*, 195-229. doi:10.1146/annurev.bi.53.070184.001211

Du, X., Li, Y., Xia, Y. L., Ai, S. M., Liang, J., Sang, P., Ji, X.L., and Liu, S. Q. (2016). Insights into Protein-Ligand Interactions: Mechanisms, Models, and Methods. *Int J Mol Sci, 17*(2). doi:10.3390/ijms17020144

Duncan, A. R., and Winter, G. (1988). The binding site for C1q on IgG. *Nature, 332*(6166), 738-740. doi:10.1038/332738a0

Dunkelberger, J. R., and Song, W. C. (2010). Complement and its role in innate and adaptive immune responses. *Cell Res, 20*(1), 34-50. doi:10.1038/cr.2009.139

Emsley, J., Cruz, M., Handin, R., and Liddington, R. (1998). Crystal structure of the von Willebrand Factor A1 domain and implications for the binding of platelet glycoprotein Ib. *J Biol Chem, 273*(17), 10396-10401.

Endo, Y., Nakazawa, N., Iwaki, D., Takahashi, M., Matsushita, M., and Fujita, T. (2010). Interactions of ficolin and mannose-binding lectin with fibrinogen/fibrin augment the lectin complement pathway. *J Innate Immun, 2*(1), 33-42. doi:10.1159/000227805

Entenza, J. M., Foster, T. J., Ni Eidhin, D., Vaudaux, P., Francioli, P., and Moreillon, P. (2000). Contribution of clumping factor B to pathogenesis of experimental endocarditis due to Staphylococcus aureus. *Infect Immun, 68*(9), 5443-5446.

Favrot, L., Blanchard, J. S., and Vergnolle, O. (2016). Bacterial GCN5-Related N-

Acetyltransferases: From Resistance to Regulation. *Biochemistry, 55*(7), 989-1002. doi:10.1021/acs.biochem.5b01269

Fletcher, S. (2015). Understanding the contribution of environmental factors in the spread of antimicrobial resistance. *Environ Health Prev Med, 20*(4), 243-252. doi:10.1007/s12199-015-0468-0

Flick, M. J., Du, X., Witte, D. P., Jirousková, M., Soloviev, D. A., et al. (2004) Leukocyte engagement of fibrin(ogen) via the integrin receptor alphaMbeta2/Mac-1 is critical for host inflammatory response *in vivo*. *J Clin Invest*. 113, 1596-1606. doi:10.1172/JCI20741

Flick, M. J., Du, X., Prasad, J. M., Raghu, H., Palumbo, J. S., Smeds, E., Hook, M., and Degen, J. L. (2013). Genetic elimination of the binding motif on fibrinogen for the S. aureus virulence factor ClfA improves host survival in septicemia. *Blood, 121*(10), 1783-1794. doi:10.1182/blood-2012-09-453894

Foster, T. (1996). Staphylococcus. In th & S. Baron (Eds.), *Medical Microbiology*. Galveston (TX).

Foster, T. J. (2005). Immune evasion by staphylococci. *Nat Rev Microbiol, 3*(12), 948-958. doi:10.1038/nrmicro1289

Foster, T. J., and Höök, M. (1998) Surface protein adhesins of *Staphylococcus aureus*. *Trends Microbiol*. 6, 484-488.

Foster, T. J., Geoghegan, J. A., Ganesh, V. K., and Hook, M. (2014). Adhesion, invasion and evasion: the many functions of the surface proteins of Staphylococcus aureus. *Nat Rev Microbiol, 12*(1), 49-62. doi:10.1038/nrmicro3161

Fowler, V.G. Jr., and Proctor, R.A. (2014) Where does a *Staphylococcus aureus* vaccine stand? *Clin Microbiol Infect.* 20, 66-75. doi: 10.1111/1469-0691.12570

Friedrich, R., Panizzi, P., Fuentes-Prior, P., Richter, K., Verhamme, I., et al. (2003). Staphylocoagulase is a prototype for the mechanism of cofactor-induced zymogen activation. *Nature* 425, 535-539.

Frost, L. S., Leplae, R., Summers, A. O., and Toussaint, A. (2005). Mobile genetic elements: the agents of open source evolution. *Nat Rev Microbiol, 3*(9), 722-732. doi:10.1038/nrmicro1235

Ganesh, V. K., Rivera, J. J., Smeds, E., Ko, Y. P., Bowden, M. G., Wann, E. R., Gurusiddappa, S., Fitzgerald, J. R., and Höök, M. (2008). A structural model of the *Staphylococcus aureus* ClfA-fibrinogen interaction opens new avenues for the design of anti-staphylococcal therapeutics. *PLoS Pathog.* 4:11. doi: 10.1371/journal.ppat.1000226

Geraci, J., Neubauer, S., Pollath, C., Hansen, U., Rizzo, F., et al. (2017). The Staphylococcus aureus extracellular matrix protein (Emp) has a fibrous structure and binds to different extracellular matrices. *Sci Rep, 7*(1), 13665. doi:10.1038/s41598-017-14168-4

Gill, S. R., Fouts, D. E., Archer, G. L., Mongodin, E. F., Deboy, R. T., et al. (2005). Insights on evolution of virulence and resistance from the complete genome analysis of an early methicillin-resistant Staphylococcus aureus strain and a biofilm-producing methicillin-resistant Staphylococcus epidermidis strain. *J Bacteriol, 187*(7), 2426-2438. doi:10.1128/JB.187.7.2426-2438.2005

Gordon, R. J., and Lowy, F. D. (2008). Pathogenesis of methicillin-resistant Staphylococcus aureus infection. *Clin Infect Dis, 46 Suppl 5*, S350-359. doi:10.1086/533591

Greenfield, N., and Fasman, G. D. (1969). Computed circular dichroism spectra for the evaluation of protein conformation. *Biochemistry.* 8, 4108-4116.

Guggenberger, C, Wolz C., Morrissey J.A., and Heesemann, J. (2012). Two distinct coagulase-dependent barriers protect *Staphylococcus aureus* from neutrophils in a three dimensional *in vitro* model. *PLoS Pathog.* 8:1. doi: 10.1371/journal.ppat.1002434

Haas, P. J., and van Strijp, J. (2007). Anaphylatoxins: their role in bacterial infection and inflammation. *Immunol Res, 37*(3), 161-175.

Hanssen, A. M., and Ericson Sollid, J. U. (2006). SCCmec in staphylococci: genes on the move. *FEMS Immunol Med Microbiol, 46*(1), 8-20. doi:10.1111/j.1574-695X.2005.00009.x

Harraghy, N., Homerova, D., Herrmann, M., and Kormanec, J. (2008). Mapping the transcription start points of the *Staphylococcus aureus eap, emp, and vwb* promoters reveals a

conserved octanucleotide sequence that is essential for expression genes. *J Bacteriol.* 190, 447-451.

Haspel, N., Ricklin, D., Geisbrecht, B. V., Kavraki, L. E., and Lambris, J. D. (2008). Electrostatic contributions drive the interaction between Staphylococcus aureus protein Efb-C and its complement target C3d. *Protein Sci, 17*(11), 1894-1906. doi:10.1110/ps.036624.108

Haupt, K., Reuter, M., van den Elsen, J., Burman, J., Hälbich, S., Richter, J., Skerka, C., and Zipfel, P. (2008). The Staphylococcus aureus protein Sbi acts as a complement inhibitor and forms a tripartite complex with host complement Factor H and C3b. *PLoS Pathog.* 4(12):e1000250.

Jensen, P. H., Weilguny, D., Matthiesen, F., McGuire, K. A., Shi, L., and Hojrup, P. (2005). Characterization of the oligomer structure of recombinant human mannan-binding lectin. J Biol Chem, 280(12), 11043-11051. doi:10.1074/jbc.M412472200

Jongerius, I., Kohl, J., Pandey, M. K., Ruyken, M., van Kessel, K. P., van Strijp, J. A., and Rooijakkers, S. H. (2007). Staphylococcal complement evasion by various convertase-blocking molecules. *J Exp Med, 204*(10), 2461-2471. doi:10.1084/jem.20070818

Jongerius, I., Garcia, B. L., Geisbrecht, B. V., van Strijp, J. A., and Rooijakkers, S. H. (2010). Convertase inhibitory properties of Staphylococcal extracellular complement-binding protein. *J Biol Chem, 285*(20), 14973-14979. doi:10.1074/jbc.M109.091975

Jorgensen, I., Rayamajhi, M., and Miao, E. A. (2017). Programmed cell death as a defence against infection. Nat Rev Immunol, 17(3), 151-164. doi:10.1038/nri.2016.147

Kang, M., Ko, Y. P., Liang, X., Ross, C. L., Liu, Q., Murray, B. E., and Hook, M. (2013). Collagen-binding microbial surface components recognizing adhesive matrix molecule (MSCRAMM) of Gram-positive bacteria inhibit complement activation via the classical pathway. *J Biol Chem, 288*(28), 20520-20531. doi:10.1074/jbc.M113.454462

Kawabata, S., Morita, T., Iwanaga, S., and Igarashi, H. (1985). Staphylocoagulase-binding region in human prothrombin. *J Biochem.* 97, 325-331.

Kelly, S. M., Jess, T. J., and Price, N. C. (2005). How to study proteins by circular dichroism.

Biochim Biophys Acta, 1751, 119-139.

Kelley, L. A., Mezulis, S., Yates, C. M., Wass, M. N., and Sternberg, M. J. (2015). The Phyre2 web portal for protein modeling, prediction and analysis. *Nat Protoc, 10*(6), 845-858. doi:10.1038/nprot.2015.053

Ko, Y. P., Liang, X., Smith, C. W., Degen, J. L., and Höök, M. (2011). Binding of Efb from *Staphylococcus aureus* to fibrinogen blocks neutrophil adherence. *J Biol Chem.* 286, 9865-9874. doi: 10.1074/jbc.M110.199687

Ko, Y.P., Kuipers A., Freitag C.M., Jongerius I., Medina E., van Rooijen W.J., Spaan A.N., van Kessel K.P., Höök M., and Rooijakkers, S.H. (2013). Phagocytosis escape by a Staphylococcus aureus protein that connects complement and coagulation proteins at the bacterial surface. *PLoS Pathog* 9:12. doi: 10.1371/journal.ppat.1003816

Ko, Y. P., and Flick, M. J. (2016). Fibrinogen is at the interface of host defense and pathogen virulence in *Staphylococcus aureus* infection. *Semin Thromb Hemost.* 42, 408-421. doi: 10.1055/s-0036-1579635

Ko, Y. P., Kang, M., Ganesh, V. K., Ravirajan, D., Li, B., and Höök, M. (2016). Coagulase and Efb of *Staphylococcus aureus* have a common fibrinogen binding motif. *MBio* 7:1. doi: 10.1128/mBio.01885-15

Köhler, S., Schmid, F., and Settanni, G. (2015). The Internal Dynamics of Fibrinogen and Its Implications for Coagulation and Adsorption. *PLoS Comput Biol, 11*(9), e1004346. doi:10.1371/journal.pcbi.1004346

Kovanen, S. M., Kivisto, R. I., Rossi, M., Schott, T., Karkkainen, U. M., Tuuminen, T., Uksila, J., Rautelin, H., and Hanninen, M. L. (2014). Multilocus sequence typing (MLST) and whole-genome MLST of Campylobacter jejuni isolates from human infections in three districts during a seasonal peak in Finland. *J Clin Microbiol, 52*(12), 4147-4154. doi:10.1128/JCM.01959-1

Kroh, H. K., Panizzi, P., and Bock, P. E. (2009). Von Willebrand factor-binding protein is a hysteretic conformational activator of prothrombin. *Proc Natl Acad Sci U S A* 106, 7786-7791. doi: 10.1073/pnas.0811750106

Kroh, H. K., and Bock, P. E. (2012). Effect of zymogen domains and active site occupation on activation of prothrombin by von Willebrand factor-binding protein. *J Biol Chem.* 287, 39149-39157. doi: 10.1074/jbc.M112.415562

Laarman AJ, Ruyken M, Malone CL, van Strijp JA, Horswill AR, Rooijakkers SH. Staphylococcus aureus metalloprotease aureolysin cleaves complement C3 to mediate immune evasion. *J Immunol*. 2011 Jun 1;186(11):6445-53.

Lacy, P. (2006). Mechanisms of degranulation in neutrophils. Allergy Asthma Clin Immunol, 2(3), 98-108. doi:10.1186/1710-1492-2-3-98

Lambert, M. (2011*).* IDSA Guidelines on the Treatment of MRSA Infections in Adults and Children *Clinical Infectious Diseases.* 15;84(4):455-463.

Lee, L. Y., Liang, X., Hook, M., and Brown, E. L. (2004). Identification and characterization of the C3 binding domain of the Staphylococcus aureus extracellular fibrinogen-binding protein (Efb). *J Biol Chem, 279*(49), 50710-50716. doi:10.1074/jbc.M408570200

Lenting, P. J., Christophe, O. D., and Denis, C. V. (2015). von Willebrand factor biosynthesis, secretion, and clearance: connecting the far ends. *Blood, 125*(13), 2019-2028. doi:10.1182/blood-2014-06-528406

Liesenborghs, L., Verhamme, P., and Vanassche, T. (2018). Staphylococcus aureus, master manipulator of the human hemostatic system. *J Thromb Haemost.* 16, 441-454. doi: 10.1111/jth.13928

Lim, K. T., Hanifah, Y. A., Yusof, M. Y., and Thong, K. L. (2012). Characterisation of the Virulence Factors and Genetic Types of Methicillin Susceptible Staphylococcus aureus from Patients and Healthy Individuals. *Indian J Microbiol, 52*(4), 593-600. doi:10.1007/s12088-012-0286-7

Lim, J. J., Grinstein, S., and Roth, Z. (2017). Diversity and Versatility of Phagocytosis: Roles in Innate Immunity, Tissue Remodeling, and Homeostasis. *Front Cell Infect Microbiol, 7*, 191. doi:10.3389/fcimb.2017.00191

Lobanovska, M., and Pilla, G. (2017). Penicillin's Discovery and Antibiotic Resistance: Lessonfor the Future? *Yale J Biol Med, 90*(1), 135-145.

Lorenz, N., Clow, F., Radcliff, F. J., and Fraser, J. D. (2013). Full functional activity of SSL7 requires binding of both complement C5 and IgA. *Immunol Cell Biol, 91*(7), 469-476. doi:10.1038/icb.2013.28

Lu, P. D., Galanakis, D. K., Ghebrehiwet, B., and Peerschke, E. I. (1999). The receptor for the globular "heads" of C1q, gC1q-R, binds to fibrinogen/fibrin and impairs its polymerization. *Clin Immunol, 90*(3), 360-367. doi:10.1006/clim.1998.4660

Malachowa, N., and DeLeo, F. R. (2010). Mobile genetic elements of Staphylococcus aureus. *Cell Mol Life Sci, 67*(18), 3057-3071. doi:10.1007/s00018-010-0389-4

Markiewski, M. M., Nilsson, B., Ekdahl, K. N., Mollnes, T. E., and Lambris, J. D. (2007). Complement and coagulation: strangers or partners in crime? *Trends Immunol, 28*(4), 184-192. doi:10.1016/j.it.2007.02.006

May, R. C., and Machesky, L. M. (2001). Phagocytosis and the actin cytoskeleton. *J Cell Sci, 114*(Pt 6), 1061-1077.

Mazzone, A., and Ricevuti, G. (1995). Leukocyte CD11/CD18 integrins: biological and clinical relevance. *Haematologica, 80*(2), 161-175.

McAdow, M., Kim, H. K., Dedent, A. C., Hendrickx, A. P., Schneewind, O., and Missiakas, D. M. (2011). Preventing *Staphylococcus aureus* sepsis through the inhibition of its agglutination in blood. *PLoS Pathog.* 7:10. doi: 10.1371/journal.ppat.1002307

McAdow, M., DeDent, A. C., Emolo, C., Cheng, A. G., Kreiswirth, B. N., Missiakas, D. M., and Schneewind, O. (2012a). Coagulases as determinants of protective immune responses against Staphylococcus aureus. *Infect Immun.* 80, 3389-3398. doi: 10.1128/IAI.00562-12

McAdow, M., Missiakas, D. M., and Schneewind, O. (2012b). *Staphylococcus aureus* secretes coagulase and von Willebrand factor binding protein to modify the coagulation cascade and establish host infections. *J Innate Immun.* 4, 141-148. doi: 10.1159/000333447

McDevitt, D., Nanavaty, T., House-Pompeo, K., Bell, E., Turner, N., McIntire, L., Foster, T., and Höök, M. (1997). Characterization of the interaction between the *Staphylococcus*

aureus clumping factor (ClfA) and fibrinogen. *Eur J Biochem.* 247, 416-424.

Merle, N. S., Church, S. E., Fremeaux-Bacchi, V., and Roumenina, L. T. (2015). Complement System Part I - Molecular Mechanisms of Activation and Regulation. *Front Immunol, 6*, 262. doi:10.3389/fimmu.2015.00262

Micsonai, A., Wien, F., Bulyaki, E., Kun, J., Moussong, E., Lee, Y. H., Goto, Y., Réfrégiers, M., and Kardos, J. (2018). BeStSel: a web server for accurate protein secondary structure prediction and fold recognition from the circular dichroism spectra. *Nucleic Acids Res.* 46, W315-W322. doi:10.1093/nar/gky497

Miller, L. G., and Kaplan, S. L. (2009). Staphylococcus aureus: a community pathogen. *Infect Dis Clin North Am, 23*(1), 35-52. doi:10.1016/j.idc.2008.10.002

Mohamed, N., Wang, M. Y., Le Huec, J. C., Liljenqvist, U., Scully, I. L., Baber, J., Begier, E., Jansen, K. U., Gurtman, A., and Anderson, A. S. (2017). Vaccine development to prevent Staphylococcus aureus surgical-site infections. *Br J Surg, 104*(2), e41-e54. doi:10.1002/bjs.10454

Moreillon, P., Entenza, J. M., Francioli, P., McDevitt, D., Foster, T. J., Francois, P., and Vaudaux, P. (1995). Role of *Staphylococcus aureus* coagulase and clumping factor in pathogenesis of experimental endocarditis. *Infect Immun.* 63, 4738-4743.

Moree, B., Connell, K., Mortensen, R. B., Liu, C. T., Benkovic, S. J., and Salafsky, J. (2015). Protein Conformational Changes Are Detected and Resolved Site Specifically by Second-Harmonic Generation. *Biophys J, 109*(4), 806-815. doi:10.1016/j.bpj.2015.07.016

Mosesson, M.W. (2005) Fibrinogen and fibrin structure and functions. *J Thromb Haemost.* 3, 1894-1904.

Nesargikar, P. N., Spiller, B., and Chavez, R. (2012). The complement system: history, pathways, cascade and inhibitors. *Eur J Microbiol Immunol (Bp), 2*(2), 103-111. doi:10.1556/EuJMI.2.2012.2.2

Noris, M., and Remuzzi, G. (2013). Overview of complement activation and regulation. *Semin Nephrol, 33*(6), 479-492. doi:10.1016/j.semnephrol.2013.08.001

Ogston, A. (1881). Report upon Micro-Organisms in Surgical Diseases. *Br Med J, 1*(1054), 369 b362-375. doi:10.1136/bmj.1.1054.369

Oikonomopoulou, K., Ricklin, D., Ward, P. A., and Lambris, J. D. (2012). Interactions between coagulation and complement--their role in inflammation. *Semin Immunopathol, 34*(1), 151-165. doi:10.1007/s00281-011-0280-x

Oki, T., Kitaura, J., Eto, K., Lu, Y., Maeda-Yamamoto, M., Inagaki, N., Nagai, H., Yamanishi, Y., Nakajima, H., Kumagai, H., and Kitamura, T. (2006). Integrin alphaIIbbeta3 induces the adhesion and activation of mast cells through interaction with fibrinogen. *J Immunol, 176*(1), 52-60.

Palma, M., Shannon, O., Quezada, H. C., Berg, A., and Flock, J. I. (2001). Extracellular fibrinogen-binding protein, Efb, from Staphylococcus aureus blocks platelet aggregation due to its binding to the alpha-chain. *J Biol Chem, 276*(34), 31691-31697. doi:10.1074/jbc.M104554200

Palta, S., Saroa, R., and Palta, A. (2014). Overview of the coagulation system. *Indian J Anaesth, 58*(5), 515-523. doi:10.4103/0019-5049.144643

Patthy, L. (1988). Detecting distant homologies of mosaic proteins. Analysis of the sequences of thrombomodulin, thrombospondin complement components C9, C8 alpha and C8 beta, vitronectin and plasma cell membrane glycoprotein PC-1. *J Mol Biol, 202*(4), 689-696.

Panizzi, P., Friedrich, R., Fuentes-Prior, P., Bode, W., and Bock, P.E. (2004) The staphylocoagulase family of zymogen activator and adhesion proteins. *Cell Mol Life Sci.* 61, 2793-2798.

Panizzi, P., Friedrich, R., Fuentes-Prior, P., Kroh, H. K., Briggs, J., Tans, G., Bode, W., and Bock, P. E. (2006a). Novel fluorescent prothrombin analogs as probes of staphylocoagulase-prothrombin interactions. *J Biol Chem.* 281, 1169-1178.

Panizzi, P., Friedrich, R., Fuentes-Prior, P., Richter, K., Bock, P. E., and Bode, W. (2006b). Fibrinogen substrate recognition by staphylocoagulase.(pro)thrombin complexes. *J Biol Chem,* 281, 1179-1187.

Pardos de la Gandara, M., Raygoza Garay, J. A., Mwangi, M., Tobin, J. N., Tsang, A., Khalida,

C., D'Orazio, B., Kost, Rhonda. G., Leinberger-Jabari, A., Coffran, C., Evering, T. H., Coller, B. S., Balachandra, S., Urban, T., Parola, C., Salvato, S., Jenks, N., Wu, D., Burgess, R., Chung, M., de Lencastre, H., and Tomasz, A. (2015). Molecular Types of Methicillin-Resistant Strains Causing Skin and Soft Tissue Infections and Nasal Colonization, Identified in Community Health Centers in New York City. Journal of Clinical Microbiology, 53(8), 2648-2658. doi:10.1128/jcm.00591-15

Peetermans, M., Vanassche, T., Liesenborghs, L., Claes, J., Vande Velde, G., Kwiecinksi, J., Jin, T., De Geest, B., Hoylaerts, M. F., Lijnen, R. H., and Verhamme, P. (2014). Plasminogen activation by staphylokinase enhances local spreading of S. aureus in skin infections. *BMC Microbiol, 14*, 310. doi:10.1186/s12866-014-0310-7

Peetermans, M., Verhamme, P., and Vanassche, T. (2015). Coagulase Activity by Staphylococcus aureus: A Potential Target for Therapy? *Semin Thromb Hemost, 41*(4), 433-444. doi:10.1055/s-0035-1549849

Perobelli, S. M., Galvani, R. G., Goncalves-Silva, T., Xavier, C. R., Nobrega, A., & Bonomo, A. (2015). Plasticity of neutrophils reveals modulatory capacity. Braz J Med Biol Res, 48(8), 665-675

Petersen, S. V., Thiel, S., and Jensenius, J. C. (2001). The mannan-binding lectin pathway of complement activation: biology and disease association. *Mol Immunol, 38*(2-3), 133-149.

Pham, C. T. (2006). Neutrophil serine proteases: specific regulators of inflammation. *Nat Rev Immunol, 6*(7), 541-550. doi:10.1038/nri1841

Pierce, M. M., Raman, C. S., and Nall, B. T. (1999). Isothermal titration calorimetry of protein-protein interactions. *Methods, 19*(2), 213-221. doi:10.1006/meth.1999.0852

Ponnuraj, K., Bowden, M. G., Davis, S., Gurusiddappa, S., Moore, D., Choe, D., Xu, Y., Höök, M., and Narayana, S. V. (2003). A "dock, lock, and latch" structural model for a staphylococcal adhesin binding to fibrinogen. *Cell* 115, 217-228.

Portman, J. J. (2010). Cooperativity and protein folding rates. *Curr Opin Struct Biol.* 20, 11-15. doi: 10.1016/j.sbi.2009.12.013

Pozzi, N., Chen, Z., Gohara, D. W., Niu, W., Heyduk, T., and Di Cera, E. (2013). Crystal

structure of prothrombin reveals conformational flexibility and mechanism of activation. *J Biol Chem.* 288, 22734-22744. doi: 10.1074/jbc.M113.466946

Redi, D., Raffaelli, C. S., Rossetti, B., De Luca, A., and Montagnani, F. (2018). Staphylococcus aureus vaccine preclinical and clinical development: current state of the art. *New Microbiol, 41*(3), 208-213.

Riedel, T., Suttnar, J., Brynda, E., Houska, M., Medved, L., and Dyr, J. E. (2011). Fibrinopeptides A and B release in the process of surface fibrin formation. *Blood, 117*(5), 1700-1706. doi:10.1182/blood-2010-08-300301

Rivera, J., Vannakambadi, G., Hook, M., and Speziale, P. (2007). Fibrinogen-binding proteins of Gram-positive bacteria. *Thromb Haemost, 98*(3), 503-511.

Robinson, J. M. (2008). Reactive oxygen species in phagocytic leukocytes. *Histochem Cell Biol, 130*(2), 281-297. doi:10.1007/s00418-008-0461-4

Rubel, C., Fernández, G.C., Dran, G., Bompadre, M.B., Isturiz, M.A., and Palermo, M.S. (2001) Fibrinogen promotes neutrophil activation and delays apoptosis. *J Immunol.* 166, 2002-2010.

Savini, V. (2018). Pet-to man traveling Staphylococci. London: Academic Press.

Seo, H. S., and Sullam, P. M. (2011). Characterization of the fibrinogen binding domain of bacteriophage lysin from Streptococcus mitis. *Infect Immun, 79*(9), 3518-3526. doi:10.1128/IAI.05088-11

Schuijs, M. J., Hammad, H., and Lambrecht, B. N. (2019). Professional and 'Amateur' Antigen-Presenting Cells In Type 2 Immunity. *Trends Immunol, 40*(1), 22-34. doi:10.1016/j.it.2018.11.001

Schultz, H., and Weiss, J. P. (2007). The bactericidal/permeability-increasing protein (BPI) in infection and inflammatory disease. Clin Chim Acta, 384(1-2), 12-23. doi:10.1016/j.cca.2007.07.005

Sethi, S., and Chakraborty, T. (2011). Role of TLR- / NLR-signaling and the associated

cytokines involved in recruitment of neutrophils in murine models of Staphylococcus aureus infection. *Virulence, 2*(4), 316-328.

Sievers, F., Wilm, A., Dineen, D., Gibson, T. J., Karplus, K., Li, W., Lopez, R., McWilliam, H., Remmert, M., Soding, J., Thompson, J. D., and Higgins, D. G. (2011). Fast, scalable generation of high-quality protein multiple sequence alignments using Clustal Omega. *Mol Syst Biol, 7*, 539. doi:10.1038/msb.2011.75

Smith, S. A., Travers, R. J., and Morrissey, J. H. (2015). How it all starts: Initiation of the clotting cascade. *Crit Rev Biochem Mol Biol, 50*(4), 326-336. doi:10.3109/10409238.2015.1050550

Smyth, D. S., Meaney, W. J., Hartigan, P. J., and Smyth, C. J. (2007). Occurrence of ssl genes in isolates of Staphylococcus aureus from animal infection. *J Med Microbiol, 56*(Pt 3), 418-425. doi:10.1099/jmm.0.46878-0

Spaan, A. N., Surewaard, B. G., Nijland, R., and van Strijp, J. A. (2013). Neutrophils versus Staphylococcus aureus: a biological tug of war. Annu Rev Microbiol, 67, 629-650. doi:10.1146/annurev-micro-092412-155746

Spickett, C. M., Jerlich, A., Panasenko, O. M., Arnhold, J., Pitt, A. R., Stelmaszynska, T., and Schaur, R. J. (2000). The reactions of hypochlorous acid, the reactive oxygen species produced by myeloperoxidase, with lipids. *Acta Biochim Pol, 47*(4), 889-899.

Stapleton, P. D., and Taylor, P. W. (2002). Methicillin resistance in Staphylococcus aureus: mechanisms and modulation. *Sci Prog, 85*(Pt 1), 57-72.

Sullivan, M. J., Petty, N. K., and Beatson, S. A. (2011). Easyfig: a genome comparison visualizer. *Bioinformatics, 27*(7), 1009-1010. doi:10.1093/bioinformatics/btr039

Sun, D. (2018). Pull in and Push Out: Mechanisms of Horizontal Gene Transfer in Bacteria. *Front Microbiol, 9*, 2154. doi:10.3389/fmicb.2018.02154

Swanson, J. A., and Baer, S. C. (1995). Phagocytosis by zippers and triggers. *Trends Cell Biol, 5*(3), 89-93.

Tacconelli, E., and Magrini, N. (2017) Global priority list of antibiotic-resistant bacteria to guide research, discovery, and development of new antibiotics. Geneva, Switzerland: WHO Press, 1-7.

Tager, M. (1974). Current views on the mechanism of coagulase action in blood clotting. *Ann N Y Acad Sci.* 236, 277-291.

Thammavongsa, V., Kim, H. K., Missiakas, D., and Schneewind O. (2015). Staphylococcal manipulation of host immune responses. *Nat Rev Microbiol*. 13(9):529-43.

Thielens, N. M., Tedesco, F., Bohlson, S. S., Gaboriaud, C., and Tenner, A. J. (2017). C1q: A fresh look upon an old molecule. Mol Immunol, 89, 73-83. doi:10.1016/j.molimm.2017.05.025

Thomas, S., Liu, W., Arora, S., Ganesh, V., Ko, Y. P., and Hook, M. (2019). The Complex Fibrinogen Interactions of the Staphylococcus aureus Coagulases. *Front Cell Infect Microbiol, 9*, 106. doi:10.3389/fcimb.2019.00106

Thomer, L., Schneewind, O., and Missiakas, D. (2013). Multiple ligands of von Willebrand factor-binding protein (vWbp) promote *Staphylococcus aureus* clot formation in human plasma. *J Biol Chem.* 288, 28283-28292. doi: 10.1074/jbc.M113.493122

Thomer, L., Emolo, C., Thammavongsa, V., Kim, H. K., McAdow, M. E., Yu, W., Kieffer, M., Schneewind, O., and Missiakas, D. (2016a). Antibodies against a secreted product of Staphylococcus aureus trigger phagocytic killing. *J Exp Med.* 213, 293-301. doi: 10.1084/jem.20150074

Thomer, L., Schneewind , O., and Missiakas, D. (2016b). Pathogenesis of *Staphylococcus aureus* Bloodstream Infections. *Annu Rev Pathol* 11, 343-364. doi: 10.1146/annurev-pathol-012615-044351

Thurman, J. M., and Holers, V. M. (2006). The central role of the alternative complement pathway in human disease. *J Immunol, 176*(3), 1305-1310.

Tong, S. Y., Davis, J. S., Eichenberger, E., Holland, T. L., and Fowler, V. G., Jr. (2015). Staphylococcus aureus infections: epidemiology, pathophysiology, clinical manifestations, and management. *Clin Microbiol Rev, 28*(3), 603-661.

doi:10.1128/CMR.00134-14

Tulinski, P., Duim, B., Wittink, F. R., Jonker, M. J., Breit, T. M., van Putten, J. P., Wagenaar, J. A., and Fluit, A. C. (2014). Staphylococcus aureus ST398 gene expression profiling during ex vivo colonization of porcine nasal epithelium. *BMC Genomics, 15*, 915. doi:10.1186/1471-2164-15-915

Vadasz, B., Chen, P., Yougbare, I., Zdravic, D., Li, J., Li, C., Carrim, N and Ni, H. (2015). Platelets and platelet alloantigens: Lessons from human patients and animal models of fetal and neonatal alloimmune thrombocytopenia. *Genes Dis,* 2(2), 173-185. doi:10.1016/j.gendis.2015.02.003

Vandenesch, F., Lina, G., and Henry, T. (2012). Staphylococcus aureus hemolysins, bi-component leukocidins, and cytolytic peptides: a redundant arsenal of membrane-damaging virulence factors? *Front Cell Infect Microbiol, 2*, 12. doi:10.3389/fcimb.2012.00012

van der Lee, R., Buljan, M., Lang, B., Weatheritt, R. J., Daughdrill, G. W., et al. (2014). Classification of intrinsically disordered regions and proteins. *Chem Rev.* 114, 6589-6631. doi: 10.1021/cr400525m

Vazquez, V., Liang, X., Horndahl, J. K., Ganesh, V. K., Smeds, E., Foster, T. J., and Hook, M. (2011). Fibrinogen is a ligand for the Staphylococcus aureus microbial surface components recognizing adhesive matrix molecules (MSCRAMM) bone sialoprotein-binding protein (Bbp). *J Biol Chem.* 286, 29797-29805. doi: 10.1074/jbc.M110.214981

Walch, M., Dotiwala, F., Mulik, S., Thiery, J., Kirchhausen, T., et al. (2014). Cytotoxic cells kill intracellular bacteria through granulysin-mediated delivery of granzymes. *Cell*, 157(6), 1309-1323. doi:10.1016/j.cell.2014.03.062

Walker, J. B., and Nesheim, M. E. (1999). The molecular weights, mass distribution, chain composition, and structure of soluble fibrin degradation products released from a fibrin clot perfused with plasmin. *J Biol Chem, 274*(8), 5201-5212. doi:10.1074/jbc.274.8.5201

Weisel, J. W. (2005). Fibrinogen and fibrin. *Adv Protein Chem, 70*, 247-299. doi:10.1016/S0065-3233(05)70008-5

Weisel, J.W., and Litvinov, R. I. (2017) Fibrin Formation, Structure and Properties. *Subcell Biochem.* 82, 405-456. doi:10.1007/978-3-319-49674-0_13

Wiedemann, C., Bellstedt, P., and Gorlach, M. (2013). CAPITO--a web server-based analysis and plotting tool for circular dichroism data. *Bioinformatics.* 29, 1750-1757. doi:10.1093/bioinformatics/btt278

Wolberg, A. S., and Campbell, R. A. (2008). Thrombin generation, fibrin clot formation and hemostasis. *Transfus Apher Sci, 38*(1), 15-23. doi:10.1016/j.transci.2007.12.005

Ugarova, T. P., Budzynski, A. Z., Shattil, S. J., Ruggeri, Z. M., Ginsberg, M. H., and Plow, E. F. (1993). Conformational changes in fibrinogen elicited by its interaction with platelet membrane glycoprotein GPIIb-IIIa. *J Biol Chem.* 268, 21080-21087

Uhlemann, A. C., Dordel, J., Knox, J. R., Raven, K. E., Parkhill, J., et al. (2014). Molecular tracing of the emergence, diversification, and transmission of S. aureus sequence type 8 in a New York community. *Proc Natl Acad Sci USA*, 111(18), 6738-6743. doi:10.1073/pnas.1401006111

Urano, T., Castellino, F. J., and Suzuki, Y. (2018). Regulation of plasminogen activation on cell surfaces and fibrin. J Thromb Haemost. doi:10.1111/jth.14157

Uribe-Querol, E., and Rosales, C. (2017). Control of Phagocytosis by Microbial Pathogens. Front Immunol, 8, 1368. doi:10.3389/fimmu.2017.01368

Voskoboinik, I., Whisstock, J. C., and Trapani, J. A. (2015). Perforin and granzymes: function, dysfunction and human pathology. *Nat Rev Immunol, 15*(6), 388-400. doi:10.1038/nri3839

Zhang, J., Suo, Y., Zhang, D., Jin, F., Zhao, H., and Shi, C. (2018). Genetic and Virulent Difference Between Pigmented and Non-pigmented *Staphylococcus aureus*. *Frontiers in microbiology*, *9*, 598. doi:10.3389/fmicb.2018.00598

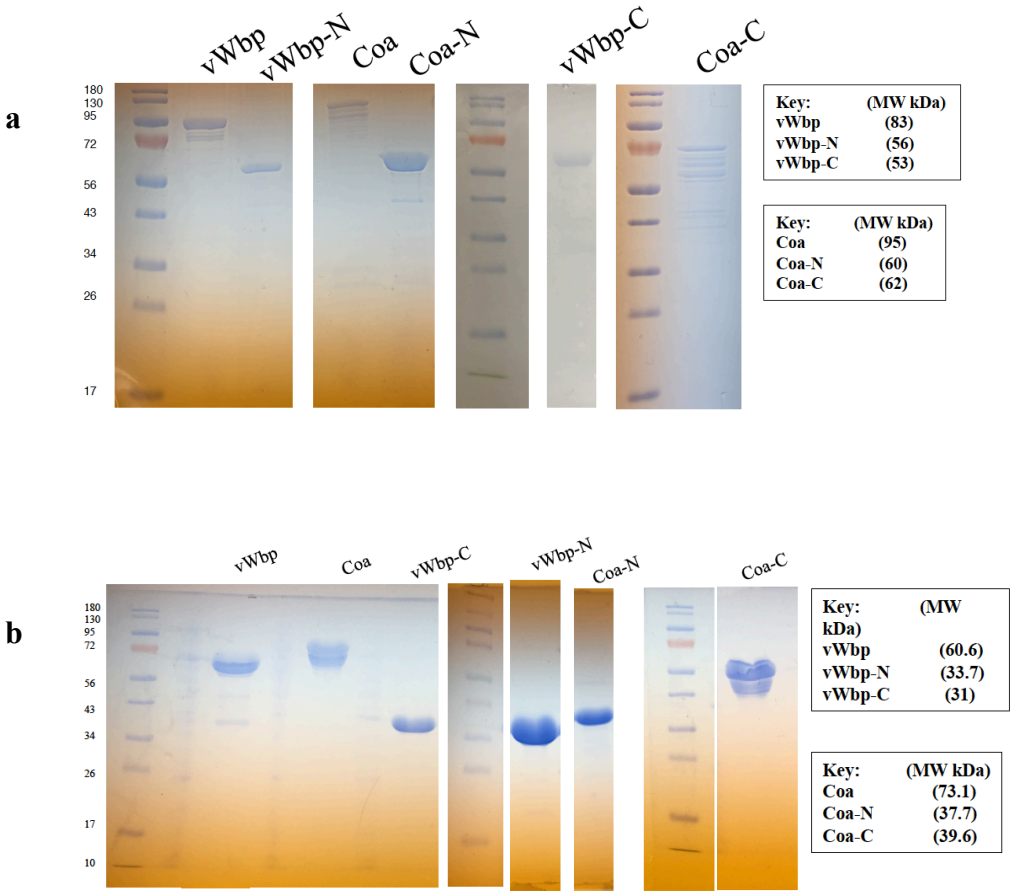

Figure A-1. Coomassie stained gel of vWbp and Coa constructs. (a) GST-tagged constructs or **(b)** His-tagged constructs. C-terminal vWbp and Coa proteins show multiple bands, suggesting extensive degradation. (Reprinted with permission from Thomas et al., 2019)

a

Protein	Algorithm	α-helix	Parallel β-sheet	Anti-Parallel β-sheet	Turns	Unordered	Others
vWbp	Bestsel	26.2	2.3	17.6	13.9		40
	CAPITO	18.8	15			57.2	
vWbp-N	Bestsel	34.4	3.6	14.9	12.3		34.8
	CAPITO	26.8	11.8			52	
vWbp-C	Bestsel	1.4	0.7	41.7	16.6		39.8
	CAPITO	4	38.2			61.6	
vWbp-N+-C	Bestsel	32	3.6	11.3	13.5		39.7
	CAPITO	29.5	6			59	

b

Protein	Algorithm	α-helix	Parallel β-sheet	Anti-Parallel β-sheet	Turns	Unordered	Others
Coa	Bestsel	20.4	3.7	18.6	14.8		42.6
	CAPITO	15.8	16			60.4	
Coa-N	Bestsel	32.2	13.8	5.1	12.7		36.2
	CAPITO	28.7	15			50	
Coa-C	Bestsel	5.3	0.08	42.7	16.2		35.8
	CAPITO	6.8	21.5			72.5	
Coa-N+-C	Bestsel	30.8	3.1	12.5	13.2		40.6
	CAPITO	27	5			63.5	

Figure A-2. Deconvolution of (a) vWbp and (b) Coa constructs. (Reprinted with permission from Thomas et al., 2019)

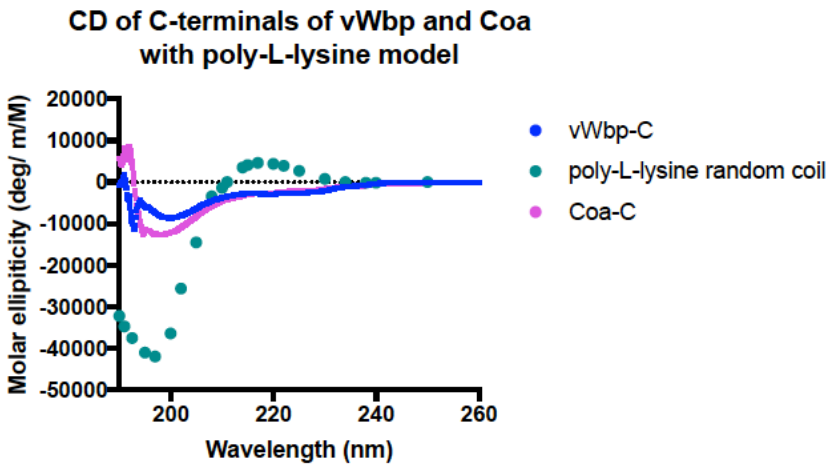

Figure A-3. Circular dichroism of C-terminals vWbp and Coa. Molar ellipiticity = deg x pathlength (mm) x concentration of peptide bonds (μM). Model used was poly-Llysine, random coil structure (Greenfield and Fasman, 1969). (Reprinted with permission from Thomas et al., 2019)

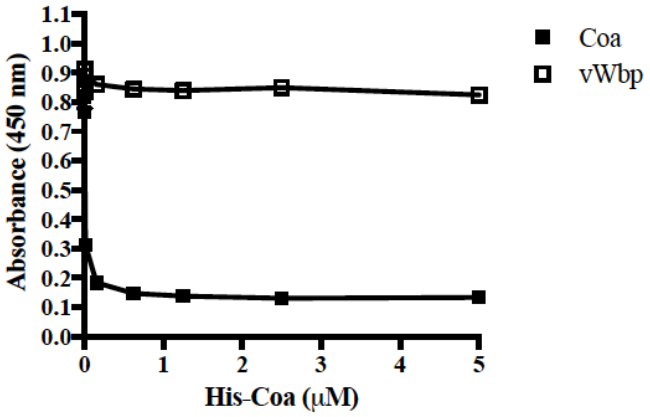

Figure A-4. vWbp and Coa do not target the same binding sites in Fg. Competition ELISA of GST-vWbp (25nM) or GST-Coa (1 nM) binding to immobilized Fg (0.5 μg/well) by His-Coa. Error bars, standard error of the mean (SEM). (Reprinted with permission from Thomas et al., 2019)

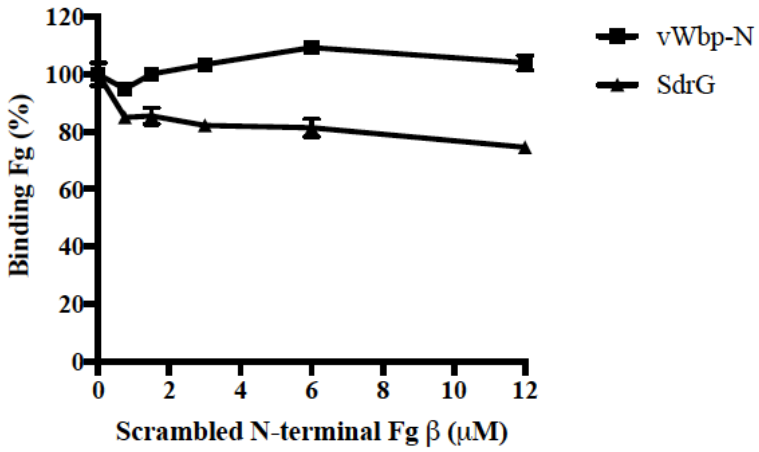

Figure A-5. vWbp and SdrG do not bind to Scrambled Fg β peptide. Inhibition of GST-vWbp-N (2 nM) or SdrG (50 nM) binding to immobilized Fg (0.5 μg/well) by scrambled Fg β (1-25) peptide. Error bars, standard error of the mean (SEM). (Reprinted with permission from Thomas et al., 2019)

Primers	Forward sequence	Reverse sequence
His-vWbp	5'- CAAG GGA TCC GTG GTT TCT GGG GAG AAG AAT C	5'-CAAT C TG CAG TTA TTT GCC ATT ATA TAC TTT ATT GAT TTG
His-vWbp-N	5'- CAAG GGA TCC GTG GTT TCT GGG GAG AAG AAT C	5'- CAAT C TG CAG TTA TTC ATC ACT TTT TGC TGC TTC
His-vWbp-C	5'- CAAG GGA TCC TCA AAA AGA AGC AAG AGA AG	5- CAAT C TG CAG TTA TTT GCC ATT ATA TAC TTT ATT GAT TTG
GST-vWbp	5' -CAA GGG ATC CCC GTG GTT TCT GGG GAG AAG AAT C	5' -CAAT GAA TTC TTA TTT GCC ATT ATA TAC TTT ATT GAT TTG
GST-vWbp-N	5' CAA GGG ATC CCC GTG GTT TCT GGG GAG AAG AAT C	5' -CAAT GAA TTC TTA TTC ATC ACT TTT TGC TGC TTC
GST-vWbp-C	5' CAA GGG ATC CCC TCA AAA AGA AGC AAG AGA AG	5' -CAAT GAA TTC TTA TTT GCC ATT ATA TAC TTT ATT GAT TTG
His-Coa-full/-N/-C	(Ko et al., 2016)	(Ko et al., 2016)
GST-Coa-full/-N/-C	(Ko et al., 2016)	(Ko et al., 2016)

Figure A-6. Sequence of oligonucleotides used in this study. (Reprinted with permission from Thomas et al., 2019)

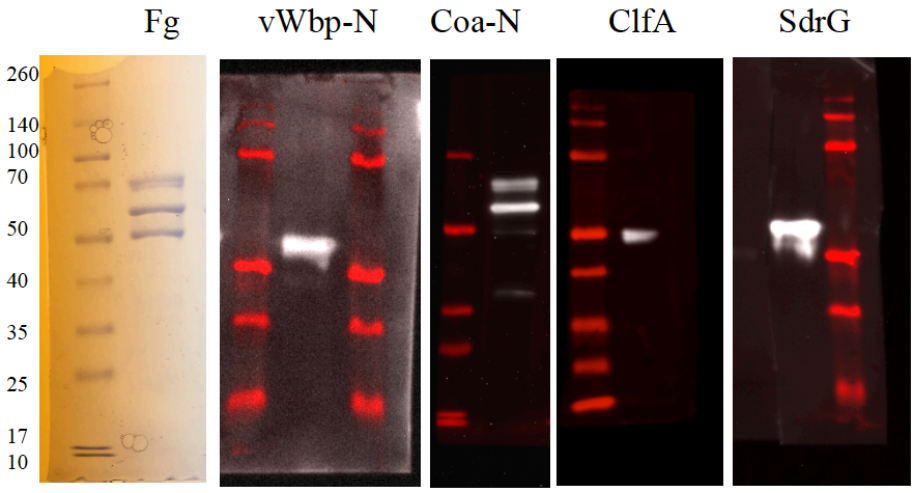

Figure A-7. The N-terminal region of vWbp binds to the N-terminal of the Fg β-chain. Far Western, Fg (5 µg/ lane) was separated on a SDS-PAGE gel and probed with vWbp-N (15 µg/ml). ClfA (15 µg/ml) and SdrG (2.5 µg/ml) were used as controls. (Reprinted with permission from Thomas et al., 2019)

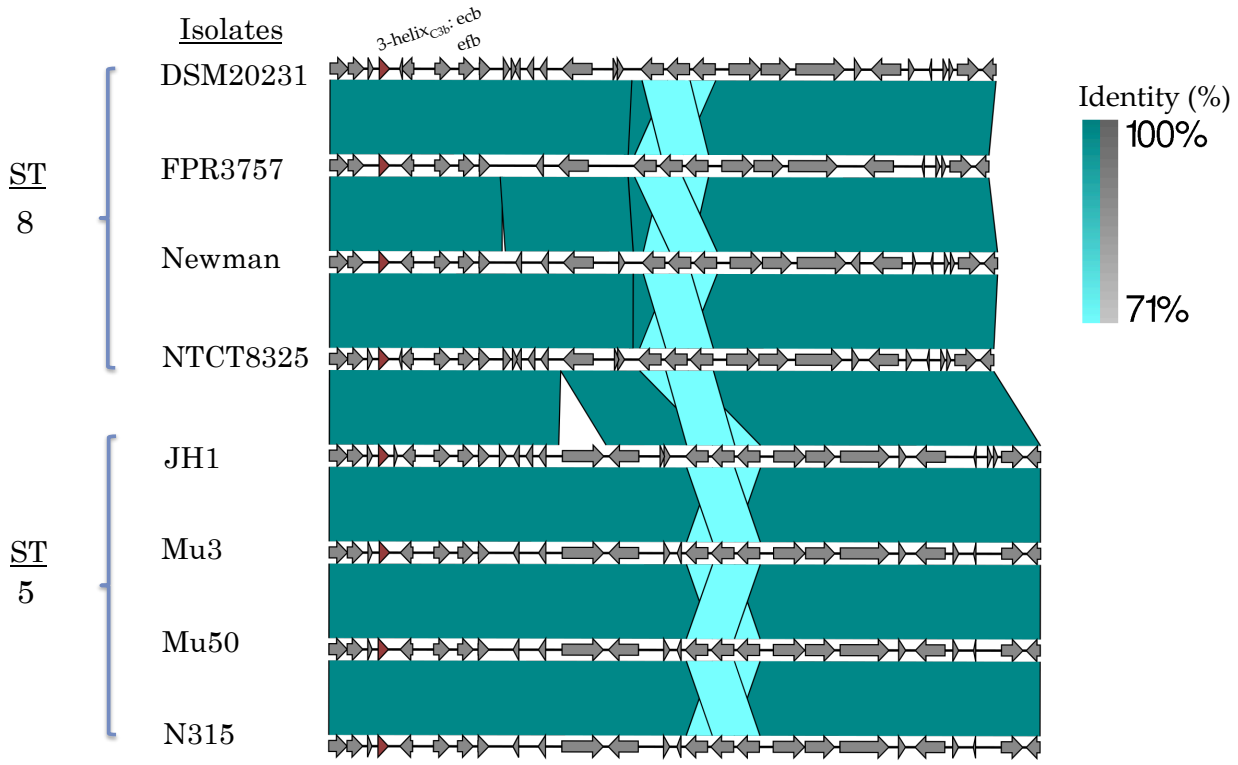

Figure A-8. Comparison of *ecb* in vSaγ island from *S. aureus* isolates. Graphic representation of the vSaγ island from the 8 identified *S. aureus* isolates. Genes, gray arrows. Ecb (*ecb),* red; Efb (*efb)*. Sequence type, ST. Nucleotide identity of 71%, turquoise; >71%, teal.